1968

Behavior of large shingle splices that simulate bridge joints , M.S. thesis (70-24)

N. Yoshida

BEHAVIOR OF LARGE SHINGLE SPLICES THAT SIMULATE BRIDGE JOINTS

by

Noriaki Yoshida

A Thesis
Presented to the Graduate Committee
of Lehigh University
in Candidacy for the Degree of
Master of Science
in
Civil Engineering

Lehigh University

1968

CERTIFICATE OF APPROVAL

This thesis is accepted and approved in partial fulfillment of the requirements of the degree of Master of Science.

_____

Dr. John W. Fisher
Professor in Charge

_____

Dr. David A. VanHorn, Chairman
Department of Civil Engineering

ACKNOWLEDGMENTS

The author wishes to express his appreciation for the supervision, advice, encouragement and review of the manuscript by his thesis Professor John W. Fisher. The interest of Professor Lynn S. Beedle is also gratefully acknowledged. The help provided by Dr. Colin O'Connor, Messrs, James Lee, Suresh Desai, Ulise C. Rivera and Hiroshi Yoshida is sincerely appreciated. Thanks are also extended to Dr. Roger G. Slutter for his advice as Engineer of Tests; to Mr. Hugh T. Sutherland for his advice on instrumentation; to Mr. Richard Sopko for the photography; to Mrs. Shirley Labert for typing the manuscript; to Mr. Jack Gera for the drafting; and to Mr. Kenneth R. Harpel and the laboratory technicians for their assistance in preparing the specimens for testing.

This study has been carried out as a part of the research project on "Studies on Simulated Bridge Joint" being conducted at Fritz Engineering Laboratory, Department of Civil Engineering, Lehigh University. Professor Lynn S. Beedle is Director of the laboratory and Professor David A. VanHorn is Head of the Department.

The project is sponsored by the Louisiana Department of Highways. Technical guidance has been provided by the Research Council on Riveted and Bolted Structural Joints through an advisory committee under the chairmanship of Mr. T. W. Spilman.

TABLE OF CONTENTS

LIST OF FIGURES

LIST OF TABLES

ABSTRACT

This paper summarizes the work on two full size simulated bridge joints and five small butt splices. One large joint was fastened with A325 bolts and the other joint with A502 Gr. 1 rivets. The test joints simulated a chord member and splice on the Baton Rouge Interstate Bridge, a three span continuous truss bridge over Mississippi River. The small butt splices provided reference data.

Each large joint consisted of three main plates and two edge angles with lap plates. The joints were fastened with one hundred twenty eight bolts or rivets. The joints were tested in a 5,000,000 lb. universal testing machine in axial tension. The joint elongation behavior, local slip behavior and the force distribution were observed for each joint. The results of the large simulated joints were compared since their joint geometry was the same. Only the type of fastener differed. The test results indicated clearly that substantial slip does occur in riveted joints. The comparison between the large riveted and bolted joints indicated that the magnitude of slip in the riveted joint was more than half the slip that occurred in the bolted joint. The joint tests also illustrated that complex bolted joints are unlikely to slip the full amount of the bolt hole clearance.

This study also confirmed that the higher allowable stresses suggested in previous investigations provided suitable behavior in the working load range and up to joint slip.

A theoretical elastic solution was also developed for the load partition in a shingle joint. It is based on previous work on symmetrical butt splices. The solution provides the stress resultants in all plate elements and at all fastener shear planes. Matrix notation is used to express the equilibrium and compatibility conditions. The solution is illustrated by considering the forces in two shingle joints.

It is believed that the theoretical solution can be used to check the load distribution in the large test joints. Also it should be extended into the inelastic region.

1. INTRODUCTION

1.1 Introduction and Purpose

High-strength bolts have continued to replace rivets in buildings, bridges and various other steel structures. Friction-type bolted joints are often used in both building and bridge construction. Friction-type bolted joints are considered directly comparable to riveted joints in both AISC and AASHO specification provisions. No change has been made in the design of friction-type joints since the A325 high-strength bolt was permitted as a replacement for the rivets on the basis of one bolt for one rivet in 1951.[1] Friction-type joints do not permit the full advantage of the high shear strength of bolts.

When reversal of movement will not occur or where stress redistribution due to joint slippage is not detrimental to behavior, bearing-type bolted joints are allowed.[2] The mechanical action of bearing-type bolted joints is directly comparable to riveted joints.[3] Since many large bridge joints may not be adversely affected by minor slips, it was desirable to evaluate the relative performance of large riveted or bolted shingle splices.

The mechanical action in a bolted bearing-type joint is the same as in a riveted joint. However, the distribution of

forces in the bolted joint may be slightly different than the distribution that exists in a riveted joint because of the deformation characteristics of the bolts and rivets.

Shingle joints also contain multiple locations where local joint slip may occur, because of the discontinuity in the plates and the non-uniform force distribution along the joint. Therefore, it was desirable to study and observe the local slip behavior, as well as the total joint slip behavior in both riveted and bolted splices.

The objective of this study was to provide comparative information on the behavior of large riveted and bolted shingle splices. It was desirable to evaluate the magnitudes and distribution of slip, the forces in the multiple plates and currently used design concepts.

1.2 Summary of Previous Studies

A considerable amount of work has been conducted on bolted and riveted joints. In general, most of these tests were done on simplified specimens or on symmetrical butt splices. Only a few large joint tests have been conducted. Very few studies have been conducted on riveted or bolted shingle joints.

In 1940, Davis, Woodruff and Davis[4] reported on an extensive series of tests of large riveted joints. These tests were conducted in connection with the design and construction of the San Francisco-Oakland Bay Bridge. As part of this study they reported on the load-slip relations and partition of load among plates of riveted shingle joints. A typical load-slip relationship for a triple-plate shingle joint is shown in Figure 1.

They also reported that unbuttoning failure occurred in fasteners of joints of considerable length connected with 7/8 in. rivets. It was noticed that the rivets in the end row took considerably more than the average share of the load and the excessive deformation caused the end fasteners to fail. The larger the joint, the less was the unit elongation ratio of the joints relative to that of the main plate (gross section). In the multiple-plate joints, stress in the outer plate was maintained at approximately the full value up to the beginning of the next butt of the joint. Therefore, in the portion where the force was transmitted the decrease in stress was similar to that in a simple lap splice joint.

Theoretical studies on symmetrical butt joints have been completed by several people. The first know study was by Arnoulevic[5] in 1909. This was followed by the work of Batho,[6]

Bleich,[7] Hrennikoff,[8] and Vogt.[9] Vogt was the first to propose an extension of the elastic studies into the inelastic and non-linear region. Francis,[10] following this, considered the behavior of double shear joints in the elastic range and beyond. Equilibrium and compatibility conditions were formulated and the partition of load was determined. Rumpf[11] adapted these methods to bolted bearing-type joints in the region from the slip load up to the ultimate load using the graphical method proposed by Francis. Fisher[12] extended these studies by developing mathematical models for the inelastic behavior of A7 and A440 steel and A325 or A490 bolts. Computer programs enabled several variables such as fasteners pitch, bolt diameter, materials and dimensions of joints to be evaluated.

All of the theoretical studies have only considered the case of the symmetrical butt or lap splice. In so far as known, no theoretical studies of shingle joints have been undertaken or developed even in the elastic range.

2. TEST SPECIMENS

2.1 Design of Test Specimens

1. Control Joint Specimens

The purpose of the control joint tests was to provide information on the slip coefficient and the slip load for the large simulated bolted and riveted joints. The pilot test specimens were designed so that the results were applicable to the large joint tests. To satisfy this condition the following criteria were adopted. All plates for the joints came from the same rolling and heat as the plates in the full size joints. All fasteners of a given size and type came from the same lot. The pitch or spacing of fasteners was the same as that used in the large joints.

Three bolted and two riveted joints of V55 steel fastened with 7/8 in. A325 bolts and A502 Gr. 1 rivets, respectively, were fabricated for the pilot test program. The ratio of the net section area of the plates to the shear area of fasteners was 60% i.e.

$$\frac{A_n}{A_s} = 0.6$$

Each joint had two lines of four fasteners. The geometry of these joints is shown in Figure 2.

2. Full Size Joint Specimens

The large test joints simulated the real joint of a chord member of three span continuous truss bridge. The test joints were designed so that major slip of the joints could be expected to occur under 5,000,000 lb. axial tension load. Each joint consisted of three main plates, 3/4 in. x 40 in., two edge angles, 8 in. x 8 in. x 3/4 in., one filler plate, 3/4 in. x 24 in., one lap plate 3/4 in. x 37-3/4 in., and one lap plate plate, 3/4 in. x 40 inches. A schematic drawing showing the joint dimensions is shown in Figure 3.

Two simulated joints were fabricated for this program, one was fastened with 7/8 in. A325 bolts and the other was fastened with 7/8 in. A502 Gr. 1 rivets. Each joint contained the same number of fasteners.

The dsign of these joints was based on current practice and the need to slip within the machine capacity. Details for the design of the large test joints are summarized hereafter.

There were two basic factors to consider when determining the required number of fasteners. One required the joints to slip under 5,000,000 lb. axial tension load. The other consideration was the geometrical proportions that existed in the actual structure. The geometry of the joint was fixed to simulate the real bridge joint.

Given factors in design were,

Materials: V55 steel plates and angles

A325 high tension bolts, 7/8 in. dia.

A502 Gr. 1 rivets, 7/8 in. dia.

Design Stress: 30 ksi in tension for V55 steel

Maximum Applied Load: 5,000,000 lb. tension

Since a major consideration was the need to slip within the machine capacity, the initial design was based on the slip resistance of the bolted joint. The slip coefficient was assumed to be equal to 0.35 a value commonly obtained in previous studies.[13,14] The bolt clamping force was taken as about 1.3 x Proof load as previous studies had indicated this would be achieved with the turn-of-nut installation.[15] Since slip would have to occur on two planes, each was assumed to contribute to the slip resistance.

Hence, the maximum number of bolts was determined by equating the slip resistance to the machine capacity.

$$P_s = 1.3 \times PL \times 0.35 \times 2n \leq 5000$$

$$n \leq \frac{5000}{35.5} \approx 140 \text{ bolts}$$

Since actual joints are designed as though the rivets or bolts are in shear, a design stress was selected so that a reasonable distribution of the bolts could be provided. Fisher and Beedle have suggested that a design stress of 30 ksi is appropriate for bearing-type joints in buildings.[16] Since these joints were for a bridge, the design stress was taken as 90% of the recommended value, or 27 ksi.

The fasteners were then proportioned in the joint proper using current design practice as follows. The design capacity of the joint was determined from the net section. The total net section of the main plates and angles (See Figure 4) is:

3 - 40 in. x 3/4 in. Plates	= 81.6 in.^{2}
2 - 8 in. x 8 in. x 3/4 in. Angles	= 21.5 in.^{2}
	103.1 in.^{2}

Design capacity = 30 x 103.1 = 3093 kips.

The number of fasteners that should be provided in each portion (A, B or C) of the joint shown in Fig. 5 was then ascertained. Fasteners in each individual portion were designed depending on the design force in the main plates and angles. The force in a main plate was assumed to be transmitted into the lap plates in proportion to their distance from the main plate. In

other words the moment couple at the discontinuity should be minimized. The forces in the two lap plates and the filler were calculated from moment equilibrium as shown in Figure 5. In portion A, the fasteners should be strong enough to transmit a force of 632 kips in single shear. This requires

$$\frac{632}{27 \times 0.601} = 39 \quad \text{use 40 fasteners.}$$

Similarly in portion B, the forces to be transmitted through the fasteners at the upper shear plane is

$$816 + 454 - 632 = 638 \text{ (kips)}$$

On the lower shear plane the force is only

$$181 + 181 = 362 \text{ (kips)}$$

Hence, the required number of fasteners in portion B is

$$\frac{638}{27 \times 0.601} = 39.4 \quad \text{use 40 fasteners.}$$

In portion C, the forces to be transmitted through the fasteners at the upper shear plane is

$$816 + 816 + 324 - 816 - 454 = 686 \text{ (kips)}$$

On the lower shear plane the force is

$$498 + 639 - 181 - 181 = 775 \text{ (kips)}$$

The required number of fasteners in portion C is

$$\frac{775}{27 \times 0.601} = 47.8 \quad \text{use 48 fasteners.}$$

The final location and distribution of the fasteners in each portion is given in Figure 3.

Since the riveted joint was to provide comparative data, the same number of fasteners were used. This would enable a direct comparison of the joint behavior at each load increment. It would also provide information on each joint behavior at the currently used design stress levels.

2.2 Fabrication of Specimens

All plates and angles came from the same rolling and heat. All fasteners of a given size and type came from the same lot. The test specimens were fabricated from 7 - 42 in. x 3/4 in. x 30 ft., 1 - 39 in. x 3/4 in. x 30 ft. 6 in., 1 - 55 in. x 3/4 in. x 40 ft. 6 in. pieces of universal mill plate and 2 - 48 in. x 8 in. x 3/4 in. x 45 feet. A 2 ft. piece was cut from each plate and angle to provide material for physical properties and other control tests.

All joints were fabricated by a local fabricator. Each plate element for all test specimens was cut from the large plates. All edges were machine-burned. The complete joint assembly was then sub-drilled and reamed near the corners of all plates. The remaining holes were then drilled from the solid joint to the required diameter. A325 shop bolts were installed in the grip areas of the bolted joint and shipping bolts were placed in the joint area since the final bolting-up was to be done in the laboratory.

A similar fabrication procedure was followed for the riveted joint. After drilling, temporary bolts were installed prior to riveting. The bolted control joints were bolted-up by the research staff. The full size bolted joint was bolted-up by a bolting crew furnished by the fabricator at Fritz Engineering Laboratory as illustrated in Figure 6. The bolts were installed with washers under the nuts and the turn-of-nut installation procedure was used. The bolt tensions were determined by measuring the changes in bolt length with an extensometer before and after the tightening sequence as shown in Figure 7. The corresponding bolt tension was then determined from the appropriate torqued tension calibration curve.

One hundred-twenty eight bolts were installed in the joint proper. The range of the variation in the clamping force

in these fasteners was 48.0 kips to 51.5 kips. Hence, the joint was clamped nearly uniformly with the one hundred-twenty eight bolts.

All riveted joints were riveted at the fabrication shop with a 60 ton Bull Riveter. Figure 8 illustrates the riveting sequence for large joints. After the large joint was riveted and the end sections of the bolted joint bolted in the shop, 10 in. holes were drilled in the end section as illustrated in Figure 9.

In addition to the test joints, five shear jigs and the standard tension coupons of V55 steel plates and the angles and A505 tension coupons of rivets were fabricated for the calibration tests. Two different kinds of shear jigs were fabricated. One was symmetric and consisted of two main plates and two lap plates. The other consisted of three main plates, one lap plate on one side and two lap plates on the other side as illustrated in Figure 17.

2.3 Instrumentation of Joints

All of the test joints were instrumented to record their performance during testing. The control joints were instrumented to record slip and joint elongation. Joint slip displacements were measured at three different levels on each side

of a joint with dial gages and cantilever gages (See Figure 10). Joint elongation was measured with dial gages between points one gage length above the top line of bolts and points one gage length below the bottom line of bolts.

Each full size joint was instrumented to record local joint slip, overall joint elongations, distribution of plate forces, and out-of-plane forces. Local joint slips were measured with cantilever gages (See Fig. 11) at six different levels on each side and at four points inside the joint. The selected locations were at points where one of the main plates was cut and midway between them as illustrated in Figures 12 and 13. Local slip was measured between two ends of the main plate where it was cut or between two different main plates at same level at intermediate points. Slip gages located inside a joint measured the slip between the lap plate and edge angles.

Overall joint elongations were measured with both dial gages and cantilever gages. These elongations were measured on each face between the second line of fasteners above and below the ends of the joint. Piano wire was used to connect the two points.

The large joints were also instrumented with SR4 electrical resistance strain gages. One hundred forty eight gages were placed on each joint, in order to evaluate the distribution

of force in the plate and angles. Three gages were placed on the surface of each lap plate and one gage on both sides of each main plate at eight different sections along the length of a joint as illustrated in Figure 14. Two gages were also placed on the flange of each angle at five different sections along the joint.

Lateral bracing was provided to prevent the large joints from moving out-of-plane and were instrumented with SR4 electrical resistance strain gages (See Figure 15). Two gages were placed on each arm of the bracings to evaluate out-of-plane force.

Figure 11 shows a cantilever gage located at the end of a full size joint. Two SR4 strain gages were placed on both sides of a thin plate cantilever. They were calibrated with a 0.0001 inches dail gage and used within the range where the deflection-strain relationship was linear.

2.4 Material Properties

The materials of the joints were calibrated in order to evaluate the individual properties. Standard tension tests of V55 steel plates and angles, standard A505 tension tests of A502 Gr. 1 rivets and direct tension and torqued tension tests of the A325 bolts were undertaken.

The average curves for the load-deformation relationship obtained from direct tension and torqued-tension tests of the bolts are shown in Figure 16. The load-deformation relationships from the torqued tension calibration tests of bolts were used to estimate the bolt clamping force.

Tension specimens of V55 steel were taken from each plate and angle. They were tested in a 120 kip universal testing machine and the load-strain curves were recorded by an automatic recorder. The results of the material tests are summarized in Table 1. The V55 plate exhibited 22 to 24% elongation.

Two different types of shear jigs were prepared to simulate the conditions in the control joints and the full size joints. One had a lap plate placed on each side of main plate. The other had two lap plates placed on one side and a single lap plate placed on the other as shown in Figure 17. The ultimate strength and load-deformation characteristics shear jigs were nearly the same as shown in Figure 17.

2.5 Testing Procedure

1. Control Joint Tests

Three bolted and two riveted control joints were tested in a 800,000 lb. universal testing machine using flat wedge grips.

The test program examined both the slip resistance and ultimate strength characteristics of these joints.

The dials and the cantilever gages were all read at zero load before the bottom grips were applied. Load was then applied in 50 kip increments up to 200 kips for the bolted joints. Load was applied in 100 kip increments for the riveted joints. Load was then applied in 10 kip increments until major slip occurred. After the joints went into bearing, load was applied continuously in 25 kip increments to obtain the ultimate strength and the deformation characteristics of the joints. At each increment all dials and cantilever gages were read.

For the bolted joints, loading was discontinued after the ultimate load was reached and it was apparent that the plates were necking down. For the riveted joints, the dial gages and cantilever gages were removed from the joint after the ultimate load was reached and the joints were loaded until failure occurred by a shearing off of the rivets.

2. Full Size Bolted Joint Test

The full size bolted joint was loaded in static tension using a 5,000,000 lb. universal testing machine with pin grips as illustrated in Figure 18. The dials, cantilever gages and the strain gages were all read before the bottom grips were applied.

The bolted joint was loaded in axial tension in three loading cycles. The joint was first loaded up to a load of 2080 kips. This corresponded to a shear stress of 13.5 ksi in the bolts. The load increment used during the first loading cycle was 300 kips. The joint was unloaded to 900 kips and the instrumentation read before all load was removed. During the first loading cycle the joint instrumentation was all checked to insure satisfactory operation.

The second loading cycle was performed in 300 kip increment up to the previously applied of 2080 kips. Total joint elongations, local slip and the force distribution were all recorded at each load increment. After the 2080 kip load level was reached, the joint was loaded in 100 kip increment up to 3090 kips which was design load. The total joint elongations and the local slips were read every load increment. The strain gages on the plates, angles and lateral bracings were read at 300 kip intervals. When the load reached 2755 kips the grips were observed to slip with a loud noise and the dial gages and some of the cantilever gages were disturbed by the shock. After all gages were read, the joint was unloaded to the load level of 600 kips before all load was removed.

The third loading cycle was continued until the slip load was reached. The joint was loaded in large increments up

to the design load. Readings of the total joint elongations and the local slips at the end of the joint (location 11 and 12) were taken at each increment. After the design load in the members was reached, the load was extended up to the slip load in 100 kip increments. The total joint elongations and the local slip at the end of the joint were read at every load increment, all other gages were read every other load increment. After the major slip occurred, loading was continued until the joint went into bearing. A minor slip occurred at a load of 4985 kips and the joint was then unloaded to a load of 2080 kips before all load was removed from the joint.

3. Full Size Riveted Joint Test

The test procedure for the full size riveted joint was very similar to that used for the full size bolted joint. After the joint was installed in the 5,000,000 lb. testing machine, all gages were read at zero load before the bottom grips were applied. Loading was also applied in three cycles. The initial loading cycle was up to a load of 2080 kips which corresponded to an average shear stress of 13.5 ksi in the rivets. A 500 kip load increment was used during the first loading cycle. The joint instrumentation was checked out during this loading cycle. The joint was then unloaded to the intermediate load level of 1000 kips before all load was removed.

The second loading cycle was applied in large increments of 1000 kips up to 2080 kips. The loading was continued in 100 kip increment until the joint slipped into bearing. First major slip occurred at a load level of 2775 kips. The loading was continued until the design load of 3090 kips was reached. Additional increments were placed on the joint until the second major slip occurred at 3330 kips and the joint went into bearing. Total joint elongations and all local slip gages were read at every load increment. All strain gages were read at every other load increment. The joint was then unloaded using about 1000 kip load increments.

The third and final loading cycle was undertaken with the intent to load the joint as high as possible. The joint was reloaded in large increments up to 3300 kips, which was the highest load level reached during the previous loading sequence. Additional load was applied in 300 kip increment and the total joint elongation, the local slip behavior and the force distribution were observed.

3. TEST RESULTS AND DISCUSSION

3.1 Pilot Test Results

The five small symmetrical butt joints were tested to evaluate the basic slip resistance of the V55 steel plate and provide an indication of the clamping force that existed in the A502 Gr. 1 rivets. The results are summarized in Table 2.

As noted previously, the clamping force in the A325 bolts was ascertained from measured bolt elongations. Since the bolts were tightened by the turn-of-nut method, no marked variation was observed in bolt tension. It was not possible to determine the clamping force in the rivets.

All bolted joints exhibited similar slip behavior. The load-deformation characteristics are summarized in Figures 19 and 20. All joints exhibited sudden major slip. The nominal slip coefficients obtained for each joint is recorded in Table 2. The average slip coefficient was $K_s = 0.36$ which was directly comparable to the average value used in the joint design. The slip measurements indicated that all joints slipped into bearing and that the total slip was equal to the bolt hole clearance of 1/16 inch.

Both riveted joints experienced slip as indicated in Figures 21 and 22. The magnitude of slip was about 20% of the

slip observed in the bolted joints. Assuming the average slip coefficients obtained during the bolted joint test are applicable, the observed slip loads in Table 2 correspond to a rivet clamping force that is about 60% as great as the bolt clamping force. Other studies have yielded comparable results.[19]

All bolted joints failed at the net section of the plate. The average ultimate strength was 89.6 ksi, which is directly comparable to the standard plate tensile strength tests. Loading of the bolted joints was discontinued after it was apparent that the tensile capacity had been exceeded and the specimen started to neck down and the load decreased with increasing deformation. The shear strength obtained for the bolts was 76 ksi in the shear jigs, hence plate failure was expected because the maximum plate capacity was less than the A325 bolt shear strength.

The two riveted control joints both failed by a simultaneous shearing of all the rivets. The average ultimate shear strength was 47 ksi, which was directly comparable to the shear strength of 45 ksi obtained with single rivets in shear jigs.

Figure 23 compares the behavior of typical riveted and bolted control joints. It is apparent that the riveted joint exhibited about the same stiffness up to slip, thereafter it always exhibited greater flexibility.

3.2 Overall Joint Behavior of the Simulated Bridge Joints

The overall joint behavior of the full size bolted and riveted joints are summarized in Figures 24 and 25 respectively.

The bolted joint exhibited a linear relationship between load and total joint elongation up to first joint slip, which was observed at a load of 4065 kips. This is apparent in Fig. 24 where the load deformation characteristics are summarized for all three load cycles. A second minor slip was observed at the maximum load level of 4985 kips.

The bolt clamping force for each bolt in the bolted joint was obtained from the appropriate bolt torqued-tension calibration curve. The one hundred twenty eight bolt in the joint provided a total clamping force of 6537 kips. The expected slip load predicted from the measured clamping force and the average slip coefficient obtained from the control joint tests was

$$6537 \times 0.36 \times 2 = 4706 \text{ kips}$$

The slip coefficient obtained from the first major slip load was

$$\frac{4065}{2 \times 6537} = 0.31$$

3.2 Overall Joint Behavior of the Simulated Bridge Joints

The overall joint behavior of the full size bolted and riveted joints are summarized in Figures 24 and 25 respectively.

The bolted joint exhibited a linear relationship between load and total joint elongation up to first joint slip, which was observed at a load of 4065 kips. This is apparent in Fig. 24 where the load deformation characteristics are summarized for all three load cycles. A second minor slip was observed at the maximum load level of 4985 kips.

The bolt clamping force for each bolt in the bolted joint was obtained from the appropriate bolt torqued-tension calibration curve. The one hundred twenty eight bolt in the joint provided a total clamping force of 6537 kips. The expected slip load predicted from the measured clamping force and the average slip coefficient obtained from the control joint tests was

$$6537 \times 0.36 \times 2 = 4706 \text{ kips}$$

The slip coefficient obtained from the first major slip load was

$$\frac{4065}{2 \times 6537} = 0.31$$

This correlated with the minimum slip coefficient that was obtained from the control tests. Hence, good agreement was obtained between the control tests and the simulated bridge shingle splice.

The magnitude of first major slip as indicated by the change in total joint elongation was 0.03 inches. This was 45% of the maximum bolt hole clearance. The magnitude of the second minor slip was 0.005 inches. Hence, the total slip of the full size bolted joint was only 0.035 inches. This was only 54% of the full bolt hole clearance. It appears that complex bolted joints do not slip the full amount of the bolt hole clearance, because of misalignment and the distribution of slip. Even though some of the slip measurements did indicate complete slip, the effect was local and did not affect significantly the overall joint behavior. The assumed slip planes that were used in the joint design were confirmed by the test. Further discussion of the distribution of the slip is given later.

The large riveted joint also exhibited a linear relationship up to the currently used shear level in the rivets of 13.5 ksi as shown in Figure 5. However, the load-deformation behavior started to exhibit non-linearity as first slip was approached. The first major slip occurred at the load level of 2775 kips. The slip magnitude was 0.010 inches. A second slip occurred at the load level of 3330 kips and its magnitude was

0.013 inches. Hence, the total slip that was observed in the riveted joint was 0.023 inches. This was 2/3 as much slip as was observed in the bolted joint at a substantially higher load level. The slip load for the full size riveted joint was estimated by assuming the rivet clamping force was the same as for the control joints. The expected slip load was between 2720 and 3040 kips. After slip had occurred a second time, the riveted joint was unloaded in large increments. Load was reapplied in 1000 kip increments up to 3000 kips and then continued in 300 kip increments. In-elastic deformations started to occur at about 3300 kips. This non-linearity was expected because of the observed behavior of the single rivets in shear.

Figure 26 compares the behavior of the full size bolted and riveted joints. The figure shows that the deformations in the riveted joint always exceeded the deformations in the bolted joint at all levels of load. Even though slightly greater slips occurred in the bolted joint, the deformation at comparable load levels were much greater in the riveted joint.

It is also apparent that substantial joint slip does occur in full size riveted joints. In fact, the magnitude of the slip was more than half the slip that was observed in the comparable bolted joint. The joint tests have also illustrated

that complex bolted joints are unlikely to slip the full amount of the bolt hole clearance. Even though some of the bolt holes do indicated complete slip (See Section 3.3), the effect is local and does not affect significantly the overall joint behavior.

3.3 Local Slip Behavior of Full Size Joints

1. Bolted Joint

The locations of the local slip gages are shown in Figure 12 for the bolted joint. The results of the local slip measurements are summarized in Figures 27 and 28.

The local load-slip behavior of the bolted joint can be characterized by two types of response. One indicates that local slip occurred gradually after the joint load exceeded 3000 kips. An examination of the load-slip data plotted in Figure 27 indicates the expected elastic response when the slip gage measurements were over a length of joint. Figure 12 indicated that this behavior was expected at gages 1, 3, 7, 11, 13 and 2, 4, 8, 12 and 14. As load was increased above 3000 kips, an increase in deformation resulted indicating that small slips were occurring at the discontinuities in the plates. These slips are clearly seen in the figures at locations (1 and 2), (7 and 8) and (11 and 12). They were the points where one of the three main plates was cut. Similar behavior has been

experience in the past.[20,21] It is comparable to the strain concentration that occurs at the end of a coverplated beam. Although location (3 and 4) was also a point where the main plate was cut, the magnitude of slip was not as great as at other locations. On the other hand, location (9 and 10) which was located at a comparable point did show gradual slip after 3000 kips. This might be due to its proximity to the more flexible end.

The second type slip response was observed at locations where no discontinuities occurred and the forces in adjacent plates were comparable. This occurred at locations 5, 6, 9, 10, 15 and 16. The load-slip curve at these locations did not show any slip or elastic deformation until sudden slip occurred.

Since the inner main plate and the edge angles were discontinuous at location (13 and 14) the load-slip curve indicated elastic deformation before major slip. The magnitude of slip was relatively small at locations (13 and 14) and (15 and 16) which measured the relative movement between the angles and the lap plate. It appeared that one side of the joint slipped a greater amount than the other (See Figures 27 and 28). The magnitude of the local slips indicated by the slip gages were between 0.01 and 0.05 inches as summarized in Figure 27. At the ends of the plates these values were always larger than

that indicated by the total elongation gages. In other words, the integrated slip along the length of a joint was usually smaller than the local slip. This is apparent from Fig. 24 which shows that total joint elongation is not as great as indicated by many of the slip gages. This condition is directly analogous to the effect that local strain concentrations have on joint or member deformations.

2. Riveted Joint

The slip gages were located at similar location on the riveted joint. Figure 13 shows the location of these gages. The results of the measurements are summarized in Figures 29 and 30. The same two basic types of response were also observed in the riveted joint. The elastic deformations that occurred as well as gradual slip are apparent at locations (1 and 2), (9 and 12) and (15 and 16), points where the plate or angles were cut. When the joint load exceeded 2000 kips, gradual slips were observed to occur at locations 1, 2, 9, 12, 13, 15 and 16. Gages (3 and 6) and (7 and 8) did not show any significant slip before major slip. This was directly comparable to the results obtained for the large bolted joint.

Gages (19 and 20) which were located inside the joint and measured the relative movement of the angles and lap plate

did not show any apparent slip or deformation even when sudden slip occurred. At two levels on the riveted joint, four additional slip gages were located to measure the relative displacement between two points on adjacent plates as shown in Figure 13. These extra gages did not show any difference in the local slip behavior.

Slip was distributed along the length of the joint as shown in Figure 30. The first major slip in the riveted joint occurred at 2775 kips. An examination of Fig. 30 indicates that larger slips were occurring at the lower end of the joint. When load was increase, a second slip occurred at 3330 kips. This resulted in a more uniform distribution of slip along the length of the joint. A comparison of Figs. 25 and 30 show that the average slip of 0.023 in. was nearly uniform along the joint length.

3.4 Axial Strain Distribution Along the Joint Length

The strain gages that were placed on each plate component were used to evaluate the distribution of force to the various plate elements throughout the joint length. The results of these measurements are summarized in Figures 31 to 39.

The strains at various locations along the joints are summarized in Figures 31 and 32 for load levels near the current working shear stress for riveted and friction-type bolted joints.

The figures indicate the change of force in the various plate elements. It is apparent that the load-transfer was similar in both joints.

An examination of Figures 31 and 32 shows that as the discontinuities in the main plates were approached, that the adjacent plates picked up most of the force as was expected. For example, between gage locations 3 and 4, plate 1 was terminated. It is apparent that the top and bottom coverplates were picking up load from the terminated plate as well as load from the other main plates. The bolted joint with its high clamping force indicated that load was also transferred into the main plates between locations 3 and 2, because the strains at location 2 exceeded the strain at location 1.

As load was increased, the strain distribution did not change even though slip occurred in both the riveted and bolted joints. This is illustrated by Figures 33 and 34 which summarize the strain distribution in the three main plates at several levels of load. The strain patterns remained the same throughout the loading range. It is also apparent that the same trends were observed in both types of joints.

Similar behavior was also observed in the edge angles of the riveted and bolted joints. Figures 35 and 36 illustrate that the average strain in the angles continually increased along the length of the joint from the point of discontinuity. It is apparent that the same trend was observed at all load levels.

It was also of interest to examine the strain distribution in the outstanding legs of the angles. Since the load transfer into the angles was along one leg, eccentricities were expected. Figures 37 and 38 summarize the strain distribution across the outstanding angle legs at various locations along the joint. The measurements indicated that a nearly uniform strain gradient existed throughout the length of the joint in the outstanding legs of the angle.

The strain measurements have all indicated that there was no significant difference in the force distributions in the riveted and bolted joints.

The strain measurements also provided an opportunity to check the assumed load distribution that was used in the design. Average forces were evaluated at each location where the main plates were discontinuous. The strains at locations 3 and 4, 5 and 6, and 7 and 8 were averaged to better approximate the plate forces at the points of termination.

The results are summarized in Fig. 39, for the design load level of 3100 kips. Both large test joints are summarized. The plate forces computed from the research strains are compared with the assumed design plate forces.

The summary of the force distributions confirm again that both joints behaved alike. At the design load level of 3100 kips, the riveted joint had slipped into bearing. The bolted joint had not slipped and load was being transferred by friction on the faying surfaces.

In the main member (Section A), the three main plates were each carrying slightly more load than predicted because the angles were not carrying their proportion of the load. Although measurements were not taken on the center plate at that location, equilibrium with the applied load indicated that the loads in each plate were comparable. As was expected, although not assumed in the design, load was transferred from all three main plates and the angles into the lap plates as these elements progressed into the joint. This resulted in substantially more load being carried by the lap plates than was assumed in the joint design. This was true for the riveted and the bolted joint. For example, at section B, the lap plates adjacent to the edge angles were carrying up to 600% more load than assumed. It is apparent that at each plate discontinuity the load tended to distribute more uniformly between the other plate elements at those sections.

The currently used design concept of distributing only the force of the discontinuous plate into the lap plates is not realistic. A more reasonable distribution would be to average

the stress resultant among the resisting plies. This would provide plate forces that more nearly approximate the observed load distribution.

3.5 Out-of Plane Forces

Because the edge angles were not continuous, it was desirable to evaluate whether or not out-of-plane movement would occur because of the eccentricitites that might be introduced. Lateral bracings were attached to the angle at the cut and were instrumented. The computed stress resultants in the joint had indicated that there was very little deviation throughout the joint.

Figure 40 shows the recorded strain in the arms of the lateral bracing. The maximum variation that was observed throughout the tests was less than 10 μ inches. Hence, the horizontal components were negligible in comparison to the applied loads.

The strain measurements throughout the joint had indicated that little if any curvature was being introduced into the joints. The strain gradients that existed in the angles were expected because of the eccentricity in the load line, however, it did not significantly effect the overall behavior of either riveted or bolted joint.

4. SUMMARY AND CONCLUSIONS

These conclusions are based on the results of five tests on compact V55 steel joints and upon two tests on large simulated bridge splices. Three compact joints and one large joint were fastened with 7/8 in. A325 bolts. The remaining two compact joints and the second large joint were fastened by 7/8 in. A502 Gr. 1 rivets.

1. The compact bolted joints gave a mean coefficient of slip for tight mill scale faying surfaces of $K_s = 0.36$. The slip loads obtained from the two compact riveted joints indicated that clamping force in the rivets was about 60% of the bolt clamping force.

2. The slip behavior of the two large simulated bridge joints was in reasonable agreement with the small control joints. The large bolted joint slipped at a load that was equivalent to a slip coefficient of 0.31. This was equal to the smallest value obtained from the compact bolted joint tests. The large riveted joint also slipped at a load equivalent to the minimum slip load obtained from the compact riveted joint tests.

3. Large and complex bolted joints are unlikely to slip the full amount of the bolt hole clearance. The large bolted joint was observed to slip 0.035 inches. This was only 54% of the hole clearance.

4. The slip that occurred in the large riveted joint was about 2/3 as much as was observed in the large bolted joint. However, the slip did occur at substantially lower loads. Other riveted joints can be expected to exhibit similar behavior.

5. The overall deformation of the large riveted joint always exceeded the comparable deformation in the large bolted joint at all load levels.

6. Slip was observed near the ends of the discontinuous plates of the large riveted and bolted joints before major slip. These slips are analogous to the strain concentrations that exist on other coverplated members and had no effect on the joint behavior.

7. The forces in each discontinous plate element were transferred primarily into the adjacent plate elements. The currently used force distribution in shingle splices is not satisfactory.

8. No significant lateral force was introduced at the point of discontinuity in the edge angles.

9. The study indicated that the higher allowable stresses suggested in Ref. 13, provided satisfactory behavior in the large bolted joint. Further study is needed to evaluate the joint strength.

In addition to the experimental study, a theoretical solution for the stress resultants in the various components of a shingle splice was developed. The solution is only applicable at present to the elastic region. Time did not permit an evaluation of the solution by comparing the results with the experimental study.

5. APPENDIX I

A THEORETICAL SOLUTION OF SHINGLE JOINTS

1. General Description of Shingle Joints

Shingle joints are usually used for connections with more than two main plates, such as the gusset plates of truss chord members or coverplates for flanges of plate girders. This type of connection is usually long and heavy. It provides a more gradual transmission of the forces throughout the joint.

The shear surfaces of a shingle joint are generally anti-symmetric as shown in Figure 42. The portion between two butt, where the plates are cut is defined here as a portion of a shingle joint. Each portion of a joint is required to develop by shear on the fasteners a load corresponding to the tension strength of a main plate.

2. Scope of Investigation

This investigation is concerned primarily with developing an elastic solution for shingle joints in which the mechanical fasteners are in state of multiple shear.

The theoretical solution of the load partition is based on the assumption that the mechanical fasteners transmit the applied load by shear and bearing, in other words no frictional forces exist.

The purpose of the theoretical work is to solve the load partitioning among the fasteners and plates in the elastic range only. In addition, this work will serve as the basis for future theoretical studies in the inelastic range.

3. Equilibrium and Compatibility Relationships

A typical anti-symmetric shingle splice joint containing three main plates is shown in Figure 42. The longitudinal line of holes parallel to the axial load is called a line and the space between each hole is called a pitch. The transverse series of holes is called a row and the space between transverse holes is called the gage as in previous papers (See Figure 41).

The lap plates and the main plates are assumed to be of the same thickness and material. The hole pattern is assumed to be completely filled and the bolts are assumed to be of the same size and material. For purposes of analysis, the joint is divided into gage strips. It is assumed that all gage strips are identical in behavior. Forces between bolts j-1 and j in plates 1, 2, 3, ---, i, ---, n are classified as P_{1j}, P_{2j}, ---, P_{ij}, --- P_{nj} respectively. Forces in a fastener j at shear surfaces between plates 1 and 2, 2 and 3, ---i and i + 1,---n-1 and n are classified as R_{1j}, R_{2j}, ---, R_{ij}, --- R_{ij}, --- R_{n-1j}

respectively as shown in Figure 41. The idealized load transfer diagrams are shown schematically in Figure 42.

As was noted previously, the fasteners are assumed to transmit all applied load by shear to the adjacent plates. Therefore, the forces in each plate are calculated from the total load P_o, and forces in the fasteners, R_{ij}, simply by addition or substraction. In addition, the direction of the load transfer to the fasteners on each shear surface in each portion of the joint is assumed not to change.

Considering the absolute values of forces in fasteners, the forces in the plates of the element j + 1 of Figure 42, can be formulated from equilibrium as

$$P_{1,\,j+1} = P_{1,\,j} + R_{1,\,j}$$

$$P_{2,\,j+1} = P_{2,\,j} - R_{1,\,j} - R_{2,\,j}$$

$$P_{3,\,j+1} = P_{3,\,j} + R_{2,\,j} - R_{3,\,j}$$

$$P_{4,\,j+1} = P_{4,\,j} + R_{3,\,j} - R_{4,\,j}$$

$$P_{5,\,j+1} = P_{5,\,j} + R_{4,\,j}$$

in matrix form, the plate forces are

$$\begin{bmatrix} P_{1,\,j+1} \\ P_{2,\,j+1} \\ P_{3,\,j+1} \\ P_{4,\,j+1} \\ P_{5,\,j+1} \end{bmatrix} = \begin{bmatrix} P_{1,\,j} \\ P_{2,\,j} \\ P_{3,\,j} \\ P_{4,\,j} \\ P_{5,\,j} \end{bmatrix} + \begin{bmatrix} 1 & 0 & 0 & 0 \\ -1 & -1 & 0 & 0 \\ 0 & 1 & -1 & 0 \\ 0 & 0 & 1 & -1 \\ 0 & 0 & 0 & 0 \end{bmatrix} \begin{bmatrix} R_{1,\,j} \\ R_{2,\,j} \\ R_{3,\,j} \\ R_{4,\,j} \end{bmatrix} \qquad (1)$$

or

$$\overline{P}_{j+1} = \overline{P}_j + B^I \cdot \overline{R}_j \qquad (1a)$$

where $\overline{P}_j$, $\overline{P}_{j+1}$ and $\overline{R}_j$ are force vectors for the plate elements j and j + 1 and fastener j respectively.

B^I is a coefficient matrix for plate forces in portion I.

Similarly, considering the direction of forces in the fasteners in other portion of the joint, coefficient matrices B^{II}, B^{III} and B^{IV} can be defined.

$$B^{II} = \begin{bmatrix} -1 & 0 & 0 & 0 \\ 1 & 1 & 0 & 0 \\ 0 & -1 & -1 & 0 \\ 0 & 0 & 1 & -1 \\ 0 & 0 & 0 & 1 \end{bmatrix} \tag{2}$$

$$B^{III} = \begin{bmatrix} -1 & 0 & 0 & 0 \\ 1 & -1 & 0 & 0 \\ 0 & 1 & 1 & 0 \\ 0 & 0 & -1 & -1 \\ 0 & 0 & 0 & 1 \end{bmatrix} \tag{3}$$

$$B^{IV} = \begin{bmatrix} -1 & 0 & 0 & 0 \\ 1 & -1 & 0 & 0 \\ 0 & 1 & -1 & 0 \\ 0 & 0 & 1 & 1 \\ 0 & 0 & 0 & -1 \end{bmatrix} \tag{4}$$

Hence, the equilibrium conditions throughout the joint can be expressed as

$$\overline{P}_{j+1} = \overline{P}_j + B^N \overline{R}_j \tag{5}$$

The compatibility conditions described hereafter assume that the fasteners of the joint are in contact with the plate, in

other words there is no space between the bearing surfaces of the plate and fastener. Justification of this assumption is given in Reference 17.

The compatibility equations will be formulated for a small element of the joint by considering Figure 43. As load is applied to the joint, the deformations are examined within the element at points j and j + 1. Due to the applied load, plate 1 will have elongated so that the distance between the holes in plate 1 is $p + e_{j+1}$. Plate 2 will have elongated and its distance will be given by $p + e'_{j+1}$. The distance p is the fastener pitch as shown in Figure 41. e_{j+1} and e'_{j+1} are the elastic elongations of the plates in element j + 1. Compatibility can be formulated by considering the total length of each plate between points j and j + 1 and the deformations of the fasteners. From Fig. 43 it can be seen that

$$\Delta_j + p + e_{j+1} = \Delta_{j+1} + p + e'_{j+1}$$

or

$$\Delta_j + e_{j+1} = \Delta_{j+1} + e'_{j+1} \qquad (6)$$

where Δ_j and Δ_{j+1} are the deformations of the j and j + 1 fasteners. They include the effects of shear, bending, and bearing of the fastener and the localized effect of bearing on

the plates. It is assumed that the fastener diameter does not change due to the applied load.

If the plate elongations are expressed as functions of load in the segments of the joint between fasteners, and the fastener deformations as functions of the fastener loads, Eq. (6) can be written as

$$\Delta(\overline{R}_j) + e(\overline{P}_{j+1}) = \Delta(\overline{R}_{j+1}) + e'(\overline{P}_{j+1})$$

or

$$\Delta(\overline{R}_{j+1}) = \Delta(\overline{R}_j) + e(\overline{P}_{j+1}) - e'(\overline{P}_{j+1}) \qquad (7)$$

where $\Delta(\overline{R}_j)$, $\Delta(\overline{R}_{j+1})$ are bolt deformations, and $e(\overline{P}_{j+1})$, $e'(\overline{P}_{j+1})$ are the elongations for plates 1 and 2.

In the elastic range the force-deformation relationships for the plates can be expressed as

$$e(\overline{P}_{j+1}) = \frac{P_{1,\,j+1} \cdot p}{EA_p}$$

$$e'(\overline{P}_{j+1}) = \frac{P_{2,\,j+1} \cdot p}{EA_p} \qquad (8)$$

where EA_p = rigidity of the plate in tension

p = pitch

The force-deformation relationship of the fastener in the elastic range is usually expressed as

$$\Delta = \frac{R}{K} \tag{9}$$

The elastic constant K has usually been determined from experimental data. Reference 18 has given a solution for the coefficient K based on the conventional beam theory. Fisher[12] described the elastic constant K synthetically in his paper. That is,

For shear: $$K_s = \frac{t_1 + t_2}{3 G_b A_b} \tag{10}$$

For bending: $$K_b = \frac{t_1^3 + 4t_1 t_2^2 + 4t_1^2 t_2 + t_2^3}{192 E I_b} \tag{11}$$

For bearing: $$K_r = \frac{2(t_1 + t_2)}{E t_1 t_2} \tag{12}$$

The localized bearing effect of fastener on the plate was found to be the same as Eq. (12). Hence, the constant K was evaluated as

$$K = \frac{2}{K_s + K_b + 2K_r} \tag{13}$$

where E = modulus of elasticity

G_b = shear modulus

A_b = fastener area

I_b = moment of inertia of a fastener

t_1 and t_2 = thickness of the plate

Now the force-deformations for fasteners j and j + 1 can be expressed as

$$\Delta(\overline{R}_j) = \frac{R_{1,\,j}}{K}$$

$$\Delta(\overline{R}_{j+1}) = \frac{R_{1,\,j+1}}{K} \qquad (14)$$

By substituting Eqs. (8) and (14) into Eq. (7), the compatibility equation can be expressed in terms of the forces in plates and fasteners as

$$\frac{R_{1,\,j+1}}{K} = \frac{R_{1,\,j}}{K} + \frac{P_{1,\,j+1}\cdot p}{A_p E} - \frac{P_{2,\,j+1}\cdot p}{A_p E}$$

or

$$R_{1,\,j+1} = R_{1,\,j} + \overline{K}(P_{1,\,j+1} - P_{2,\,j+1}) \qquad (15)$$

where

$$\overline{K} = \frac{K \cdot P}{A_p E} \tag{16}$$

Equation (15) expresses the forces $\overline{R}_{j+1}$ as functions of the forces $\overline{R}_j$. In portion I, Eq. (15) can be applied to other shear surfaces and similar equations are obtained.

$$R_{2,\,j+1} = R_{2,\,j} + \overline{K}(-P_{2,\,j+1} + P_{3,\,j+1})$$

$$R_{3,\,j+1} = R_{3,\,j} + \overline{K}(-P_{3,\,j+1} + P_{4,\,j+1}) \tag{15a}$$

$$R_{4,\,j+1} = R_{4,\,j} + \overline{K}(-P_{4,\,j+1} + P_{5,\,j+1})$$

Using matrix notation, the bolt forces in portion I are

$$\begin{bmatrix} R_{1,\,j+1} \\ R_{2,\,j+1} \\ R_{3,\,j+1} \\ R_{4,\,j+1} \end{bmatrix} = \begin{bmatrix} R_{1,\,j} \\ R_{2,\,j} \\ R_{3,\,j} \\ R_{4,\,j} \end{bmatrix} + \overline{K} \begin{bmatrix} 1 & -1 & 0 & 0 & 0 \\ 0 & -1 & 1 & 0 & 0 \\ 0 & 0 & -1 & 1 & 0 \\ 0 & 0 & 0 & -1 & 1 \end{bmatrix} \begin{bmatrix} P_{1,\,j+1} \\ P_{2,\,j+1} \\ P_{3,\,j+1} \\ P_{4,\,j+1} \\ P_{5,\,j+1} \end{bmatrix} \tag{17}$$

or

$$\bar{R}_{j+1} = \bar{R}_j + \bar{K}C^I\bar{P}_{j+1} \tag{17a}$$

where C^I is a coefficient matrix for fastener forces in portion I. Similarly, considering the directions of the deformations of the fasteners in other portions we obtain coefficient matrices C^{II}, C^{III} and C^{IV} as

$$C^{II} = \begin{bmatrix} -1 & 1 & 0 & 0 & 0 \\ 0 & 1 & -1 & 0 & 0 \\ 0 & 0 & -1 & 1 & 0 \\ 0 & 0 & 0 & -1 & 1 \end{bmatrix} \tag{18}$$

$$C^{III} = \begin{bmatrix} -1 & 1 & 0 & 0 & 0 \\ 0 & -1 & 1 & 0 & 0 \\ 0 & 0 & 1 & -1 & 0 \\ 0 & 0 & 0 & -1 & 1 \end{bmatrix} \tag{19}$$

$$C^{IV} = \begin{bmatrix} -1 & 1 & 0 & 0 & 0 \\ 0 & -1 & 1 & 0 & 0 \\ 0 & 0 & -1 & 1 & 0 \\ 0 & 0 & 0 & 1 & -1 \end{bmatrix} \tag{20}$$

The compatibility equation can now be expressed as

$$\bar{R}_{j+1} = \bar{R}_j + \bar{K}C^N\bar{P}_{j+1} \qquad (21)$$

4. Example of the Force Distribtuion in Fasteners of a Lap Splice

For illustrative purposes a simple lap splice is shown in Figure 44. For this particluar joint, the coefficient matrices B and C can be expressed as

$$B = \begin{bmatrix} 1 \\ -1 \end{bmatrix} \qquad C = \begin{bmatrix} 1 & -1 \end{bmatrix} \qquad (22)$$

The forces in the plates and fasteners as expresses by Eqs. (5) and (21) can be written in terms of P_o and R_1.

Hence at element 1

$$\begin{bmatrix} P_{11} \\ P_{21} \end{bmatrix} = \begin{bmatrix} 0 & 0 \\ 1 & 0 \end{bmatrix} \begin{bmatrix} P_o \\ R_1 \end{bmatrix}$$

$$\begin{bmatrix} R_1 \end{bmatrix} = \begin{bmatrix} 0 & 1 \end{bmatrix} \begin{bmatrix} P_o \\ R_1 \end{bmatrix} \qquad (23)$$

where P_o is the total load in the plate of a strip. To determine the unknown bolt force R_1, the boundary condition at the end of plate 2, that is $P_{2,4} = 0$ will be used. At each element, the forces in the plate can be expressed as a function of the initial

plate force P_o and the bolt force R_1. Hence the forces in other elements are

at element 2

$$\begin{bmatrix} P_{12} \\ P_{22} \end{bmatrix} = \begin{bmatrix} P_{11} \\ P_{21} \end{bmatrix} + \begin{bmatrix} 1 \\ -1 \end{bmatrix} \begin{bmatrix} R_1 \end{bmatrix} = \begin{bmatrix} 0 & 0 \\ 1 & 0 \end{bmatrix} \begin{bmatrix} P_o \\ R_1 \end{bmatrix} + \begin{bmatrix} 1 \\ -1 \end{bmatrix} \begin{bmatrix} 0 & 1 \end{bmatrix} \begin{bmatrix} P_o \\ R_1 \end{bmatrix}$$

$$= \begin{bmatrix} 0 & 1 \\ 1 & -1 \end{bmatrix} \begin{bmatrix} P_o \\ R_1 \end{bmatrix} \qquad (24)$$

$$\begin{bmatrix} R_2 \end{bmatrix} = \begin{bmatrix} R_1 \end{bmatrix} + \bar{K} \begin{bmatrix} 1 & -1 \end{bmatrix} \begin{bmatrix} P_{12} \\ P_{22} \end{bmatrix} = \begin{bmatrix} 0 & 1 \end{bmatrix} \begin{bmatrix} P_o \\ R_1 \end{bmatrix} + \bar{K} \begin{bmatrix} 1 & -1 \end{bmatrix} \begin{bmatrix} 0 & 1 \\ 1 & -1 \end{bmatrix} \begin{bmatrix} P_o \\ R_1 \end{bmatrix}$$

$$= \begin{bmatrix} -\bar{K} & 2\bar{K} + 1 \end{bmatrix} \begin{bmatrix} P_o \\ R_1 \end{bmatrix}$$

for element 3

$$\begin{bmatrix} P_{13} \\ P_{23} \end{bmatrix} = \begin{bmatrix} 0 & 1 \\ 1 & -1 \end{bmatrix} \begin{bmatrix} P_o \\ R_1 \end{bmatrix} + \begin{bmatrix} 1 \\ -1 \end{bmatrix} \begin{bmatrix} -\bar{K} & 1 + 2\bar{K} \end{bmatrix} \begin{bmatrix} P_o \\ R_1 \end{bmatrix} = \begin{bmatrix} -\bar{K} & 2 + 2\bar{K} \\ 1 + \bar{K} & -2 - 2\bar{K} \end{bmatrix} \begin{bmatrix} P_o \\ R_1 \end{bmatrix}$$

$$\begin{bmatrix} R_3 \end{bmatrix} = \begin{bmatrix} -\bar{K} & 1 + 2\bar{K} \end{bmatrix} \begin{bmatrix} P_o \\ R_1 \end{bmatrix} + \bar{K} \begin{bmatrix} 1 & -1 \end{bmatrix} \begin{bmatrix} -\bar{K} & 2 + 2\bar{K} \\ 1 + \bar{K} & -2 - 2\bar{K} \end{bmatrix} \begin{bmatrix} P_o \\ R_1 \end{bmatrix} \qquad (25)$$

$$= \begin{bmatrix} -2\bar{K} - 2\bar{K}^2 & 1 + 6\bar{K} + 4\bar{K}^2 \end{bmatrix} \begin{bmatrix} P_o \\ R_1 \end{bmatrix}$$

for element 4

$$\begin{bmatrix} P_{14} \\ P_{24} \end{bmatrix} = \begin{bmatrix} -\bar{K} & 2 + 2\bar{K} \\ 1 + \bar{K} & -2 - 2\bar{K} \end{bmatrix} \begin{bmatrix} P_o \\ R_1 \end{bmatrix} + \begin{bmatrix} 1 \\ -1 \end{bmatrix} \begin{bmatrix} -2\bar{K} - 2\bar{K}^2 & 1 + 6\bar{K} + 4\bar{K}^2 \end{bmatrix} \begin{bmatrix} P_o \\ R_1 \end{bmatrix}$$

$$= \begin{bmatrix} -3\bar{K} - 2\bar{K}^2 & 3 + 8\bar{K} + 4\bar{K}^2 \\ 1 + 3\bar{K} + 2\bar{K}^2 & -3 - 8\bar{K} - 4\bar{K}^2 \end{bmatrix} \begin{bmatrix} P_o \\ R_1 \end{bmatrix} \qquad (26)$$

Enforcing the boundary condition at the end of plate 2 results in

$$P_{24} = (1 + 3\bar{K} + 2\bar{K}^2)P_o + (-3 - 8\bar{K} - 4\bar{K}^2)R_1 = 0$$

$$R_1 = \frac{1 + 3\bar{K} + 2\bar{K}^2}{3 + 8\bar{K} + 4\bar{K}^2} P_o = \frac{1 + \bar{K}}{3 + 2\bar{K}} P_o \qquad (27)$$

Since the bolt forces R_2 and R_3 are a function of P_o and R_1 they may be expressed as

$$R_2 = \frac{1}{3 + 2\bar{K}} P_o \qquad (28)$$

$$R_3 = \frac{1 + \bar{K}}{3 + 2\bar{K}} P_o \qquad (29)$$

If the ratio of the rigidities in the plates and fasteners is assumed, then

$$\overline{K} = \frac{K \cdot p}{A_p E} = 0.05$$

The forces in three fasteners can then be expressed as

$$R_1 = 0.339\ P_o$$

$$R_2 = 0.322\ P_o$$

$$R_3 = 0.339\ P_o$$

5. Solution of a Joint with Multiple-Main Plates

The theoretical solution of a shingle joint with multiple-main plates can be obtained by consideration of the joint shown in Figure 45. The joint has three main plates, two lap plates and four fasteners in each portion of the joint.

Considering the calculation procedure described in previous section and referring to Fig. 45, the unknown forces in this case are R_{11}, R_{21}, R_{31}, R_{41}, R_{15}, R_{25}, R_{29}, R_{39}, $R_{3,13}$, and $R_{4,13}$. The boundary conditions provided at the ends of the

plates are

$$P_{25} = P_{39} = P_{4,13} = P_{1,17} = P_{5,17} = 0$$

$$P_{2,17} = P_{3,17} = P_{4,17} = P_o \tag{30}$$

Since there are only eight boundary conditions for ten unknown fastener forces, some particular characteristic conditions of the joint will be used to determine these unknown forces.

In this particular problem, the joint is anti-symmetric. Therefore, the bottom half below the principal shear surfaces can be considered instead of the whole joint. The forces on the principal shear surfaces,

$$\bar{R}_o = \{R_{11}, R_{12}, R_{13}, R_{14}, R_{25}, R_{26}, R_{27}, R_{28}, R_{39}, R_{3,10}, R_{3,11}, R_{3,12} R_{4,13}, R_{4,14}, R_{4,15}, R_{4,16}\} \tag{31}$$

are assumed to be represented by the values which were obtained in the discontinuous lap splice shown in Figure 46. The discontinuous lap splice can be solved by the methods described in References 12 and 17. The top and bottom half of the joint can be assumed to act as solid bodies and different sectional rigidities are applied in the different portions.

When the forces on the principal shear surfaces are obtained the remaining unknowns in the bottom half of the joint are R_{21}, R_{31} and R_{41} and the resulting boundary conditions are,

$$P_{15} = P_{29} = P_{3,13} = 0 \tag{32}$$

as shown in Figure 46. All other forces in the plates and fasteners can be expressed as functions of the forces in the first fastener. These three unknowns can be determined from the three boundary conditions. The remaining joint forces can then be obtained.

Coefficients Matrices B^N and C^N

Coefficient matrices B^N and C^N in Eqs. (5) and (21) can be written for each portion considering the directions of the fastener forces, as

$$B^I = \begin{bmatrix} -1 & -1 & 0 & 0 \\ 0 & 1 & -1 & 0 \\ 0 & 0 & 1 & -1 \\ 0 & 0 & 0 & 1 \end{bmatrix} \quad C^I = \begin{bmatrix} 0 & 0 & 0 & 0 \\ -1 & 1 & 0 & 0 \\ 0 & -1 & 1 & 0 \\ 0 & 0 & -1 & 1 \end{bmatrix} \tag{33}$$

The first row of C^I corresponds to the fastener forces on the principal shear surface (which are obtained as solutions of a discontinuous lap splice as in the previous step).

Similarly in other portions of the joint, the coefficient matrices are of the form

$$B^{II} = \begin{bmatrix} -1 & -1 & 0 \\ 0 & 1 & -1 \\ 0 & 0 & 1 \end{bmatrix}, \qquad C^{II} = \begin{bmatrix} 0 & 0 & 0 \\ -1 & 1 & 0 \\ 0 & -1 & 1 \end{bmatrix} \tag{34}$$

$$B^{III} = \begin{bmatrix} -1 & -1 \\ 0 & 1 \end{bmatrix} \qquad C^{III} = \begin{bmatrix} 0 & 0 \\ -1 & 1 \end{bmatrix} \tag{35}$$

Again the first rows of C^{II} and C^{III} correspond to the fastener forces on the principal shear surfaces.

Initial values of plates or fastener.

In matrix form

$$\begin{bmatrix} P_{11} \\ P_{21} \\ P_{31} \\ P_{41} \end{bmatrix} = \begin{bmatrix} 1 & 0 & 0 & 0 & 0 \\ 1 & 0 & 0 & 0 & 0 \\ 1 & 0 & 0 & 0 & 0 \\ 0 & 0 & 0 & 0 & 0 \end{bmatrix} \begin{bmatrix} P_o \\ 1 \\ R_{21} \\ R_{31} \\ R_{41} \end{bmatrix} \tag{36}$$

$$\begin{bmatrix} R_{11} \\ R_{21} \\ R_{31} \\ R_{41} \end{bmatrix} = \begin{bmatrix} 0 & R_{11} & 0 & 0 & 0 \\ 0 & 0 & 1 & 0 & 0 \\ 0 & 0 & 0 & 1 & 0 \\ 0 & 0 & 0 & 0 & 1 \end{bmatrix} \begin{bmatrix} P_o \\ 1 \\ R_{21} \\ R_{31} \\ R_{41} \end{bmatrix} \tag{37}$$

where in the unknown vector the real unknowns are R_{21}, R_{31}, and R_{41}. The second element, 1, corresponds to the values on the principal shear surfaces. The forces in plates and fasteners are calculated by means of Eqs. (5) and (21), that is,

$$\overline{P}_{j+1} = \overline{P}_j + B \cdot \overline{R} \tag{5}$$

$$\overline{R}_{j+1} = \overline{R}_j + \overline{K} \cdot C \cdot \overline{P}_{j+1} \tag{21}$$

The result of the fastener forces on the principal shear surface which are obtained as solutions of the discontinuous lap splice in Fig. 46 are

$$[R_{1,1}, R_{1,2}, R_{1,3}, R_{1,4}, R_{2,5}, R_{2,6}, R_{2,7}, R_{2,8}, R_{3,9}, R_{3,10}, R_{3,11}, R_{3,12}, R_{4,13}, R_{4,14}, R_{4,15}, R_{4,16}]$$

$$= [0.2164,\ 0.1968,\ 0.1872,\ 0.1872,\ 0.1842,$$
$$0.1758,\ 0.1739,\ 0.1784,\ 0.1784,\ 0.1739,$$
$$0.1758,\ 0.1842,\ 0.1872,\ 0.1872,\ 0.1968,$$
$$0.2164]$$

Using the fastener forces on the principal shear surface in the matrix of fasteners forces, the forces in the 2nd element of plates becomes

$$\begin{bmatrix} P_{1,2} \\ P_{2,2} \\ P_{3,2} \\ P_{4,2} \end{bmatrix} = \begin{bmatrix} 1 & 0 & 0 & 0 & 0 \\ 1 & 0 & 0 & 0 & 0 \\ 1 & 0 & 0 & 0 & 0 \\ 0 & 0 & 0 & 0 & 0 \end{bmatrix} \begin{bmatrix} P_o \\ 1 \\ R_{21} \\ R_{31} \\ R_{41} \end{bmatrix}$$

$$+ \begin{bmatrix} -1 & -1 & 0 & 0 & 0 & 0.2164 & 0 & 0 & 0 \\ 0 & 1 & -1 & 0 & 0 & 0 & 1 & 0 & 0 \\ 0 & 0 & 1 & -1 & 0 & 0 & 0 & 1 & 0 \\ 0 & 0 & 0 & 1 & 0 & 0 & 0 & 0 & 1 \end{bmatrix} \begin{bmatrix} P_o \\ 1 \\ R_{21} \\ R_{31} \\ R_{41} \end{bmatrix}$$

$$= \begin{bmatrix} 1 & -0.2164 & -1 & 0 & 0 \\ 1 & 0 & 1 & -1 & 0 \\ 1 & 0 & 0 & 1 & -1 \\ 0 & 0 & 0 & 0 & 1 \end{bmatrix} \begin{bmatrix} P_o \\ 1 \\ R_{21} \\ R_{31} \\ R_{41} \end{bmatrix}$$

at the 2nd fastener,

$$\overline{K} = \frac{K \cdot P}{A_p E} = \frac{3.879 \times 10^3 \times 3.5}{6.75 \times 29 \times 10^3} = 0.0695$$

$$\begin{bmatrix} R_{1,2} \\ R_{2,2} \\ R_{3,2} \\ R_{4,2} \end{bmatrix} = \begin{bmatrix} 0 & 0.2164 & 0 & 0 & 0 \\ 0 & 0 & 1 & 0 & 0 \\ 0 & 0 & 0 & 1 & 0 \\ 0 & 0 & 0 & 0 & 1 \end{bmatrix} \begin{bmatrix} P_o \\ 1 \\ R_{21} \\ R_{31} \\ R_{41} \end{bmatrix}$$

$$+ \overline{K} \begin{bmatrix} 0 & 0 & 0 & 0 & 1 & -0.2164 & -1 & 0 & 0 \\ -1 & 1 & 0 & 0 & 1 & 0 & 1 & -1 & 0 \\ 0 & -1 & 1 & 0 & 1 & 0 & 0 & 1 & -1 \\ 0 & 0 & -1 & 1 & 0 & 0 & 0 & 0 & 1 \end{bmatrix} \begin{bmatrix} P_o \\ 1 \\ R_{21} \\ R_{31} \\ R_{41} \end{bmatrix}$$

$$= \begin{bmatrix} 0 & 0.2164 & 0 & 0 & 0 \\ 0 & 0.0150 & 1.139 & -0.0695 & 0 \\ 0 & 0 & -0.0695 & 1.139 & -0.0695 \\ -0.0695 & 0 & 0 & -0.0695 & 1.139 \end{bmatrix} \begin{bmatrix} P_o \\ 1 \\ R_{21} \\ R_{31} \\ R_{41} \end{bmatrix}$$

Same calculation procedure were repeated until $P_{4,17}$ and the three boundary conditions gave a three order simultaneous equation to determine the initial fastener forces. All other forces in plate and fasteners are to be obtained as function of the initial fastener forces.

Theoretical solution of load partition among the plates is summarized in Figure 47. The calculation procedure is shown in the flow chart in Figures 48(1) and (2). The solution of the load partition was referred with the work in the past[4] and comparable.

6. TABLES AND FIGURES

TABLE 1

SUMMARY OF MATERIAL PROPERTY CALIBRATIONS

Specimens	Type of Test	Number of Test	Yield Stress (ksi)	Standard Deviation	Ultimate Strength (ksi)
A325 Bolt	Direct Tension	6	93	1.60	98
	Torqued Tension	6	82	1.56	86
	Shear Jig	2	42	1.80	76
A502 Gr. 1 Rivet	Tension Coupon	6	53	1.75	65
	Shear Jig	6	27	1.80	45
V55 Plate	Tension Coupon	9	59	1.40	88

TABLE 2

SUMMARY OF TESTS OF CONTROL JOINTS

Specimen	Clamping Force (kips)	Slip Load (kips)	Slip Coefficient	Ultimate Load (kips)	Failure Mode
CBJ-1	432	361	0.42	518	Plate
CBJ-2	429	263	0.35	500	Plate
CBJ-3	430	324	0.31	492	Plate
CRJ-1	-	190	-	475	Rivet Shear
CRJ-2	-	169	-	481	Rivet Shear

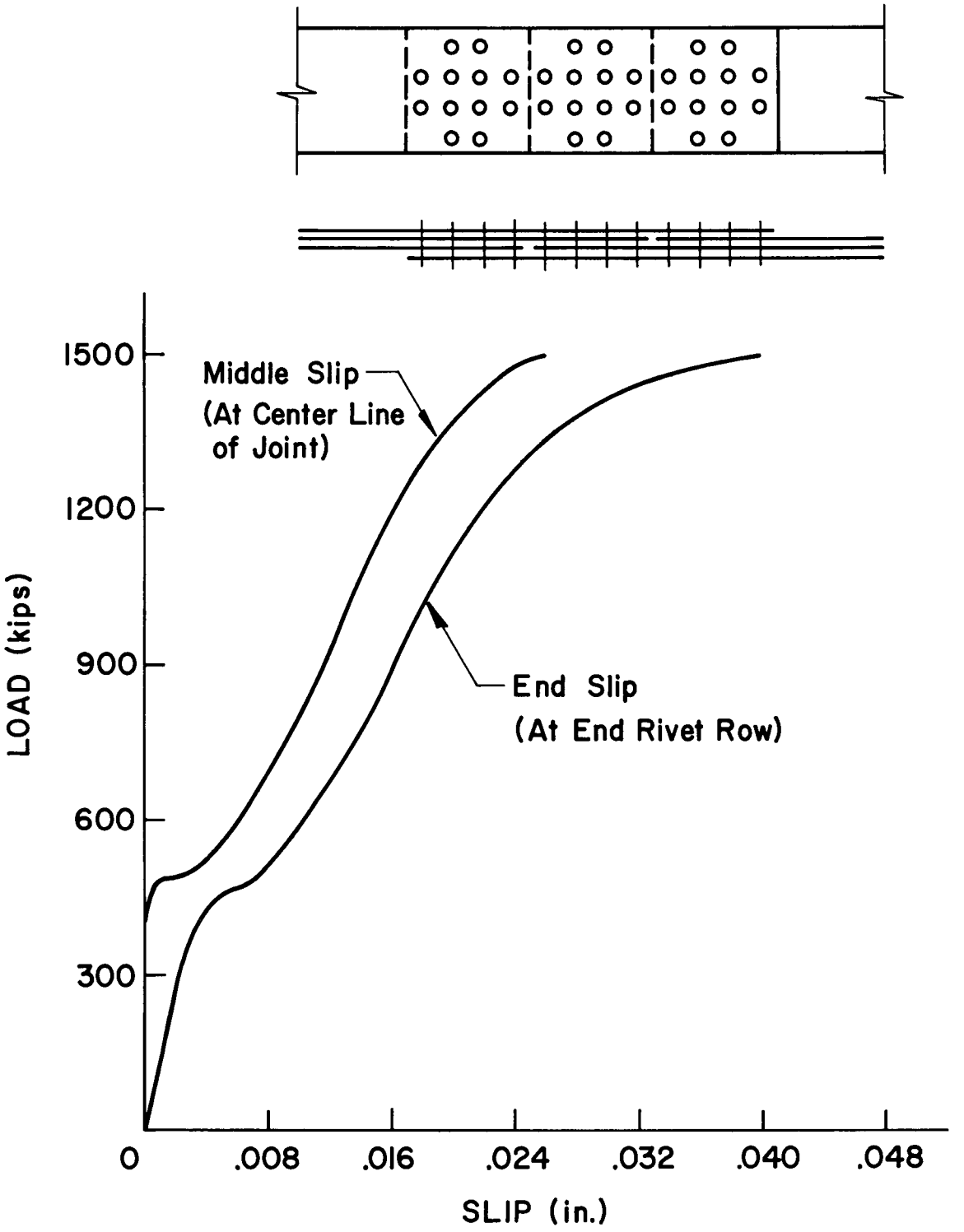

Fig. 1 Load-Slip Relations of Triple-Plates Shingle Joint

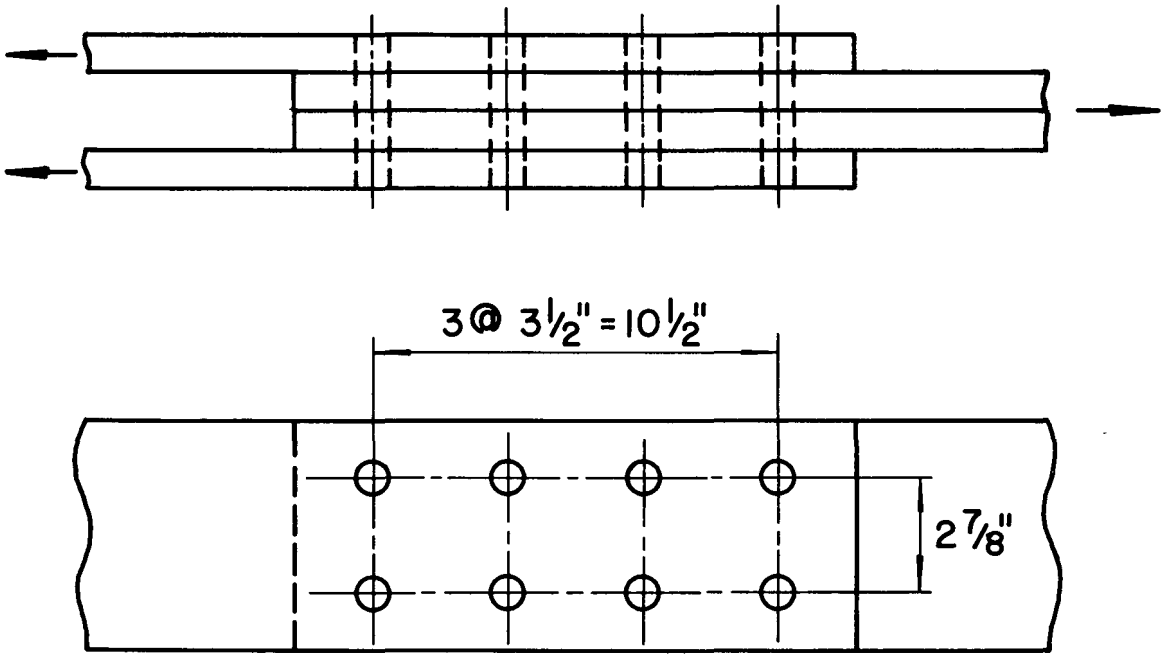

V55 STEEL PLATES

7/8" ϕ A325 BOLTS OR A502 Gr. I RIVETS

Fig. 2 Control Test Specimen

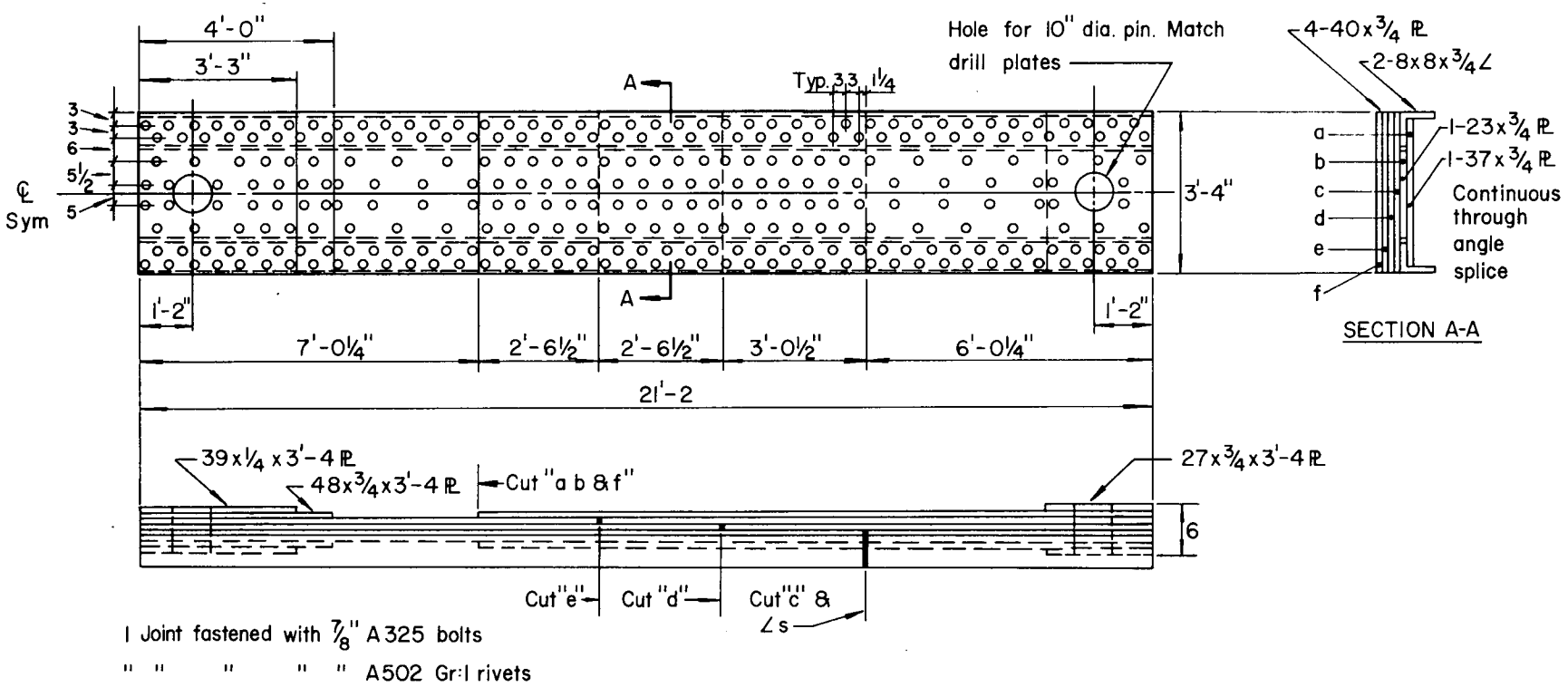

LARGE TEST JOINTS

Scale - 1/2"=1'-0"

Fig. 3 Full Size Simulated Joint Test Specimen

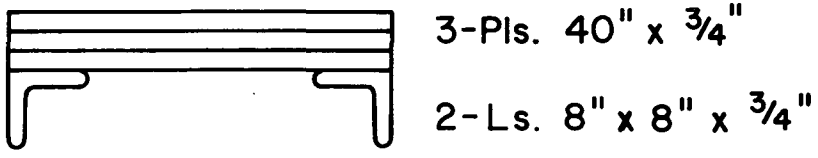

Fig. 4 Main Section of Large Joint

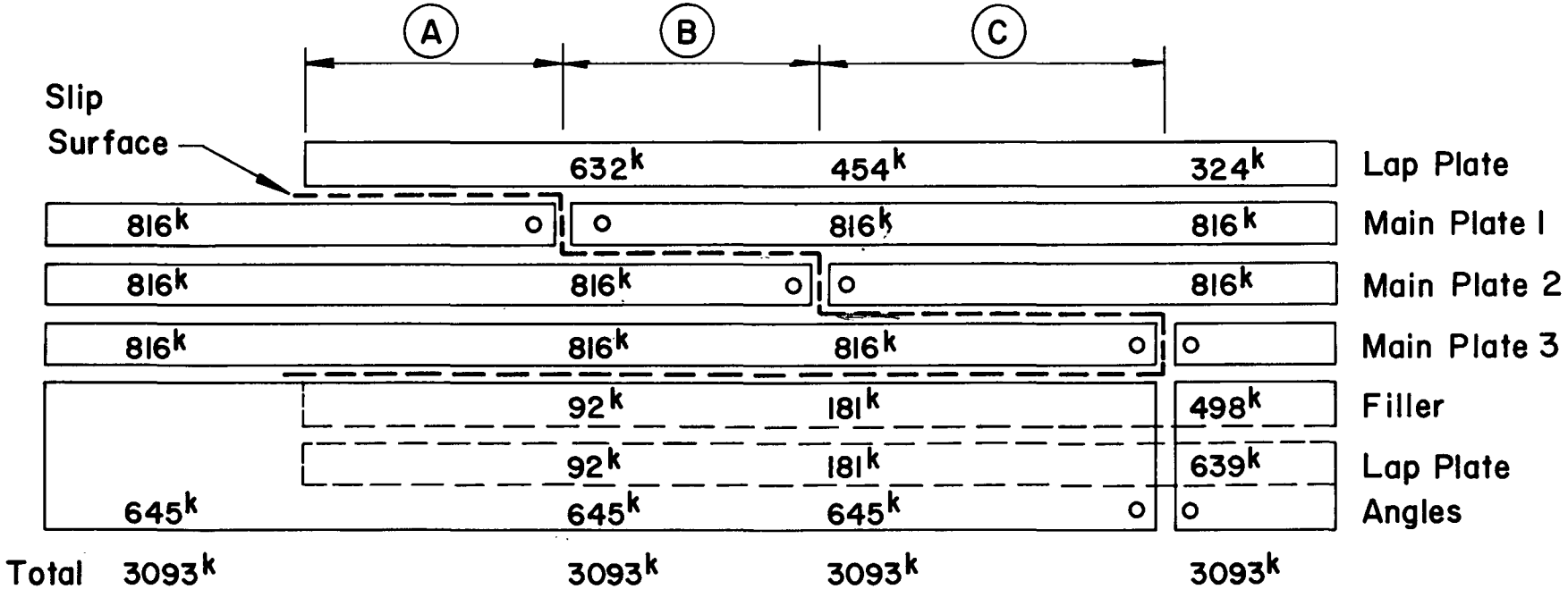

Fig. 5 Force Transmission Diagram for Design of Large Joint

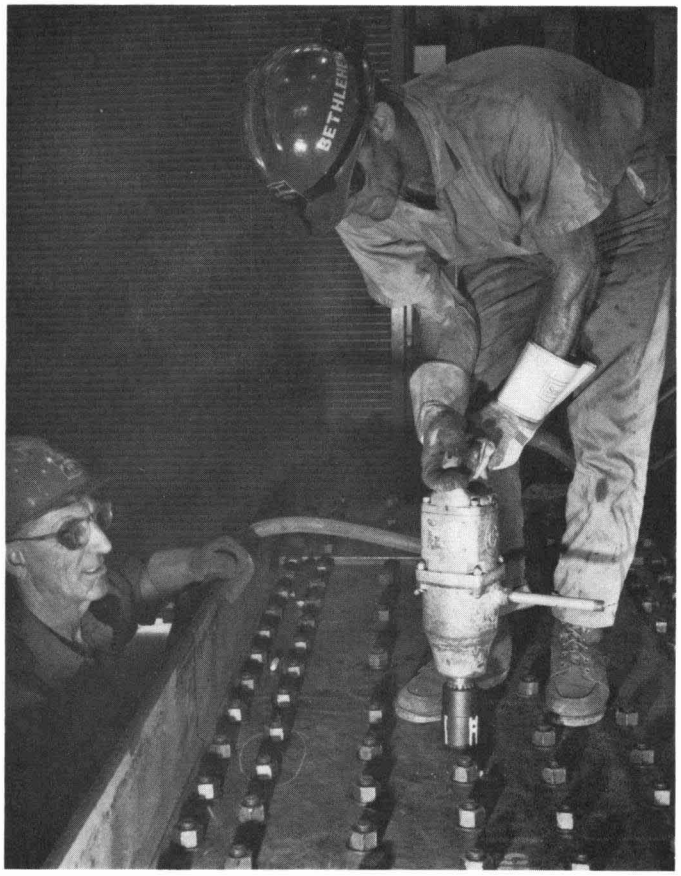

Fig. 6 Bolting-up to Simulated Joint

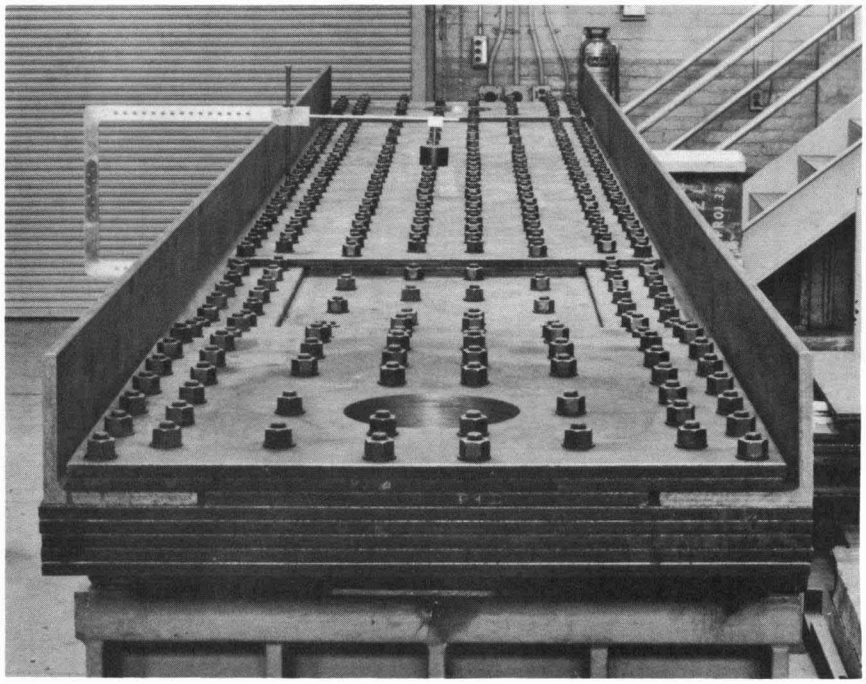

Fig. 7(1) Measuring the Changes in Bolt Length with Extensometer

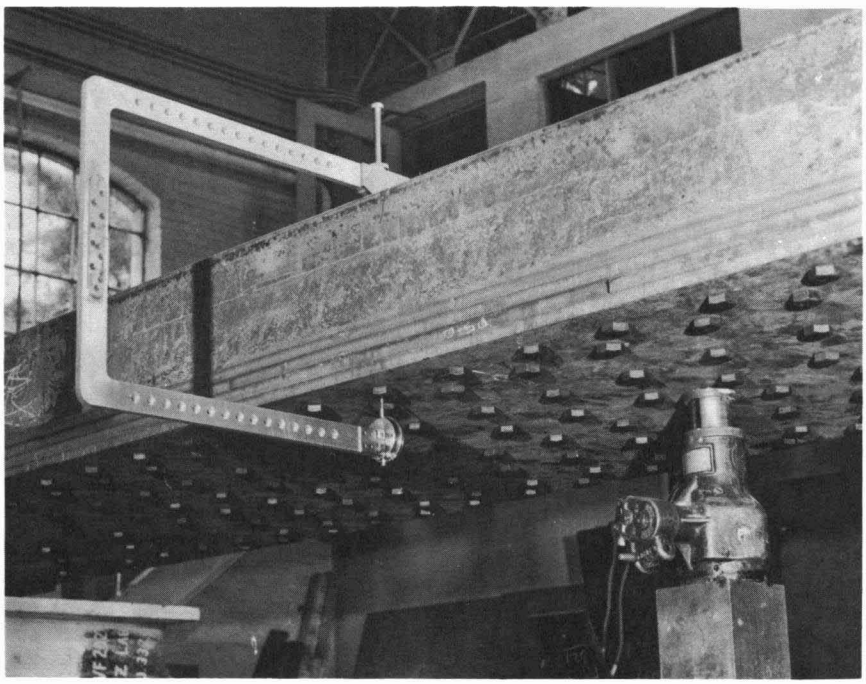

Fig. 7(2) Measuring the Changes in Bolt Length with Extensometer

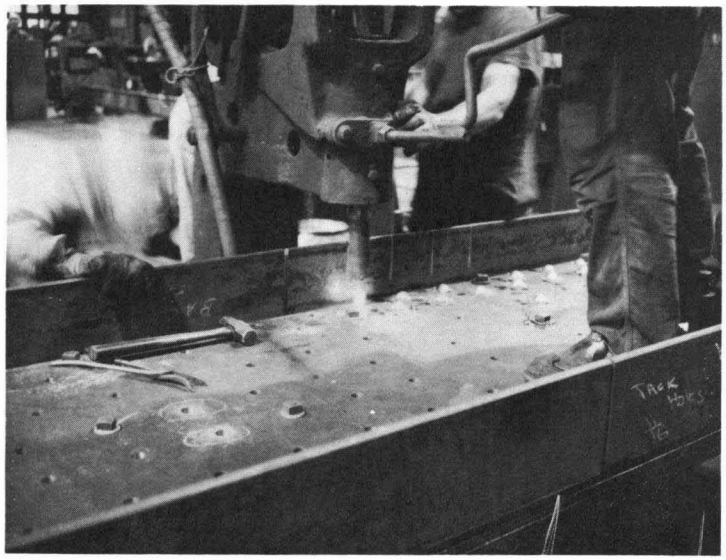

Fig. 8 Riveting-up to Simulated Joint

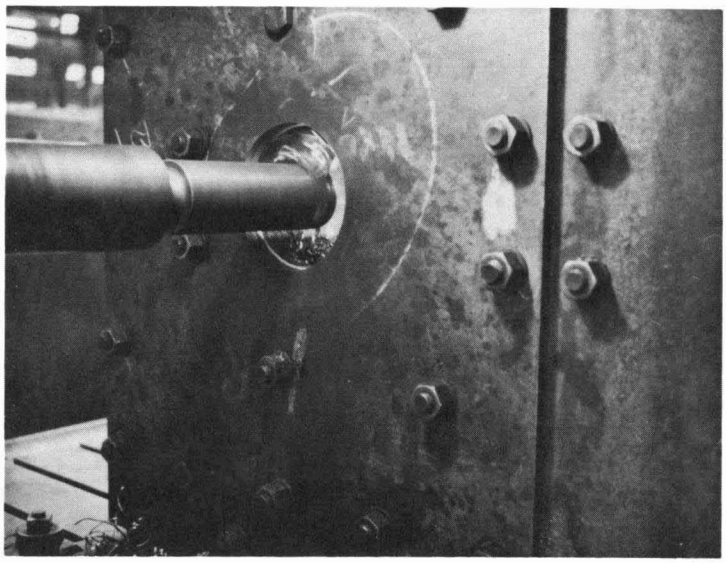

Fig. 9 Drilling 10-in. Pin Hole in Simulated Joint

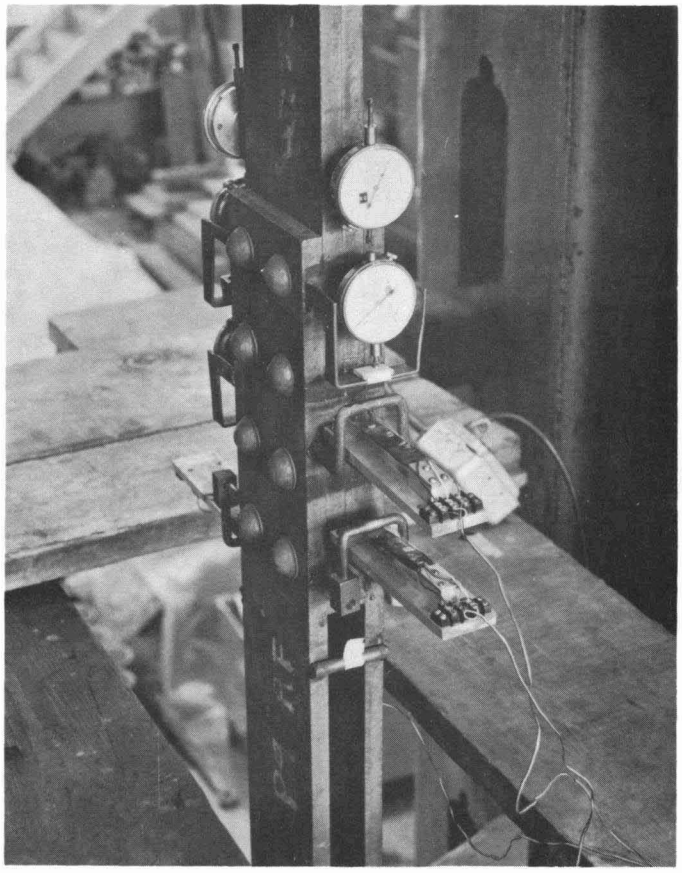

Fig. 10 Instrumentation of Control Joint

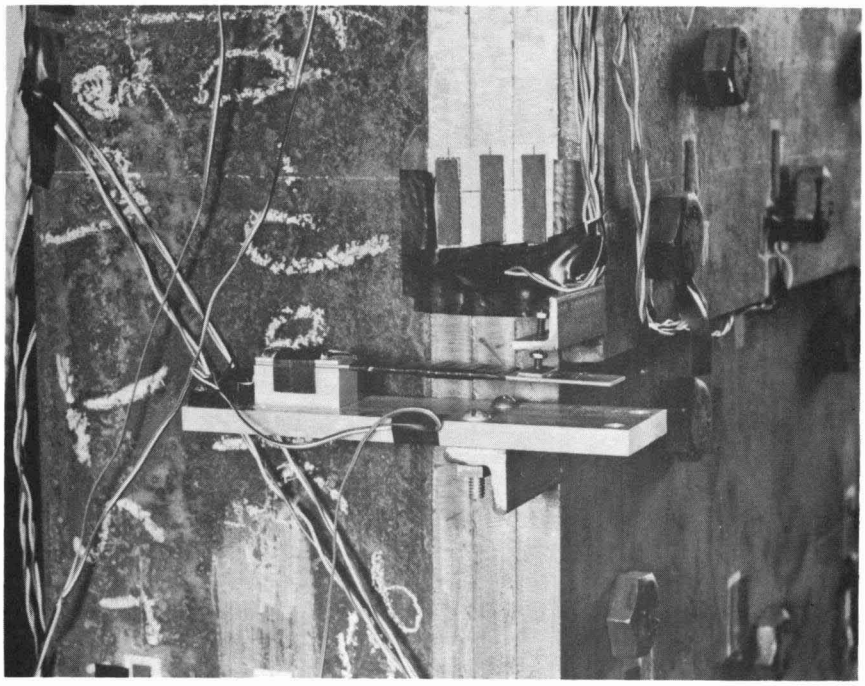

Fig. 11 Cantilever Gage

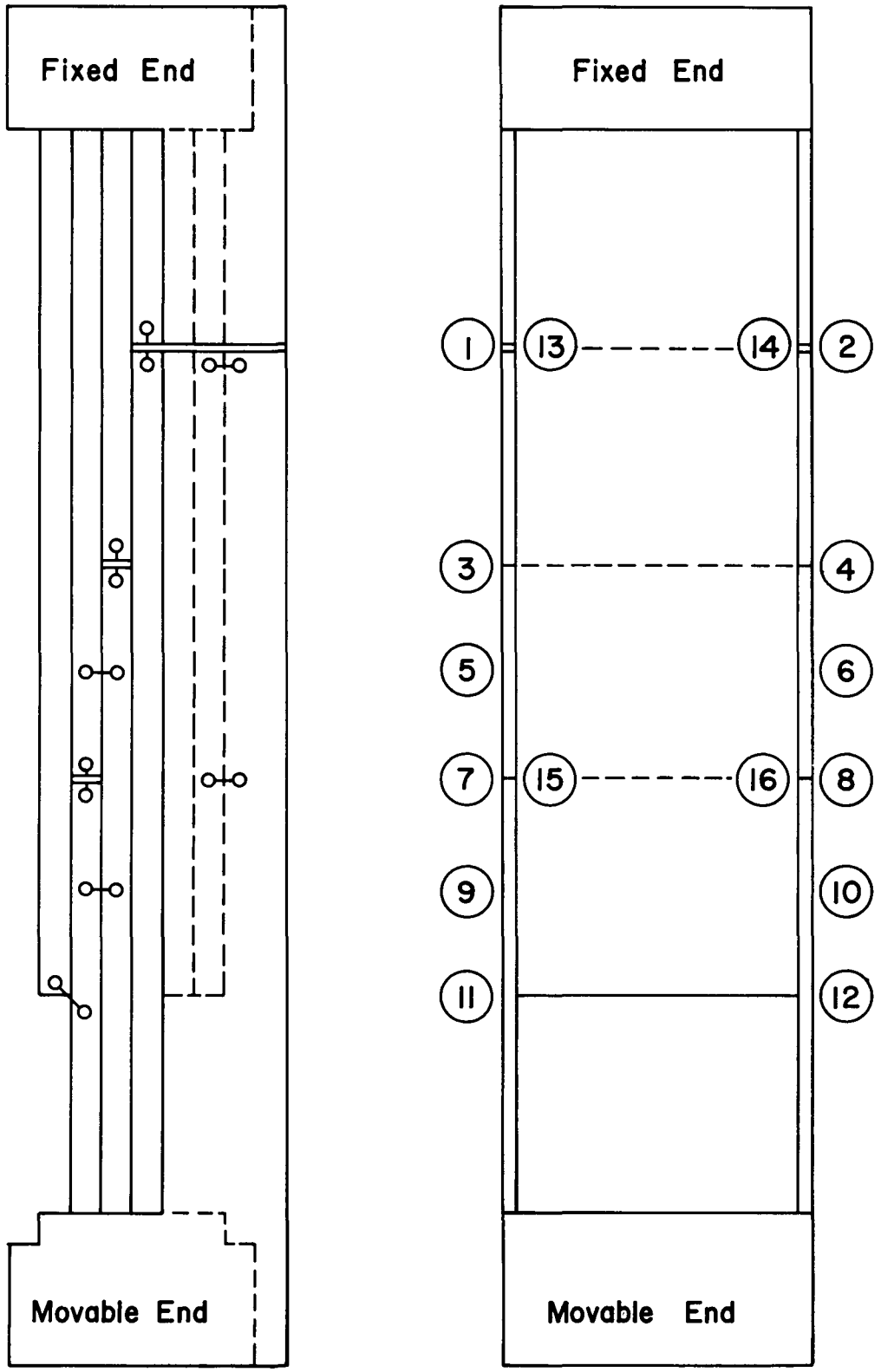

Fig. 12 Location of Local Slip Measuring for Bolted Joint

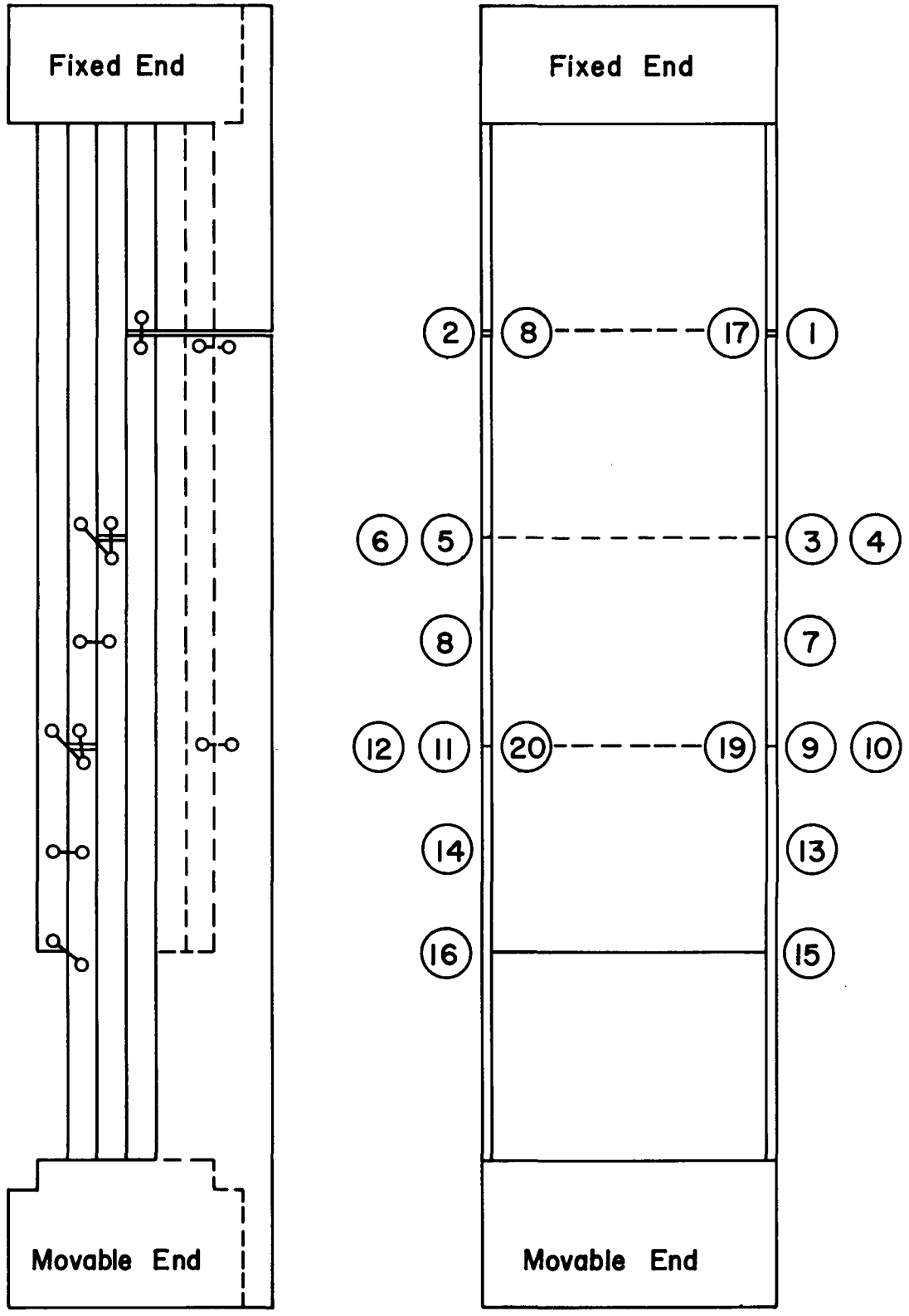

Fig. 13 Location of Local Slip Measuring for Riveted Joint

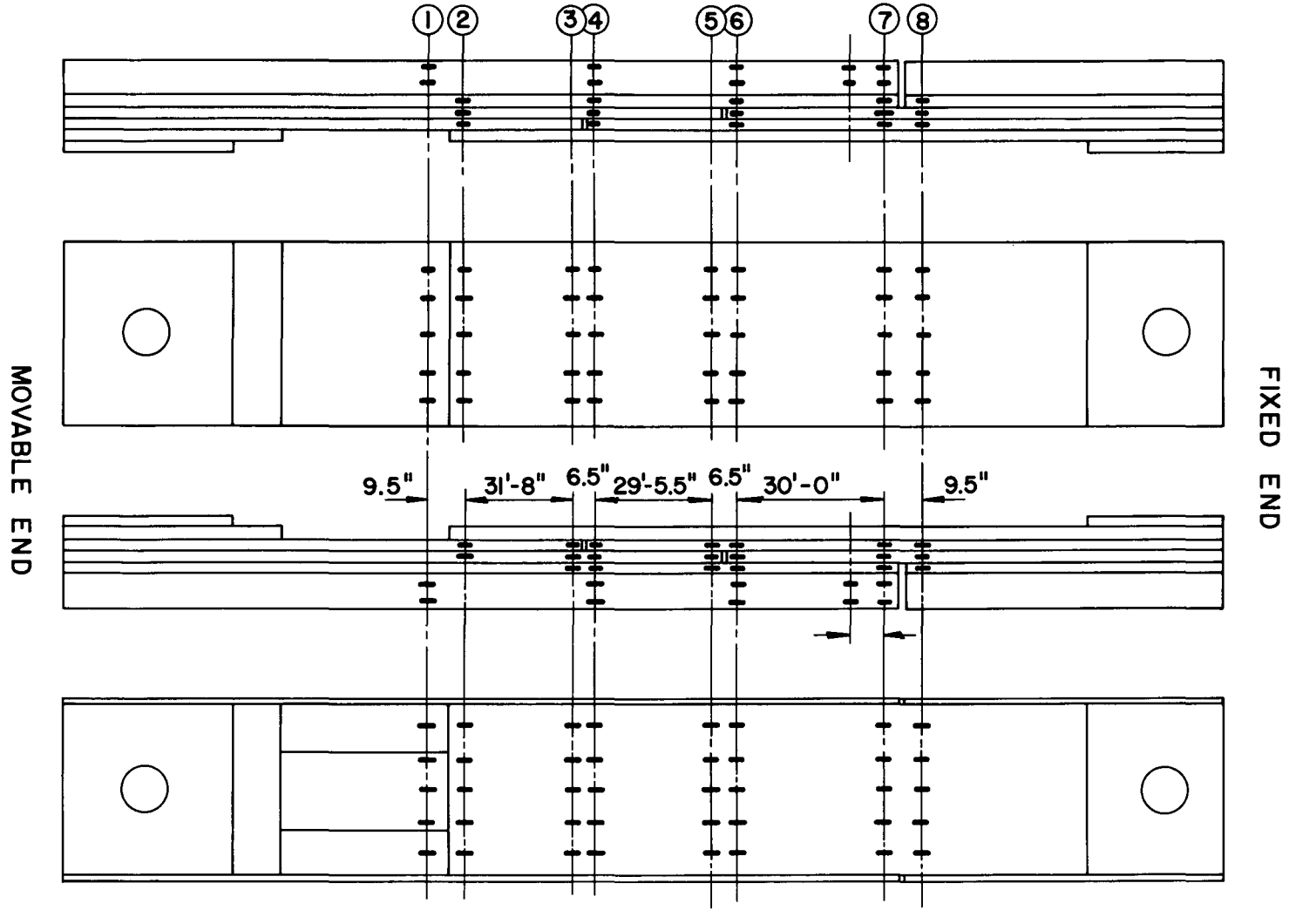

Fig. 14 Location of SR4 Strain Gages for Simulated Joint

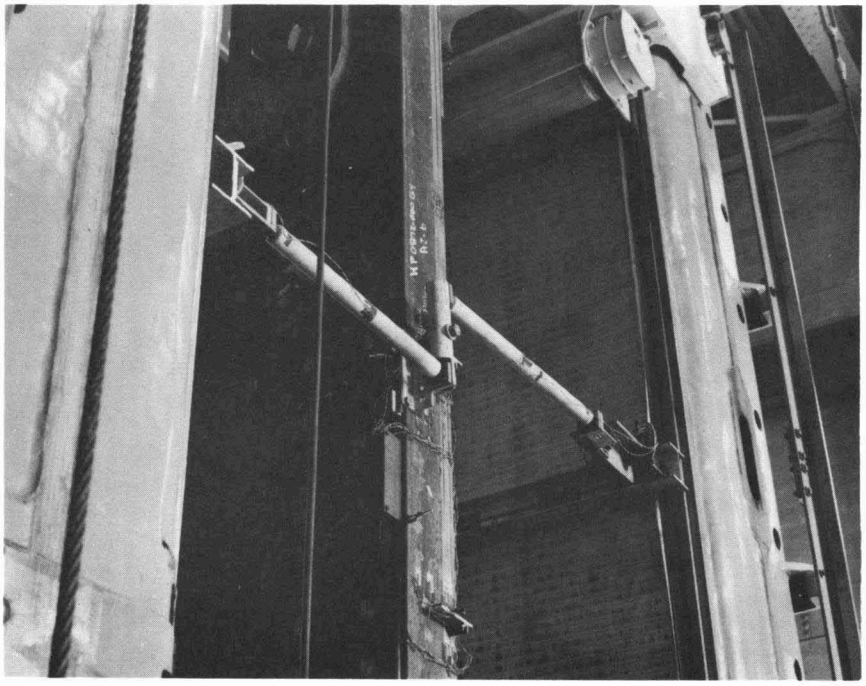

Fig. 15 Lateral Bracing

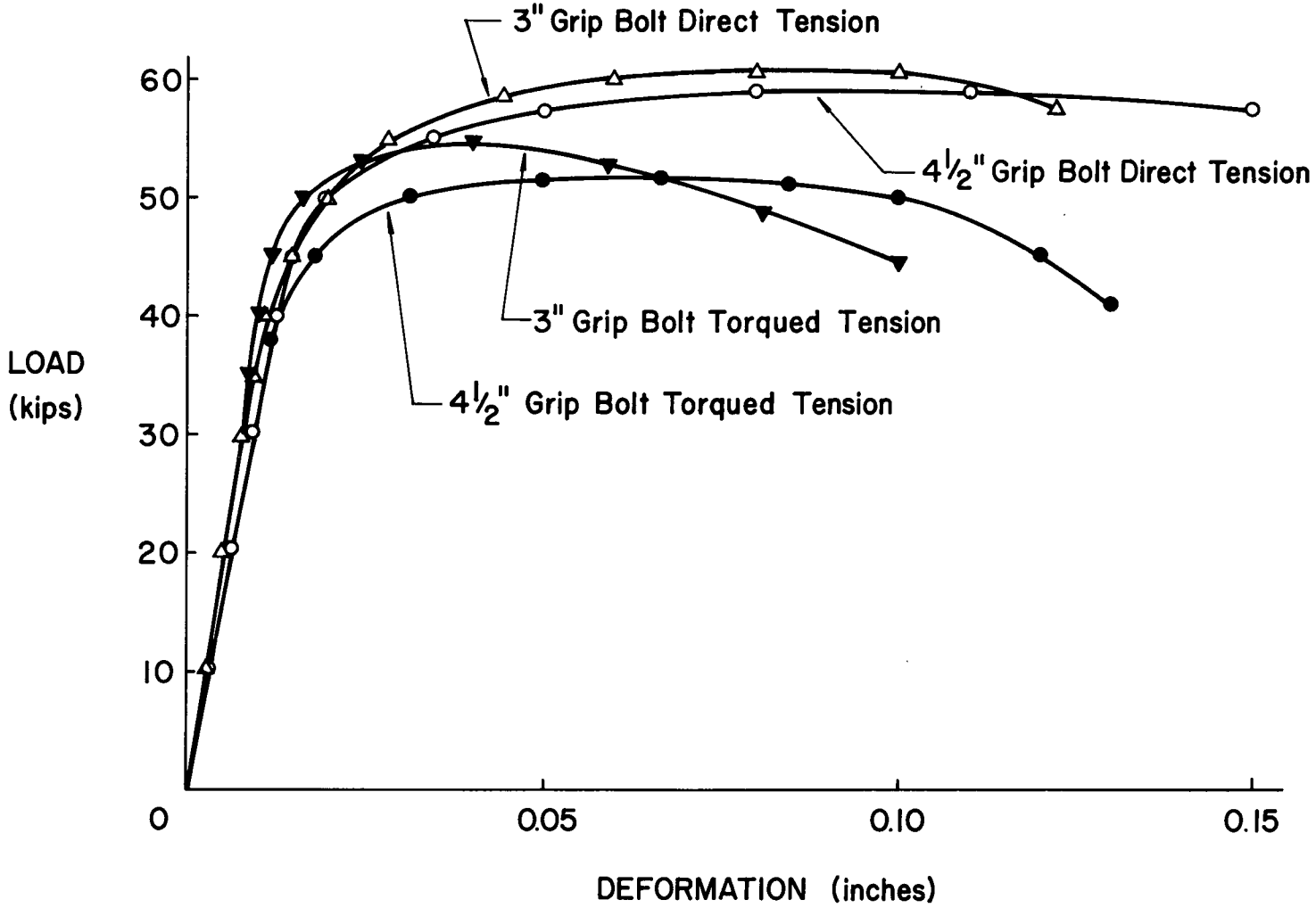

Fig. 16 A325 Bolt Tension Calibration Curves

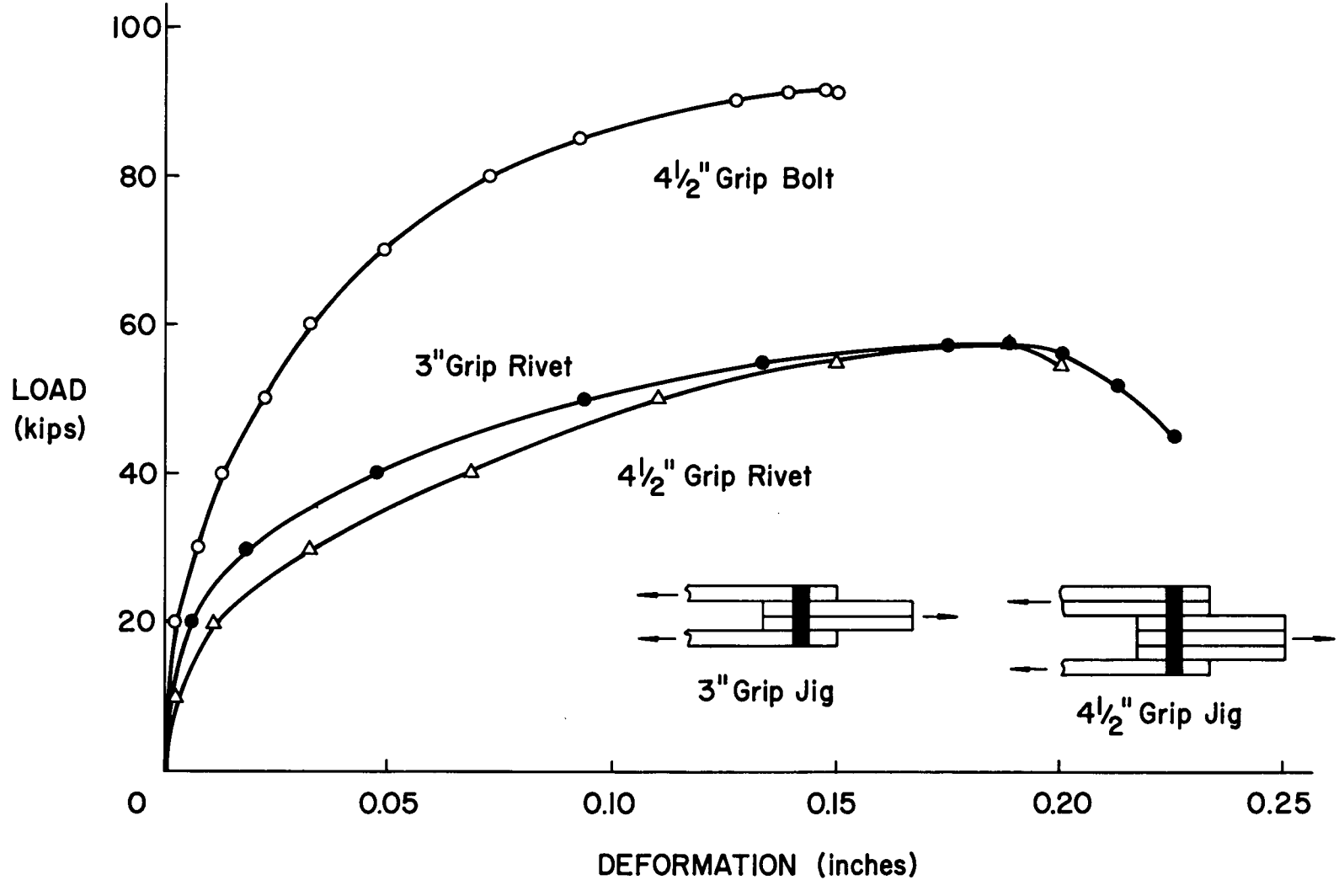

Fig. 17 Load- Deformation Curves of Shear Jig Tests

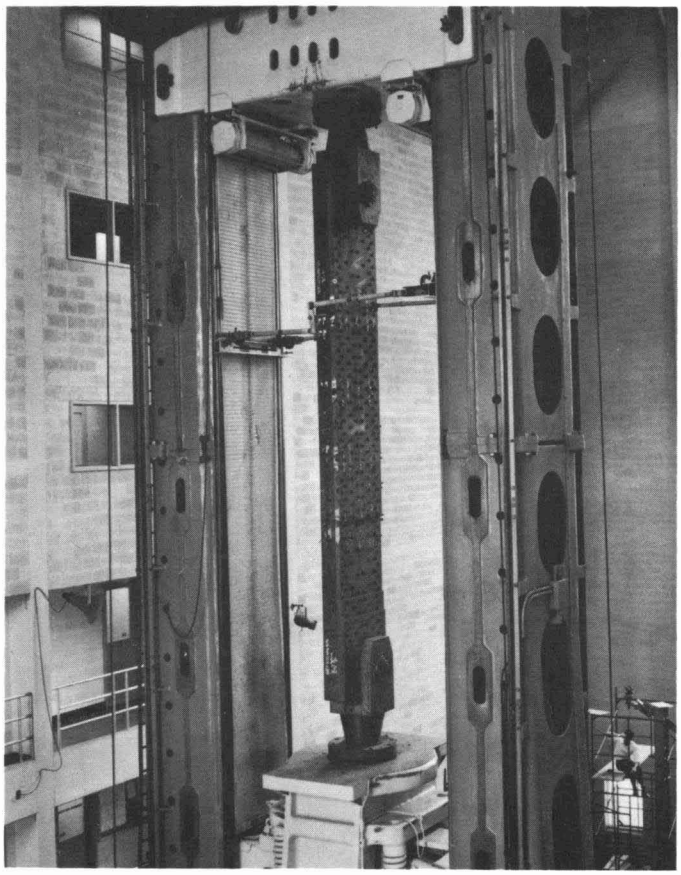

Fig. 18 Simulated Joint in a 5,000,000 lb. Machine

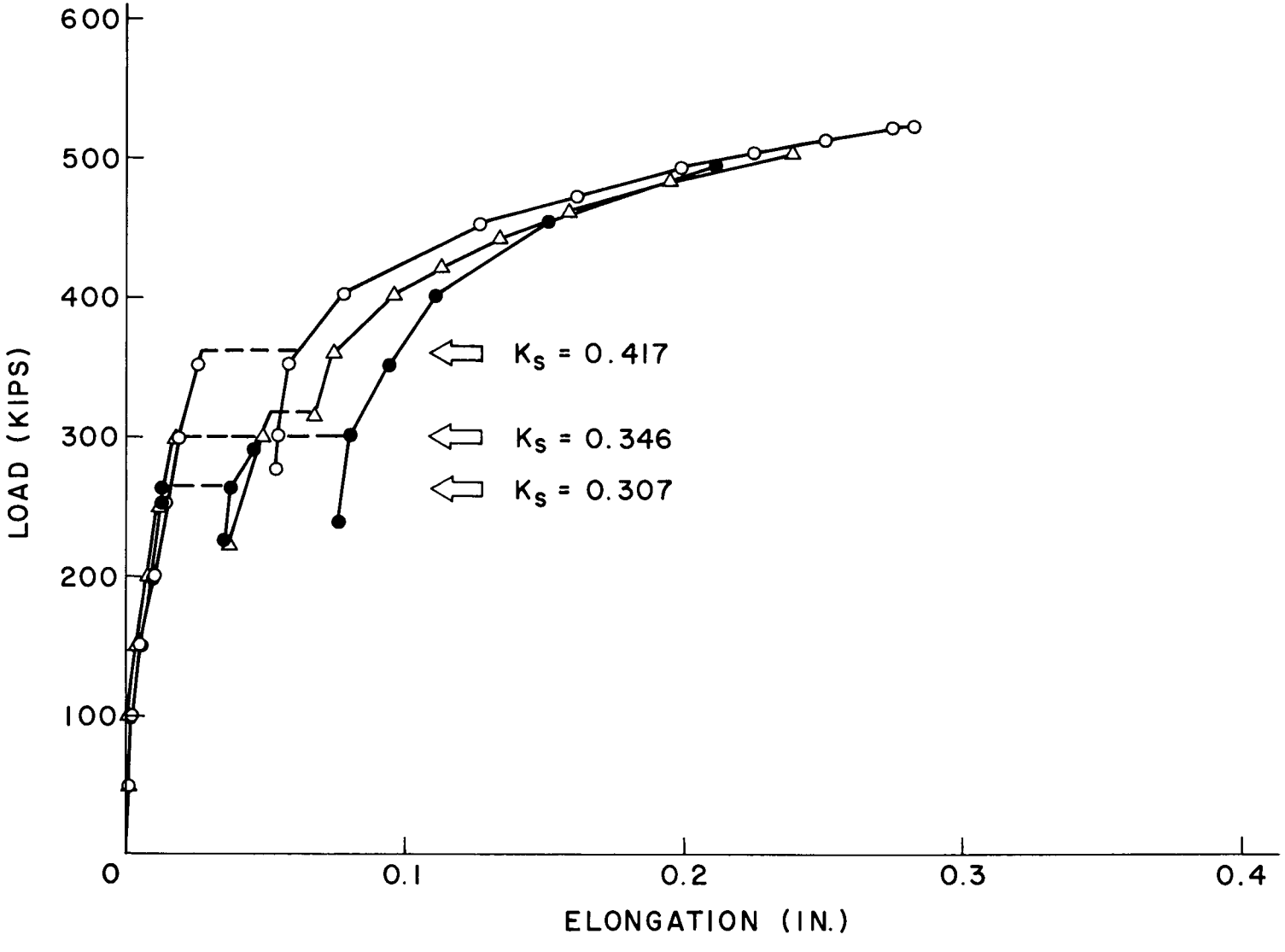

Fig. 19 Joint Elongation Curves of Bolted Control Joints

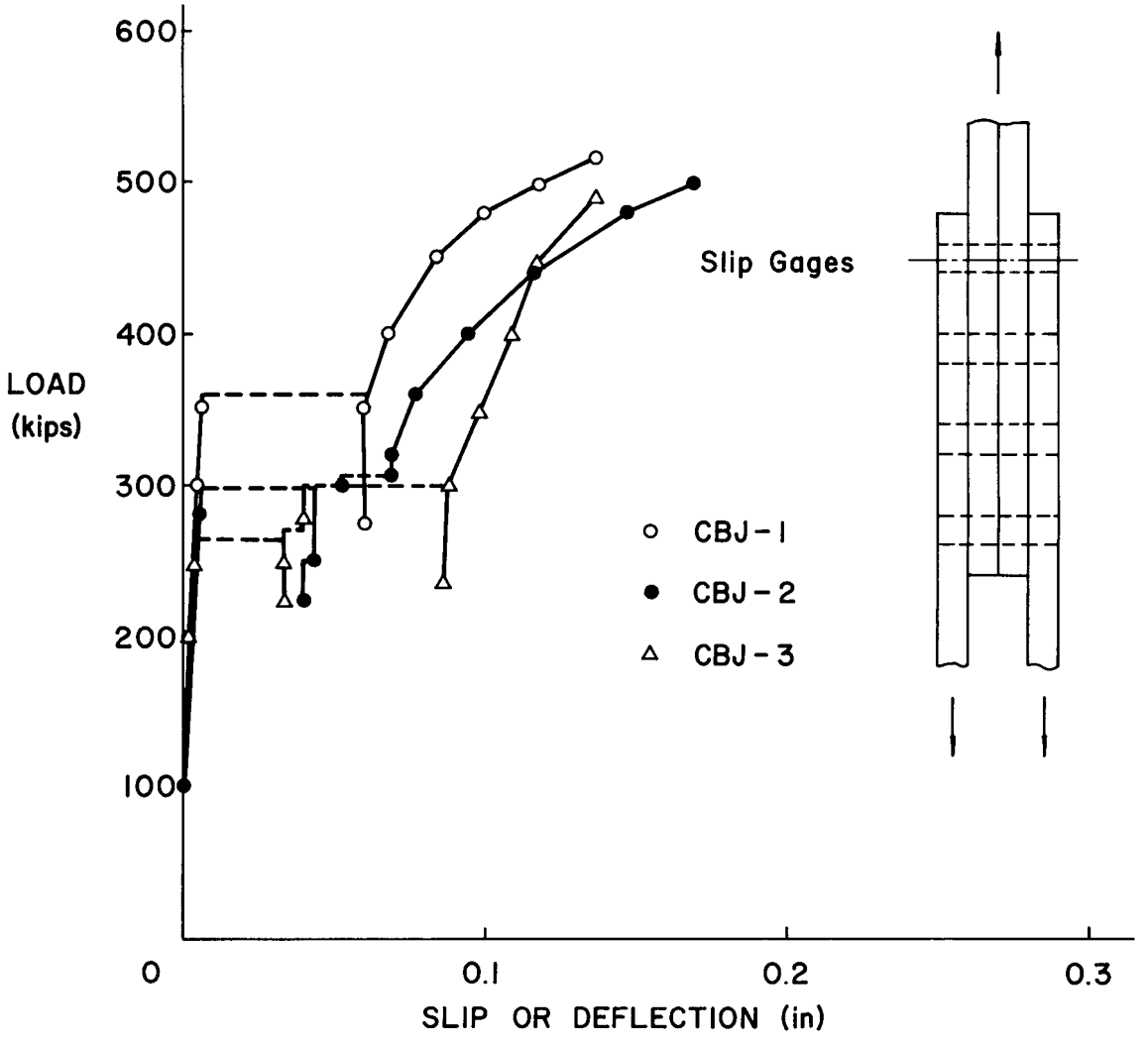

Fig. 20 Local Load-Slip Curves of Control Bolted Joints

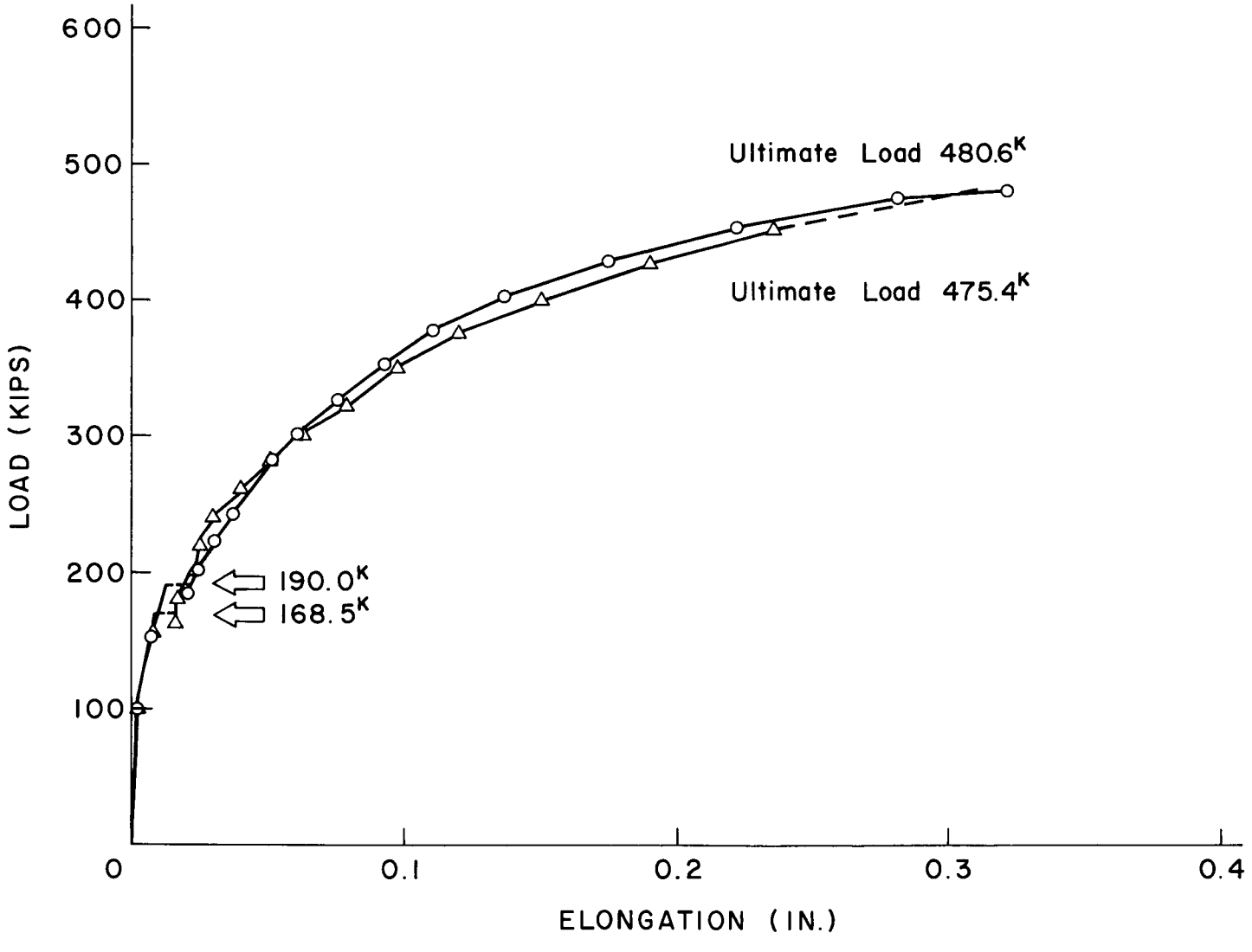

Fig. 21 Joint Elongation Curves of Riveted Control Joints

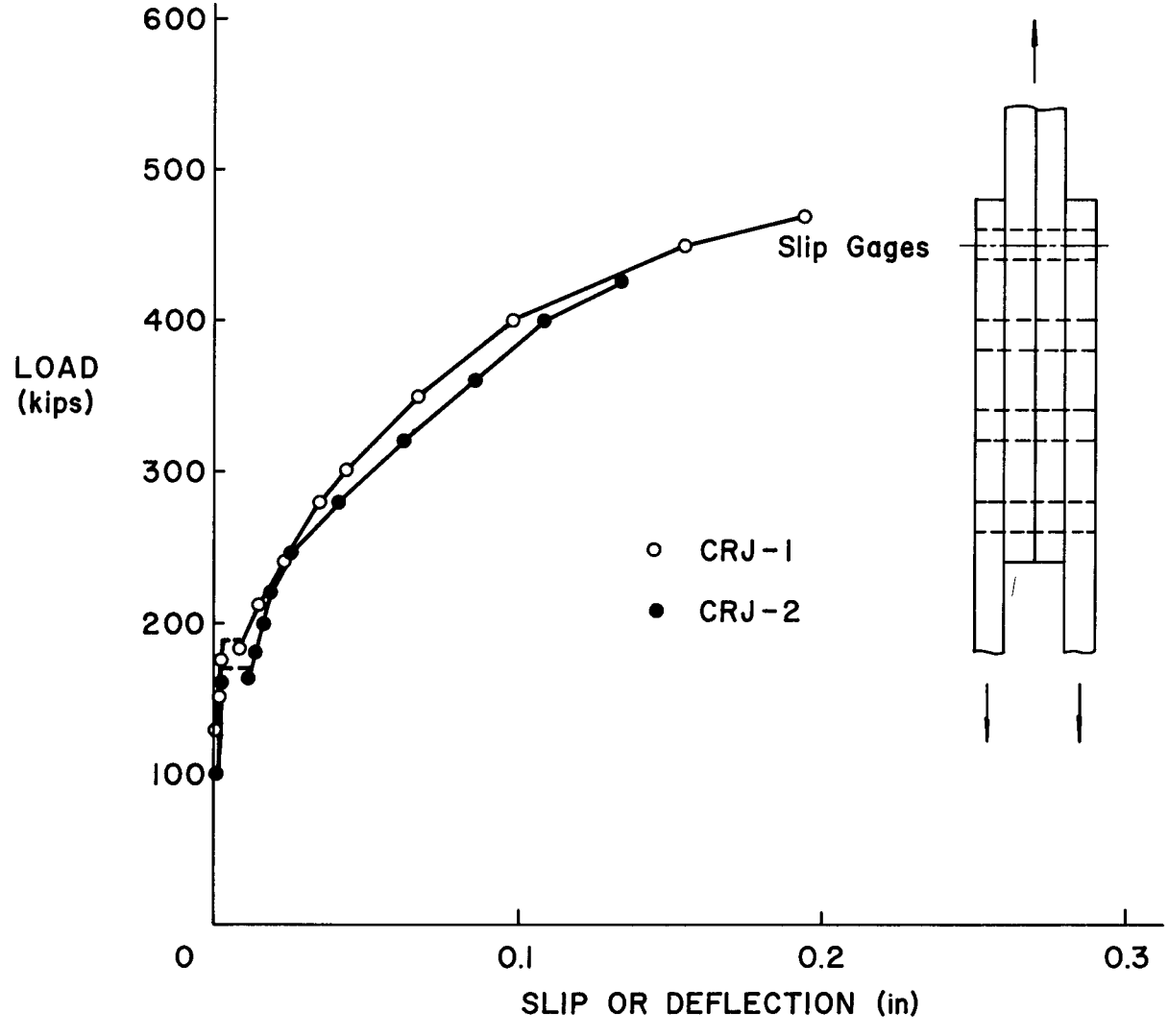

Fig. 22 Local Load-Slip Curves of Control Riveted Joints

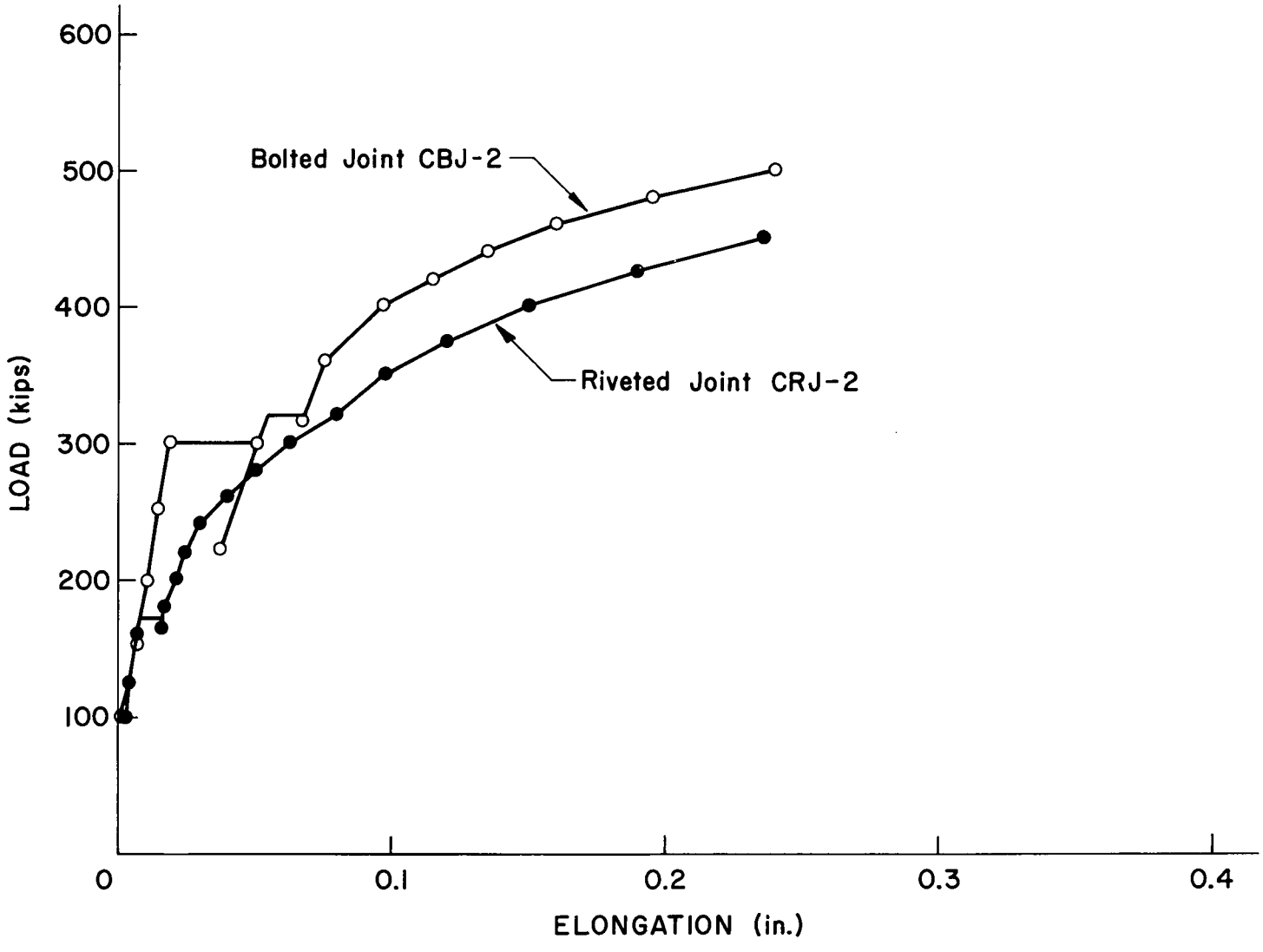

Fig. 23 Comparison of Joint Elongation Curves of Bolted and Riveted Joints

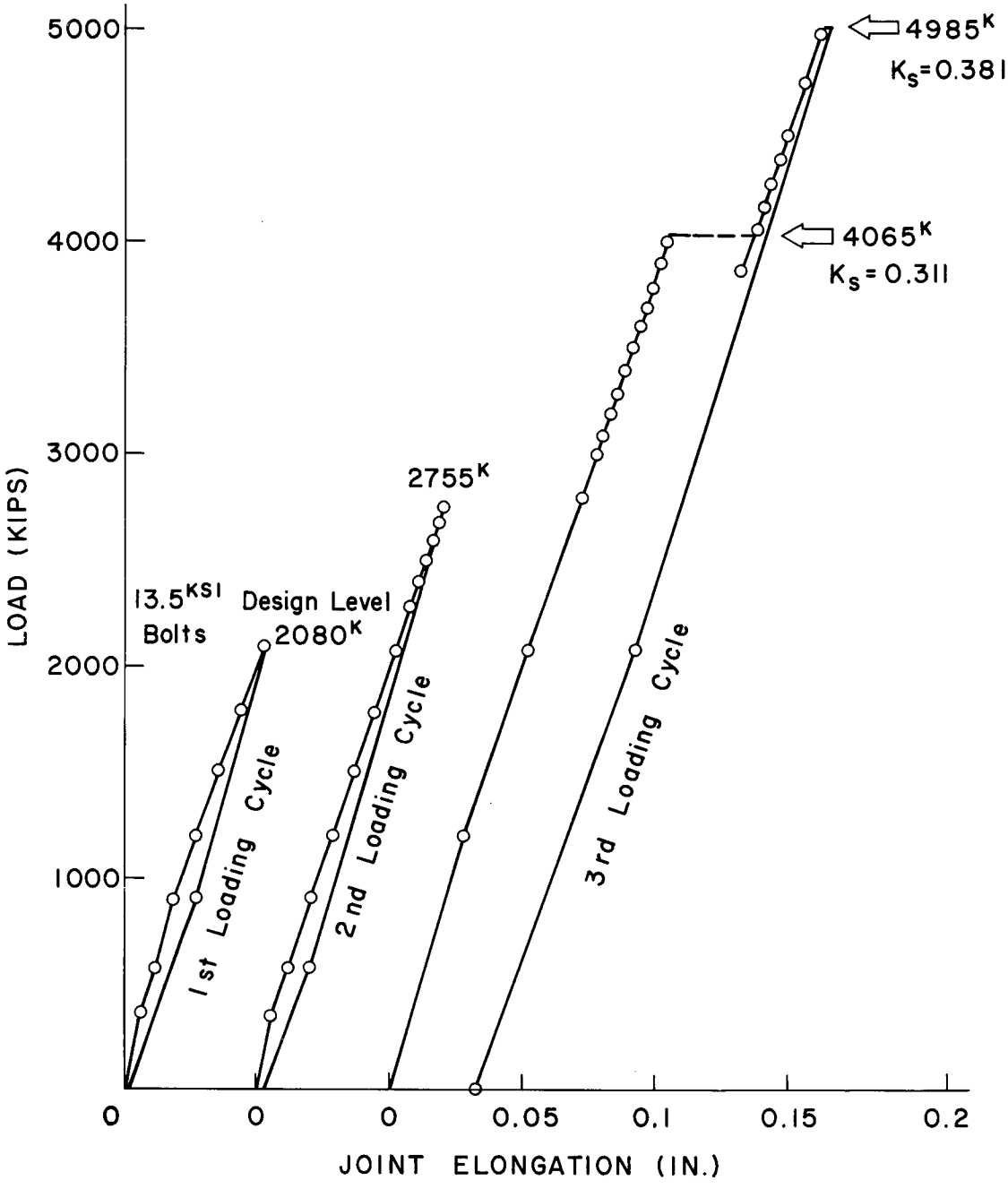

Fig. 24 Load-Deformation Curves of Bolted Joint

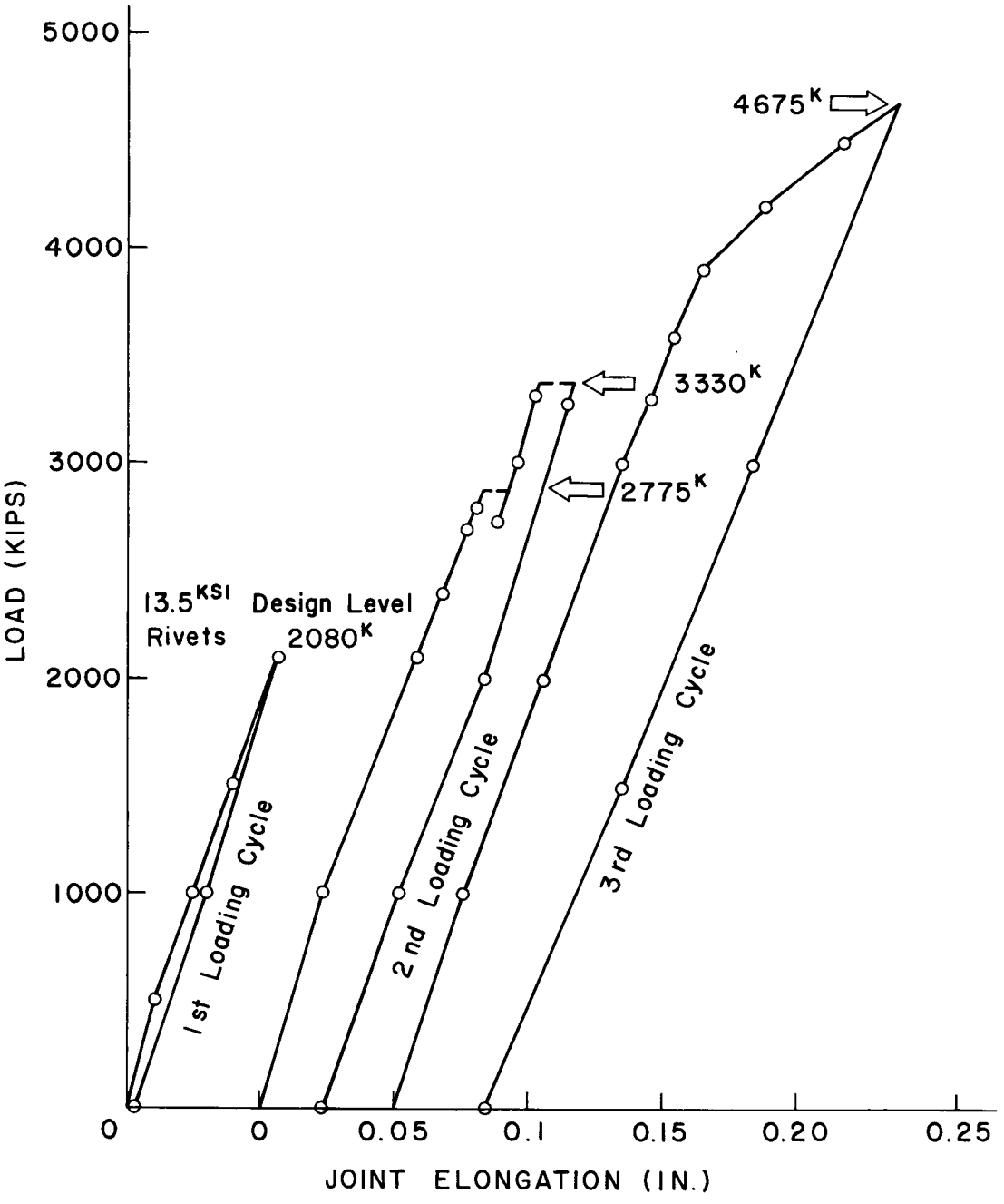

Fig. 25 Load-Deformation Curves of Riveted Joint

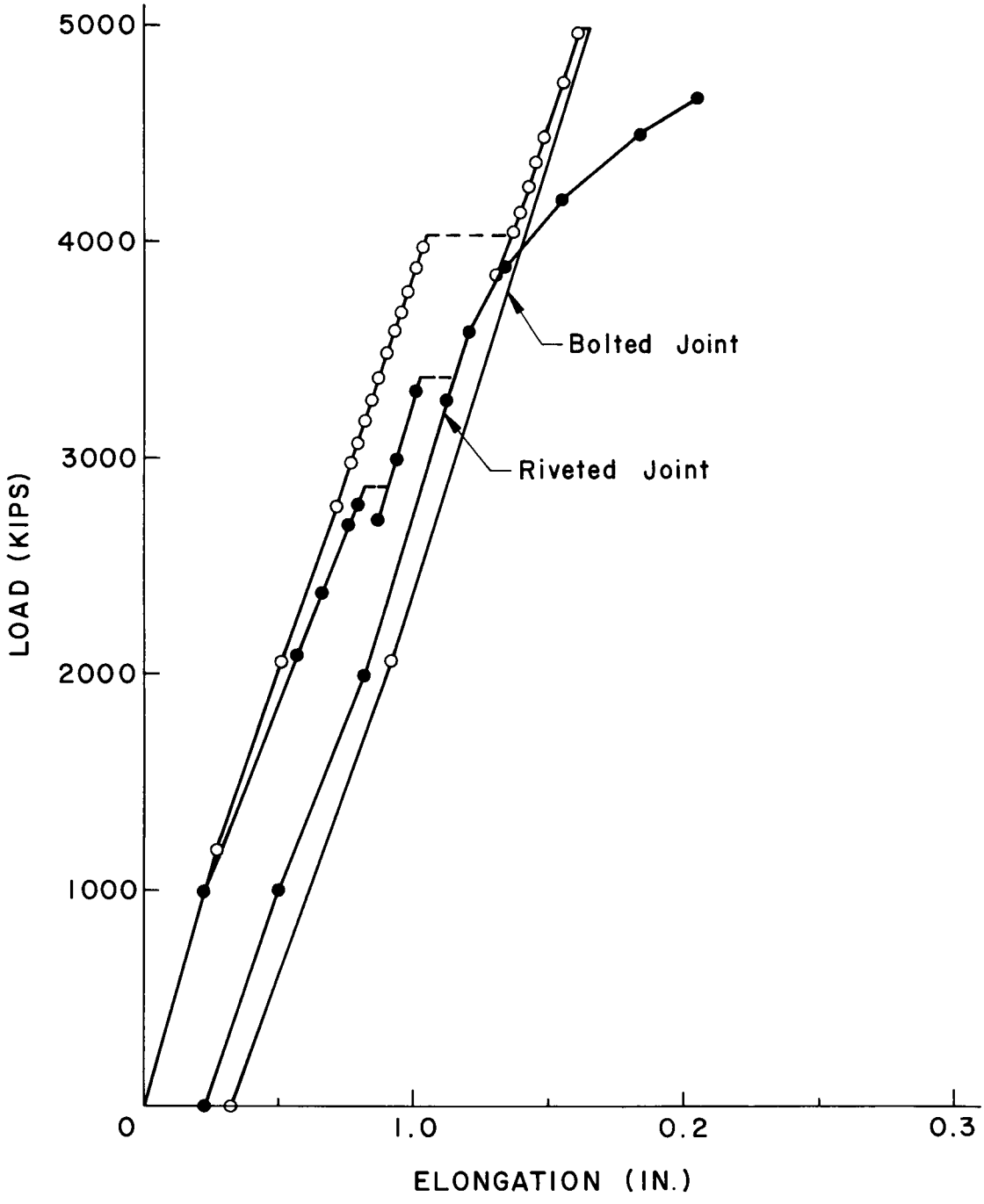

Fig. 26 Comparison of Load-Deformation Curves of Bolted and Riveted Joints

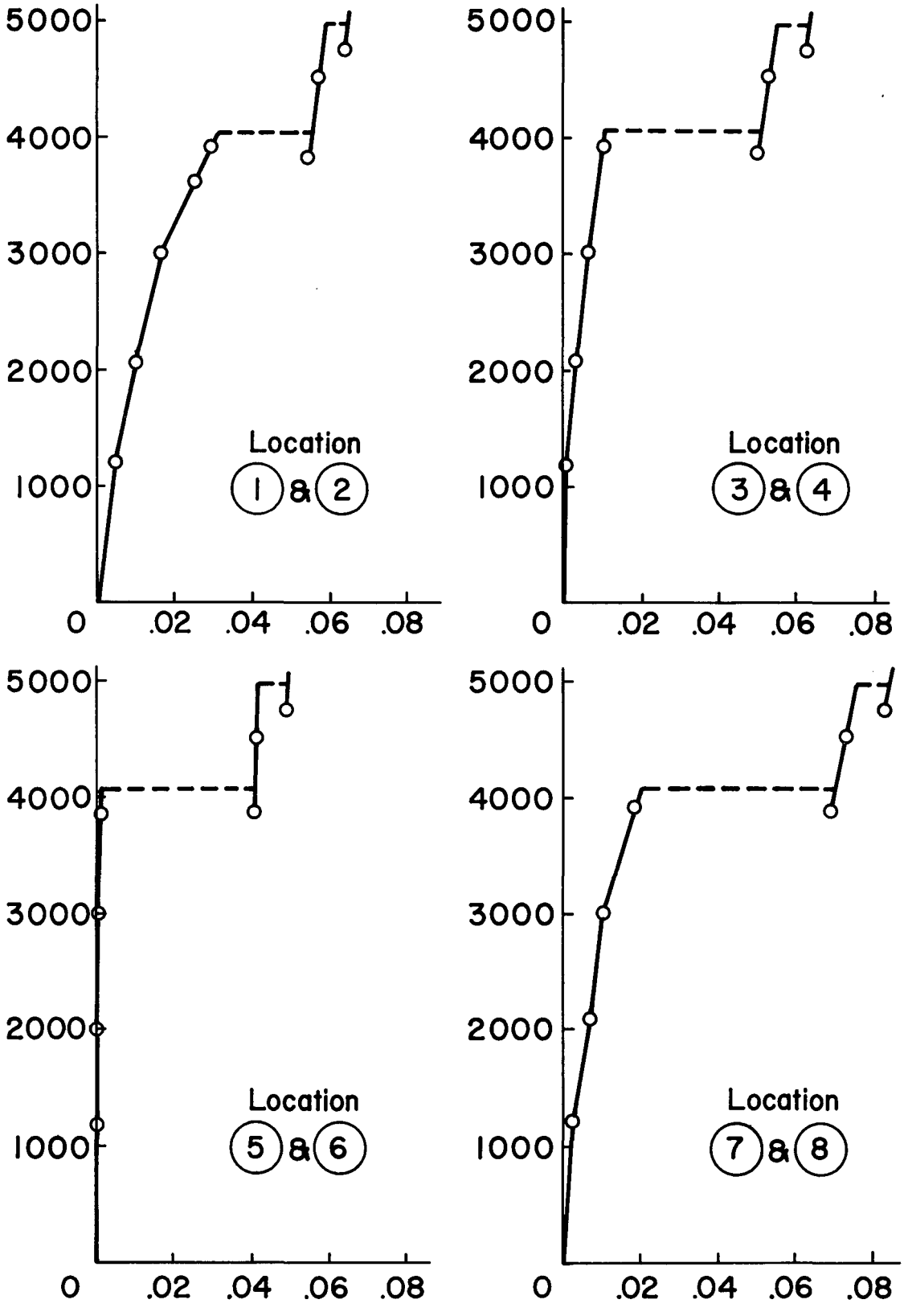

Fig. 27(1) Local Slip Behaviors of Large Bolted Joints

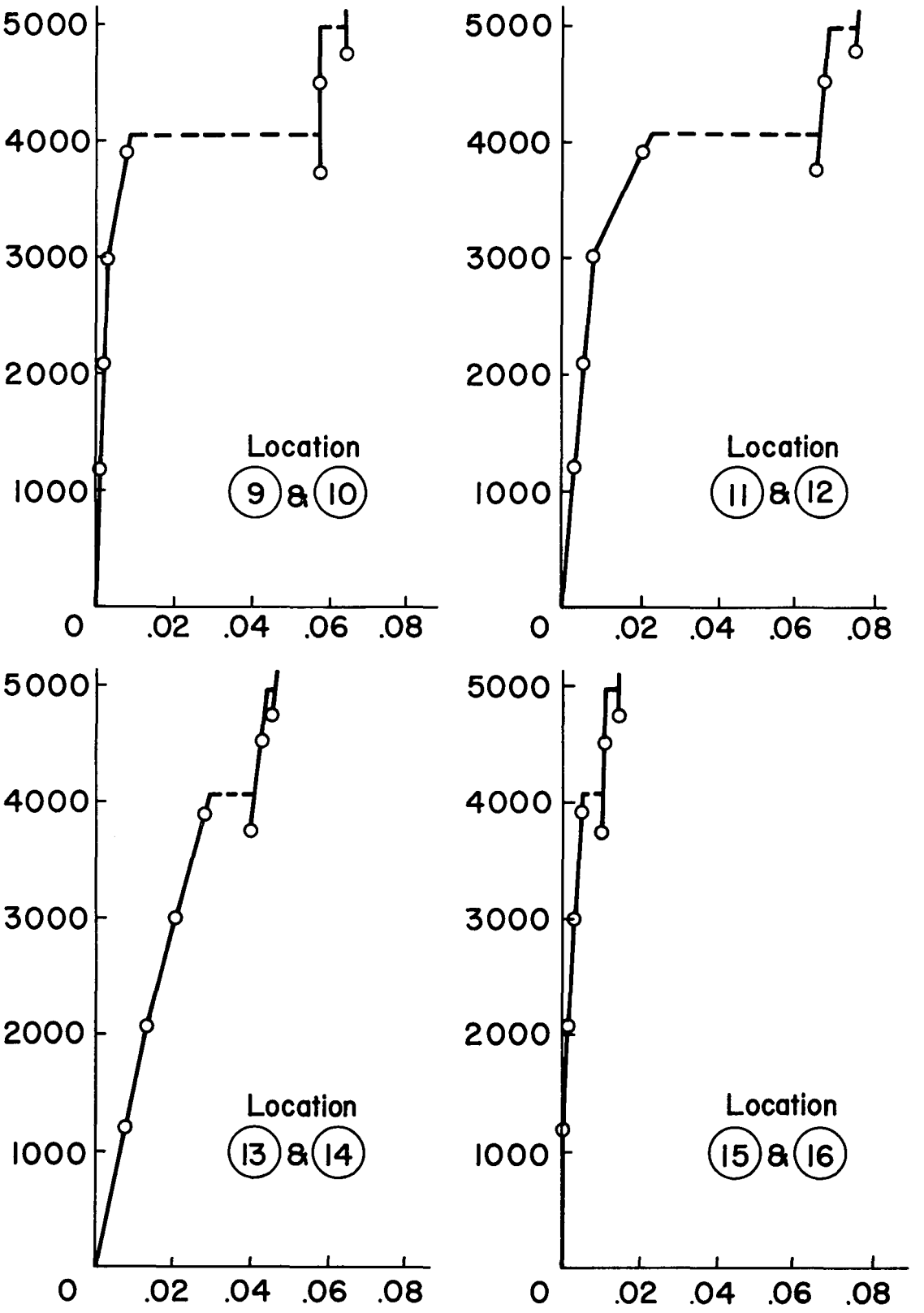

Fig. 27(2) Local Slip Behaviors of Large Bolted Joints

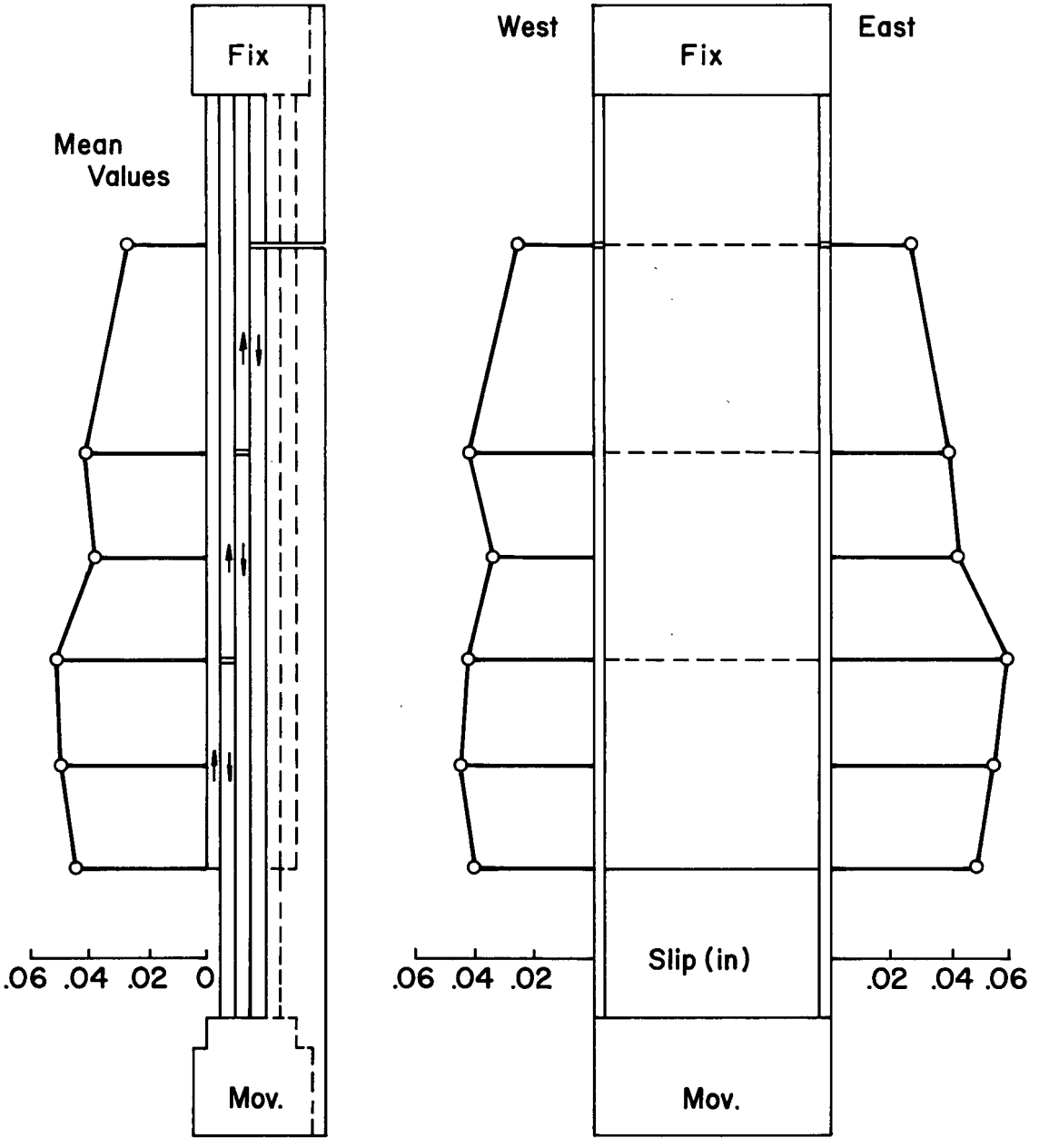

Fig. 28 Major Slip Distribution of Bolted Joint

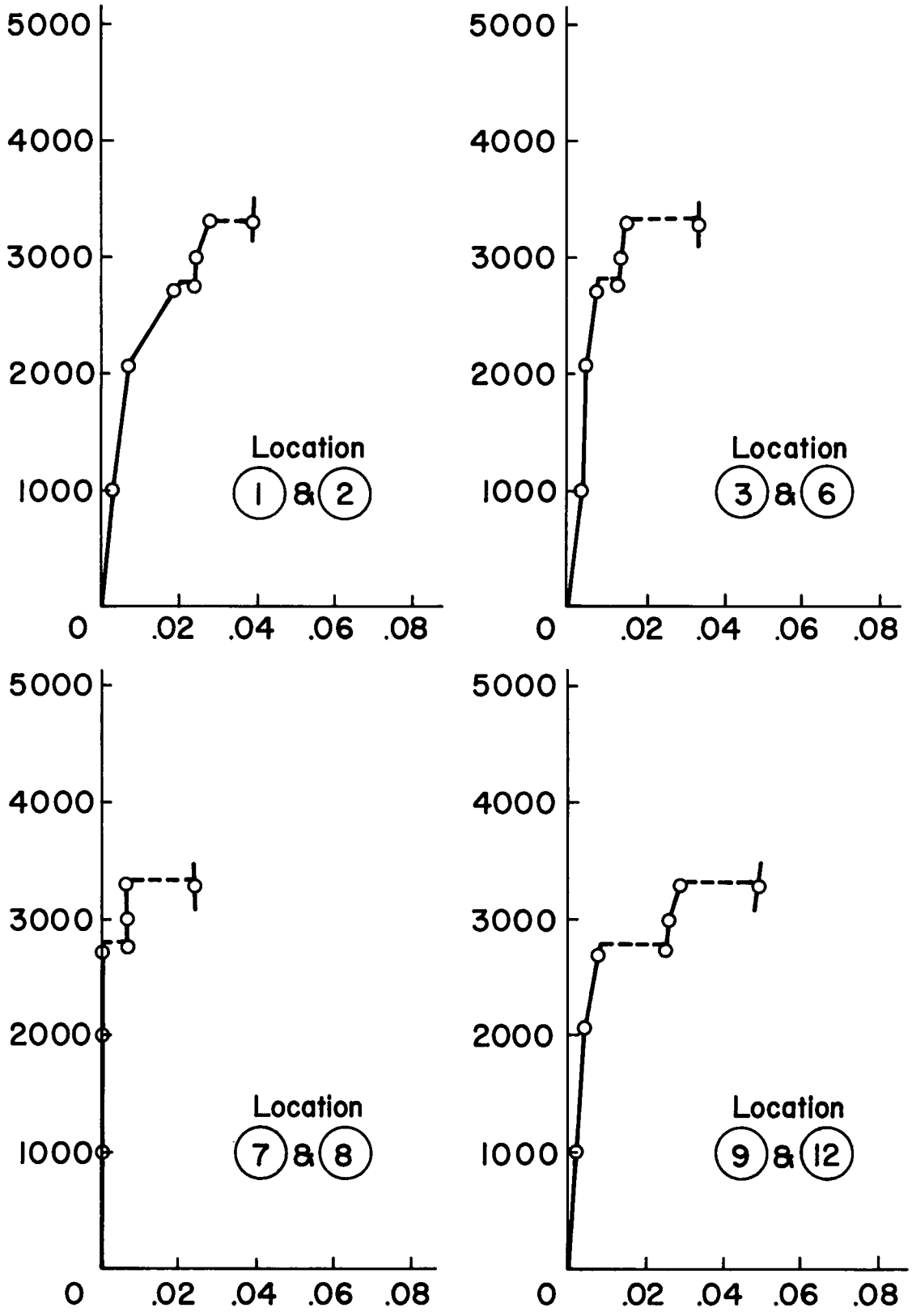

Fig. 29(1) Local Slip Behaviors of Large Riveted Joint

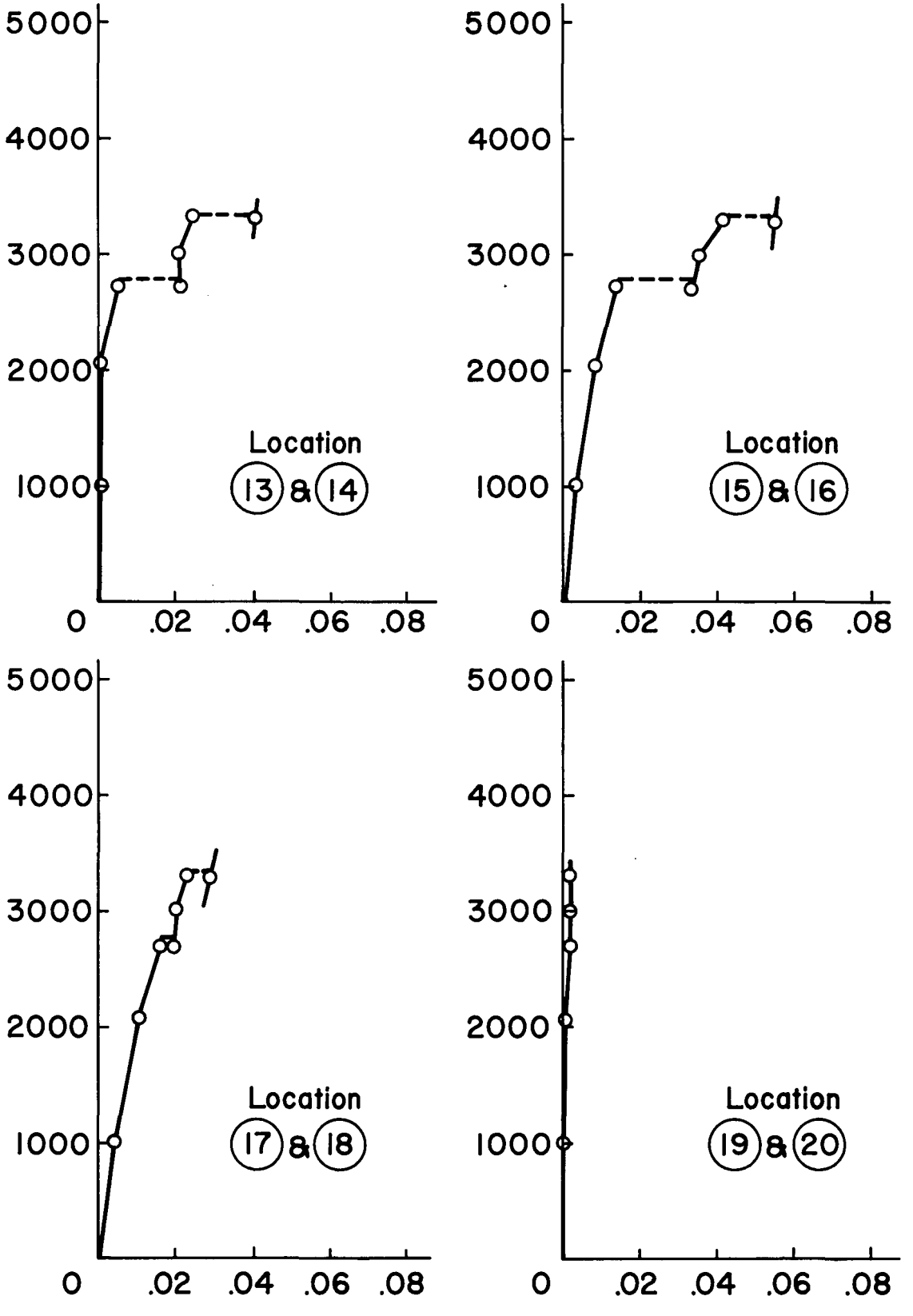

Fig. 29(2) Local Slip Behaviors of Large Riveted Joint

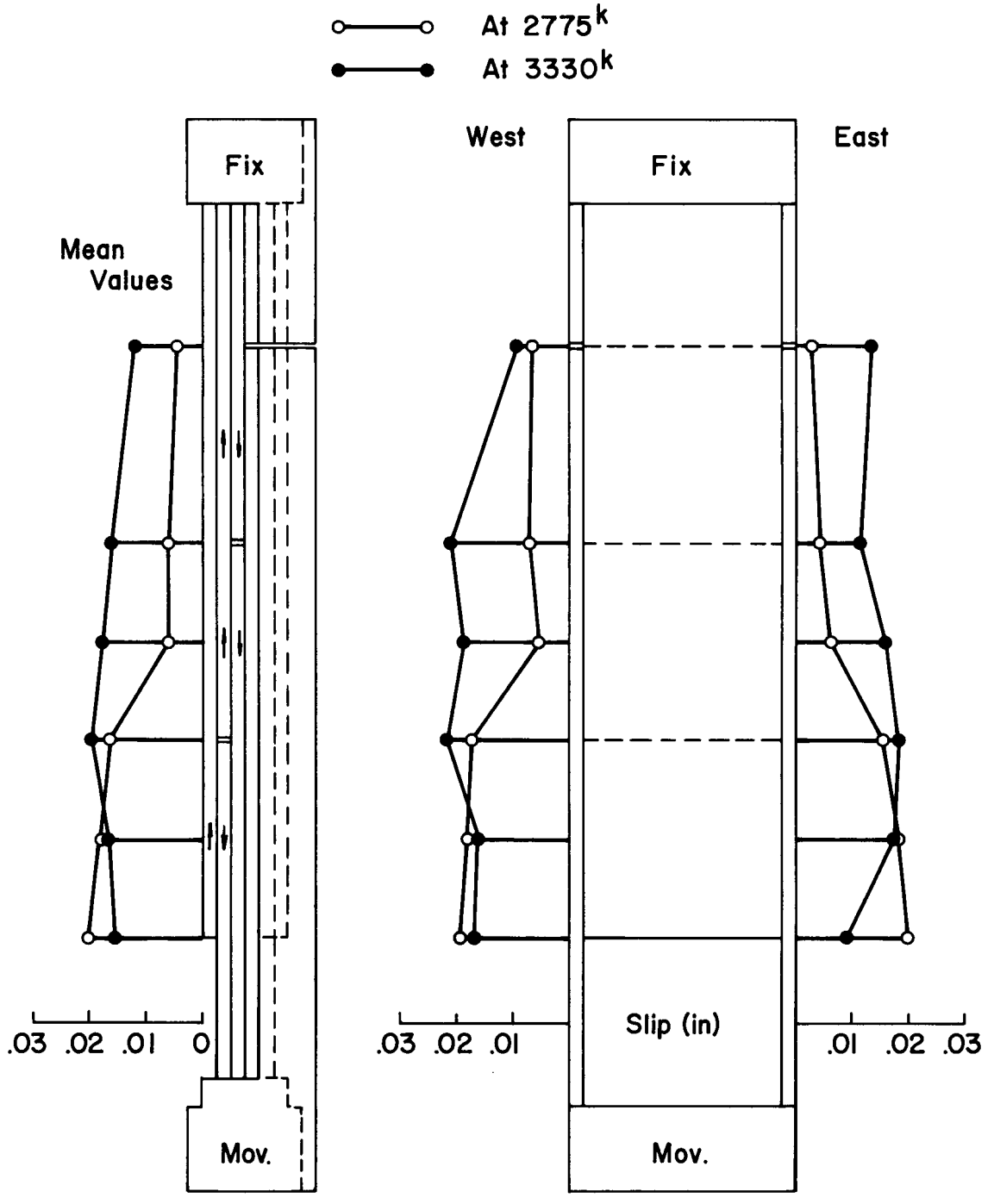

Fig. 30 Major Slip Distribution of Riveted Joint

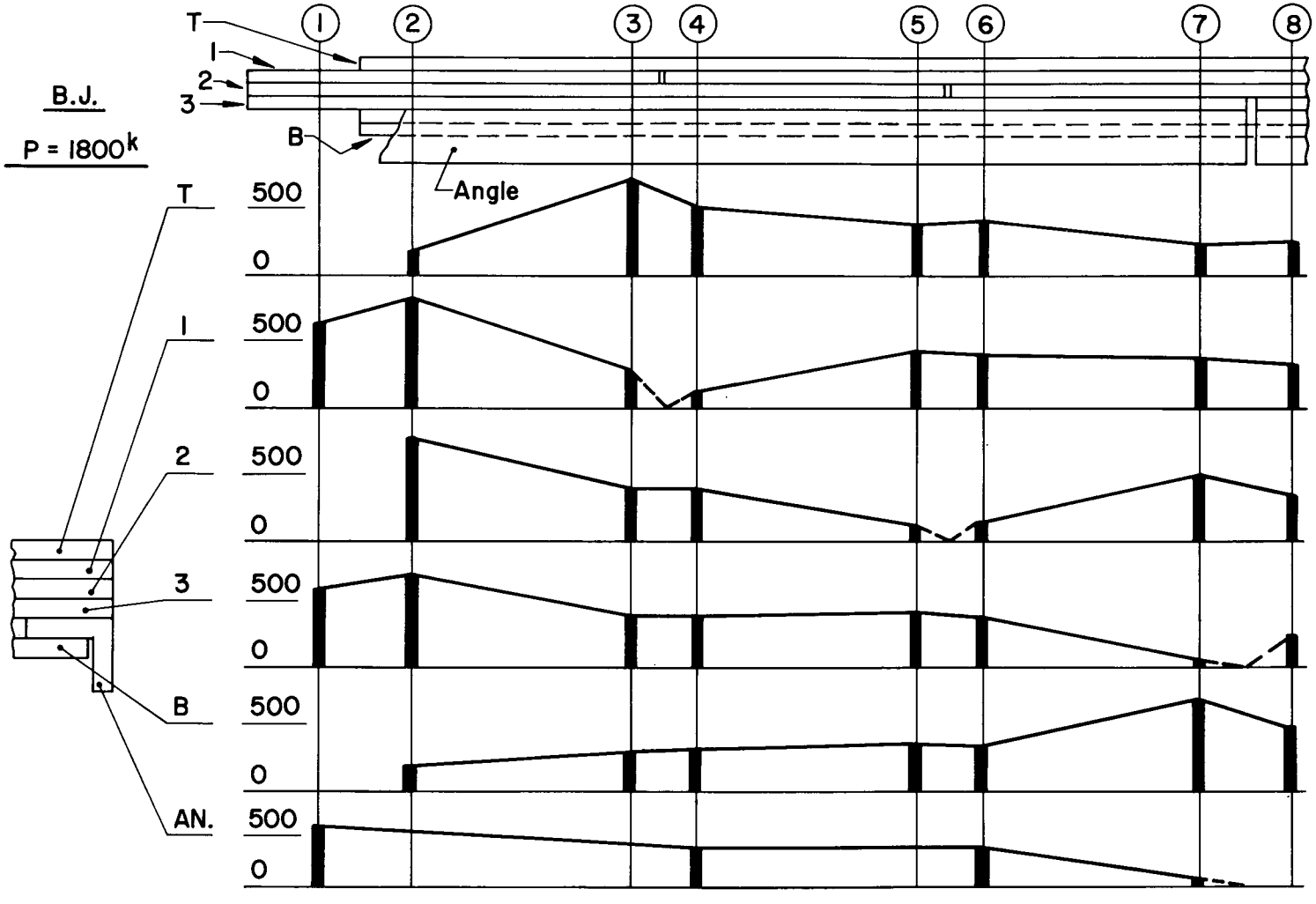

Fig. 31 Strain Distribution in Plates and Angles of Large Bolted Joint

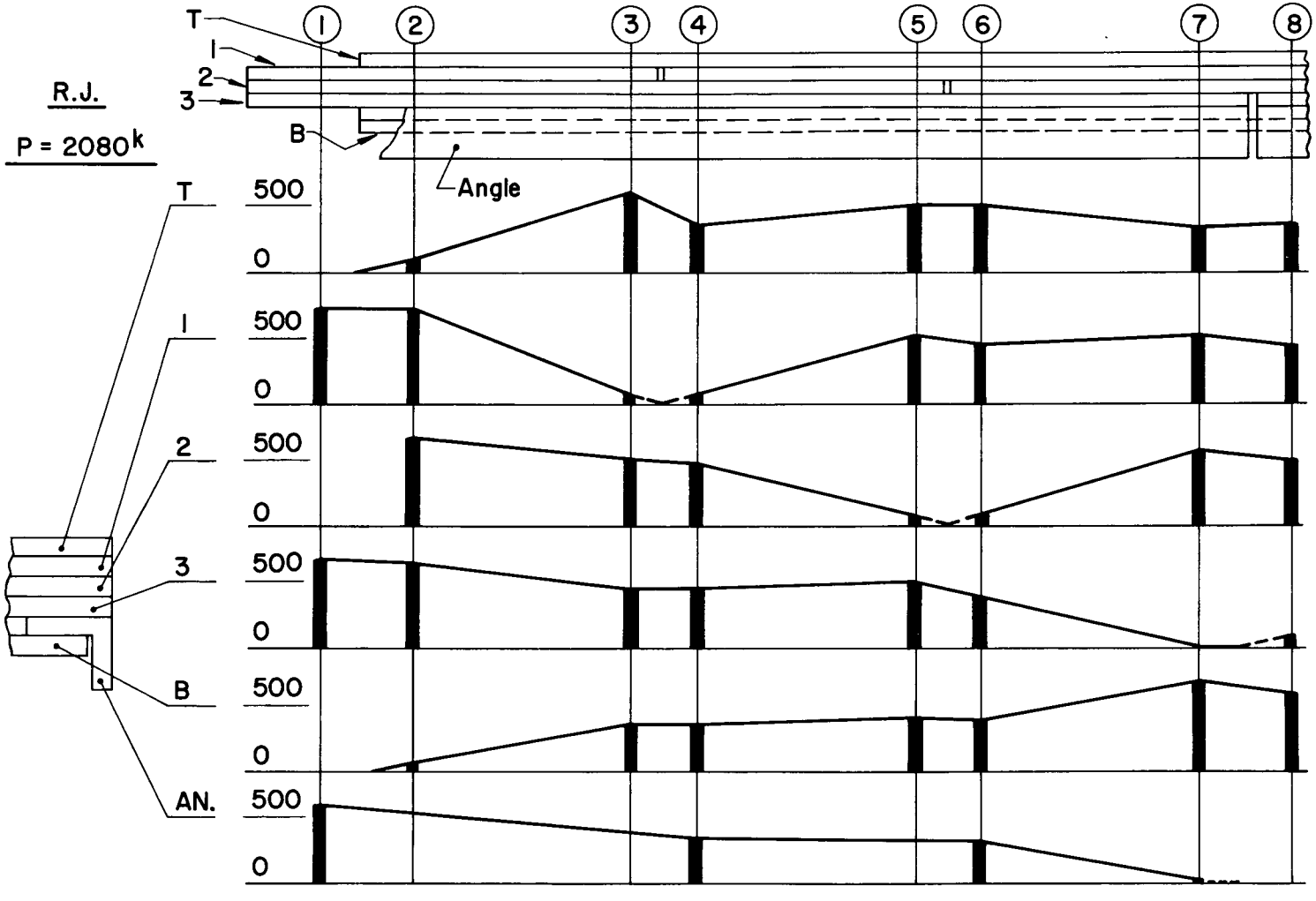

Fig. 32 Strain Distribution in Plates and Angles of Large Riveted Joint

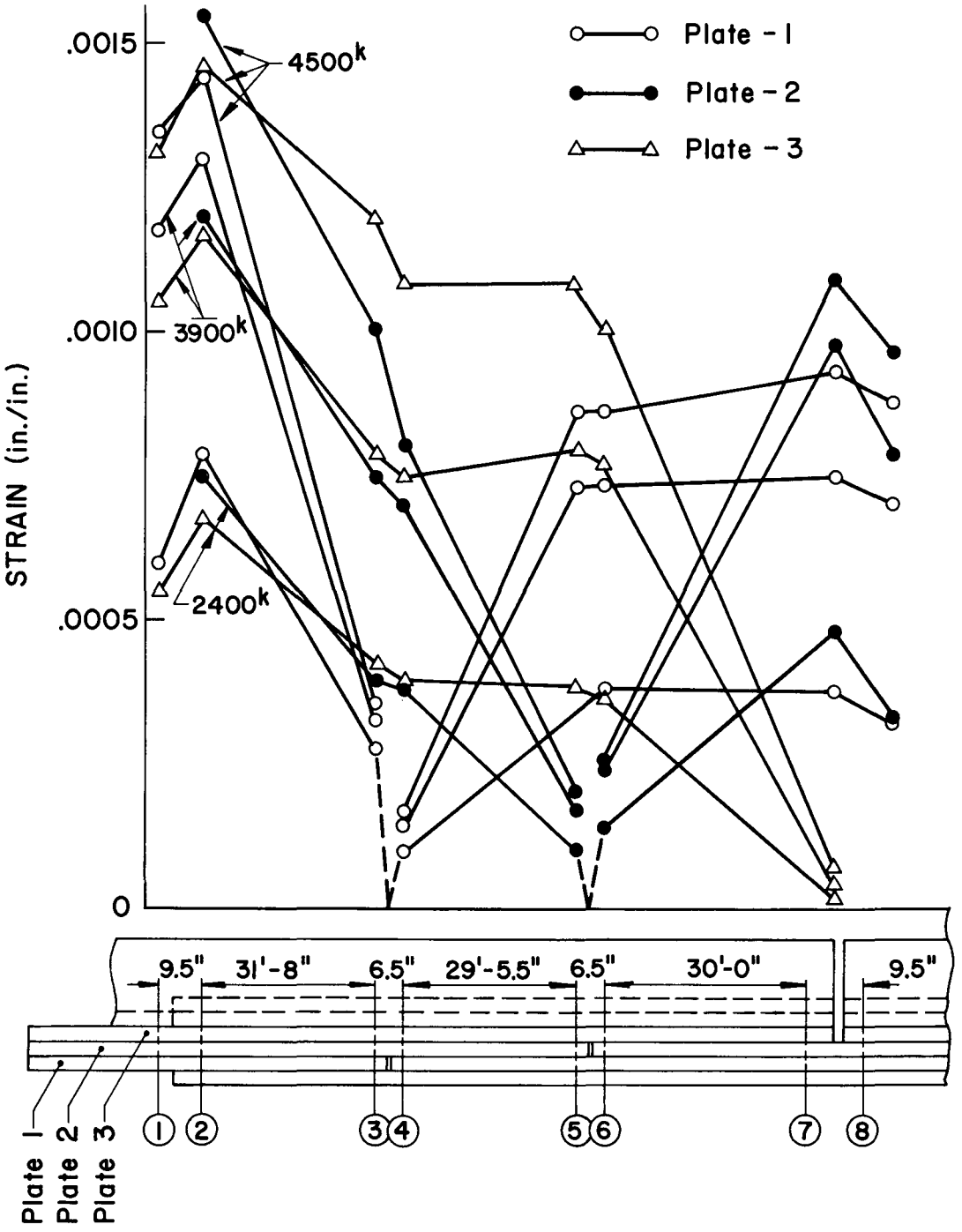

Fig. 33 Strain Distribution in Plates of Bolted Joint

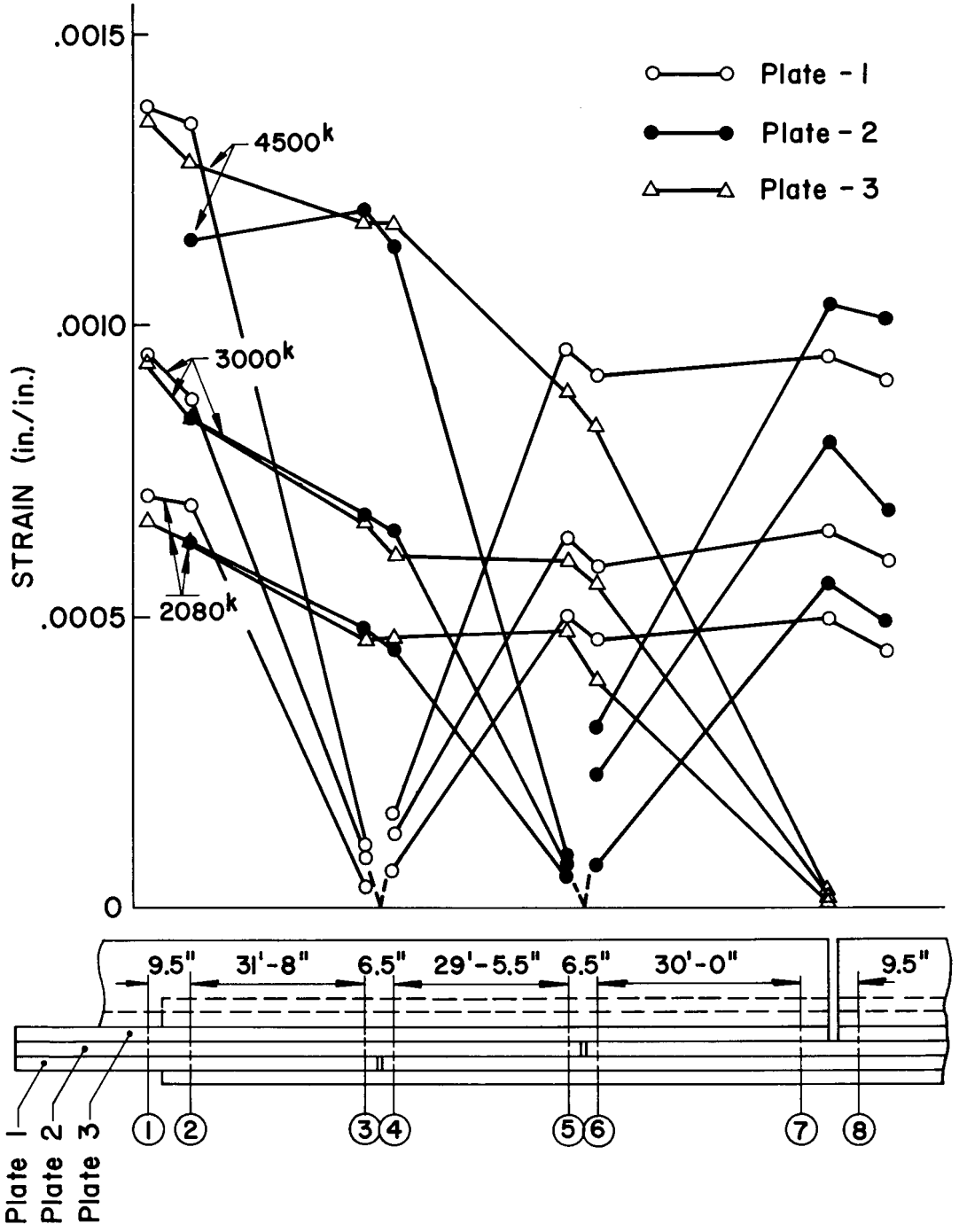

Fig. 34 Strain Distribution in Plates of Riveted Joint

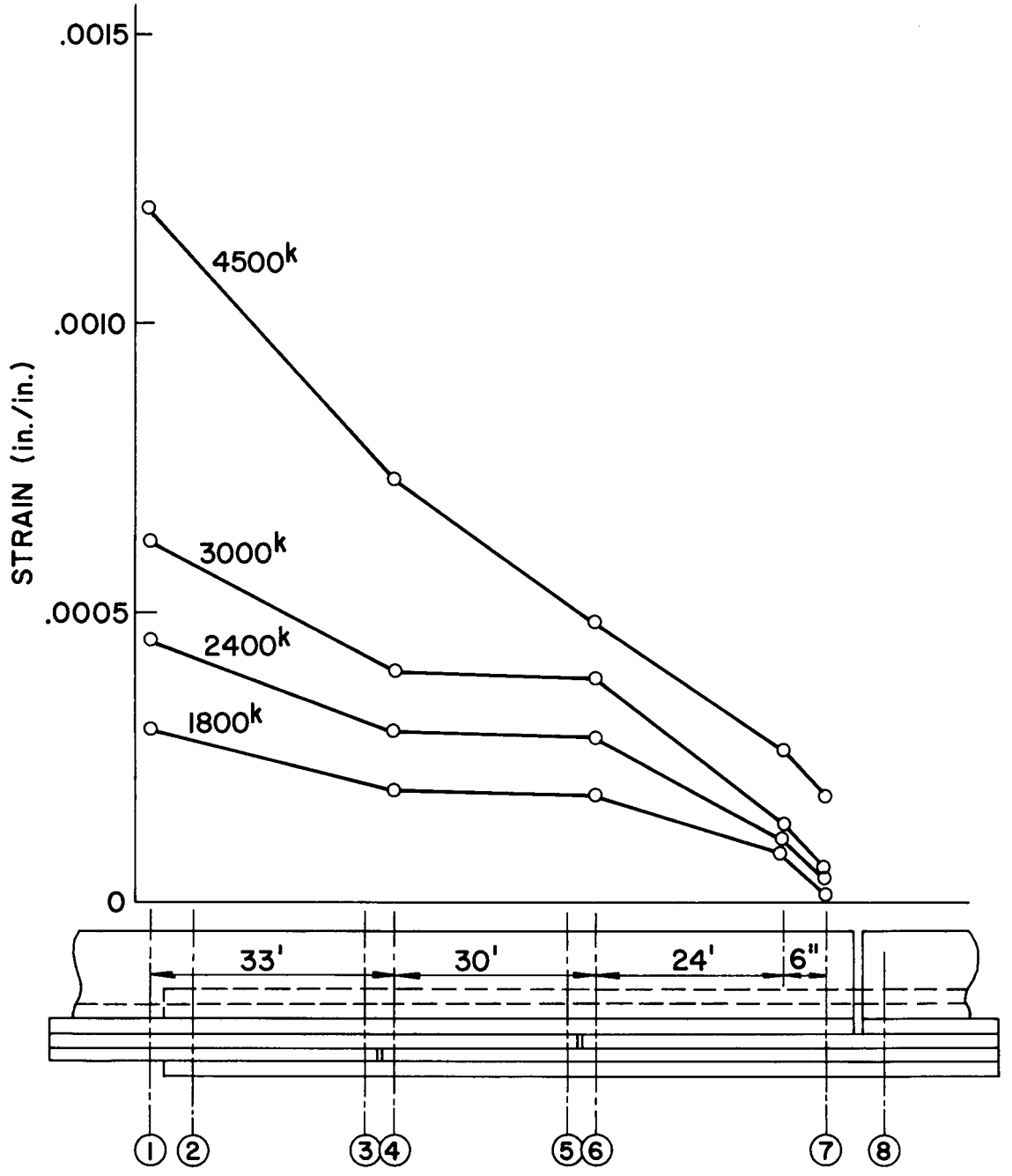

Fig. 35 Strain Distribution in Angles of Bolted Joint

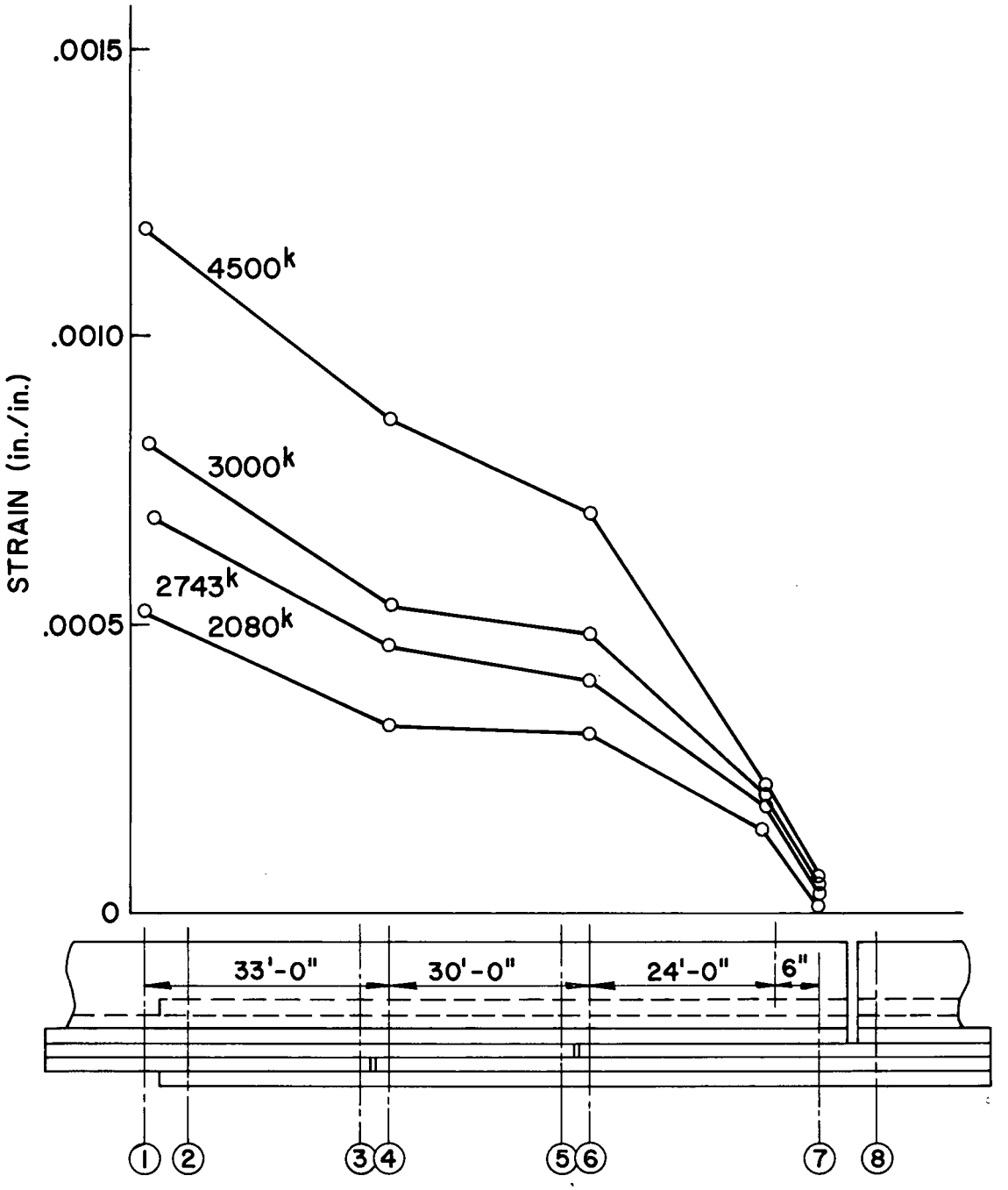

Fig. 36 Strain Distribution in Angles of Riveted Joint

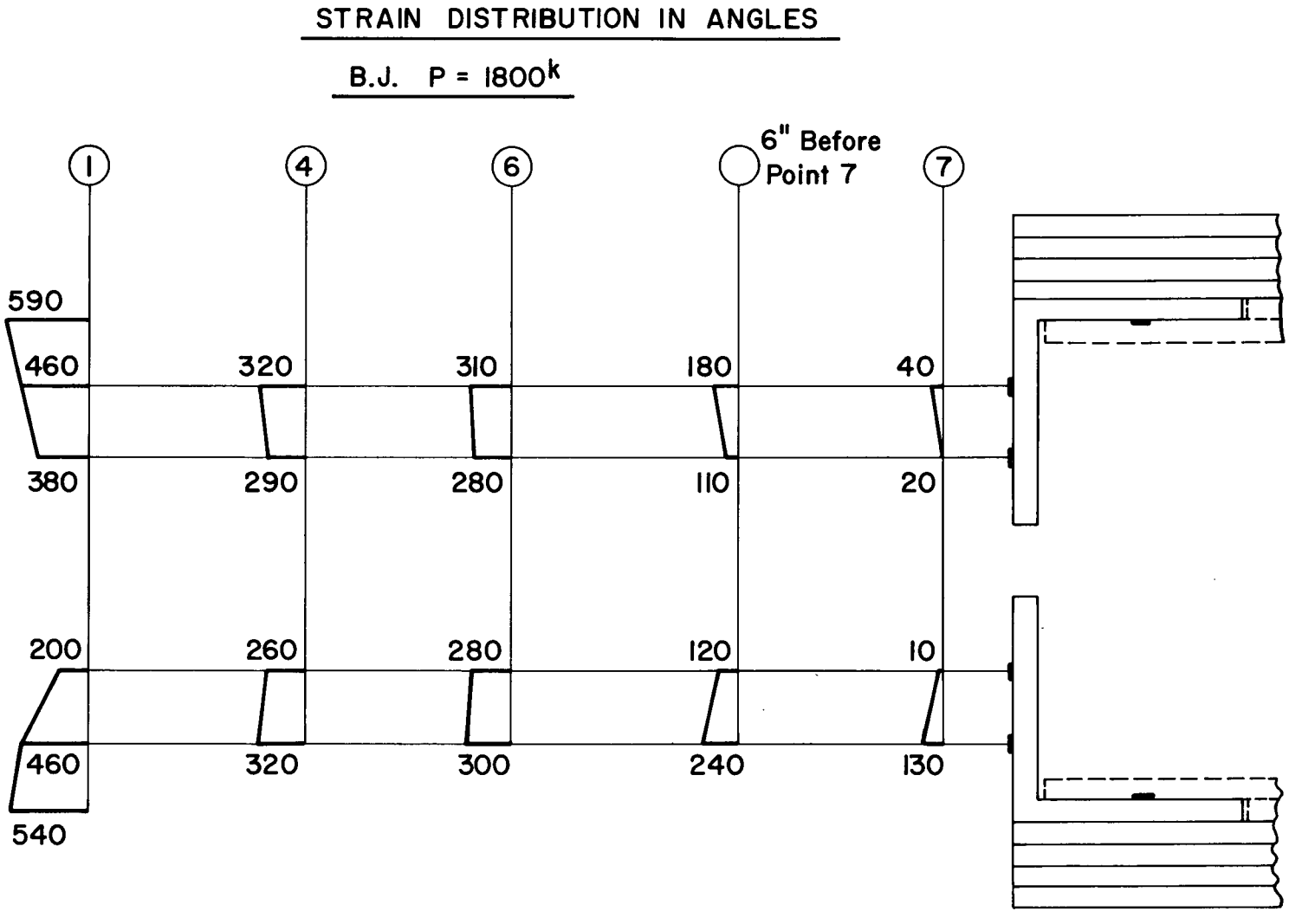

Fig. 37 Strain Distribution in Outstanding Legs of Angles of Bolted Joint

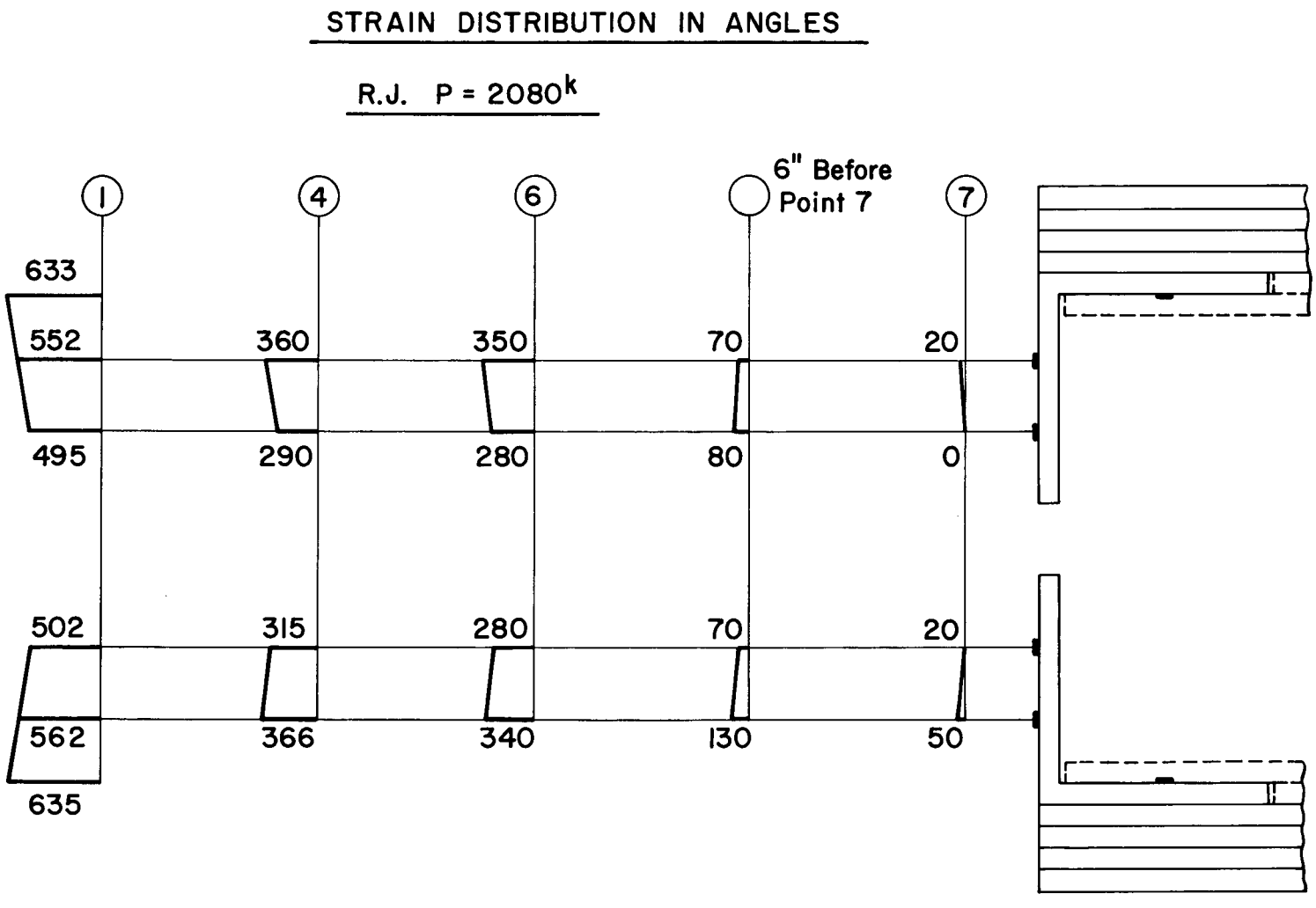

Fig. 38 Strain Distribution in Outstanding Legs of Angles of Riveted Joint

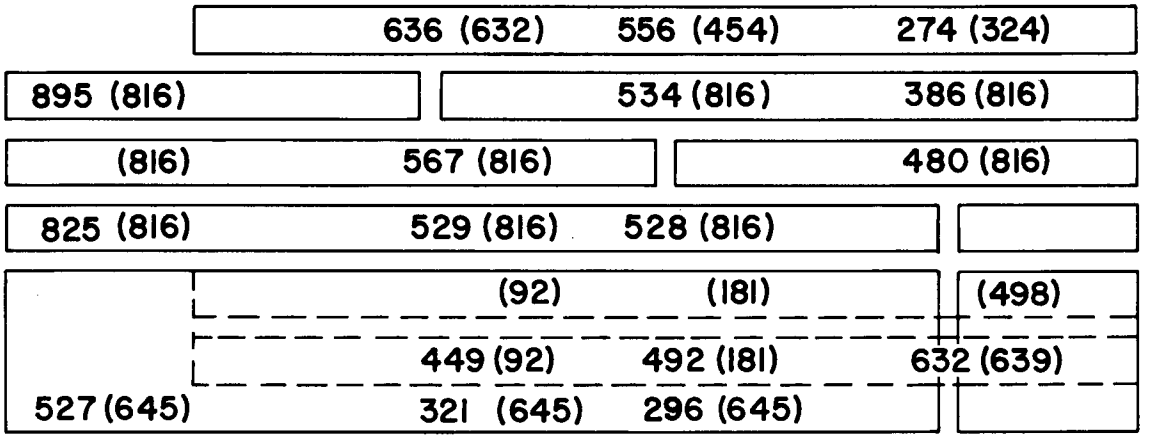

BOLTED JOINT Load in Kips

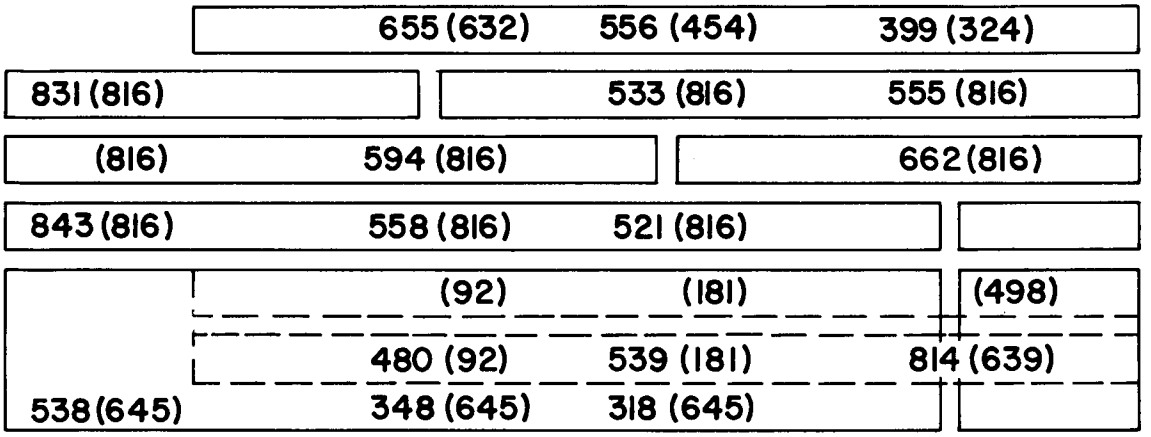

RIVETED JOINT Load in Kips

( ) : Load for Design

At Design Load of 3100 kips

Fig. 39 Load Distribution at Design Load Level

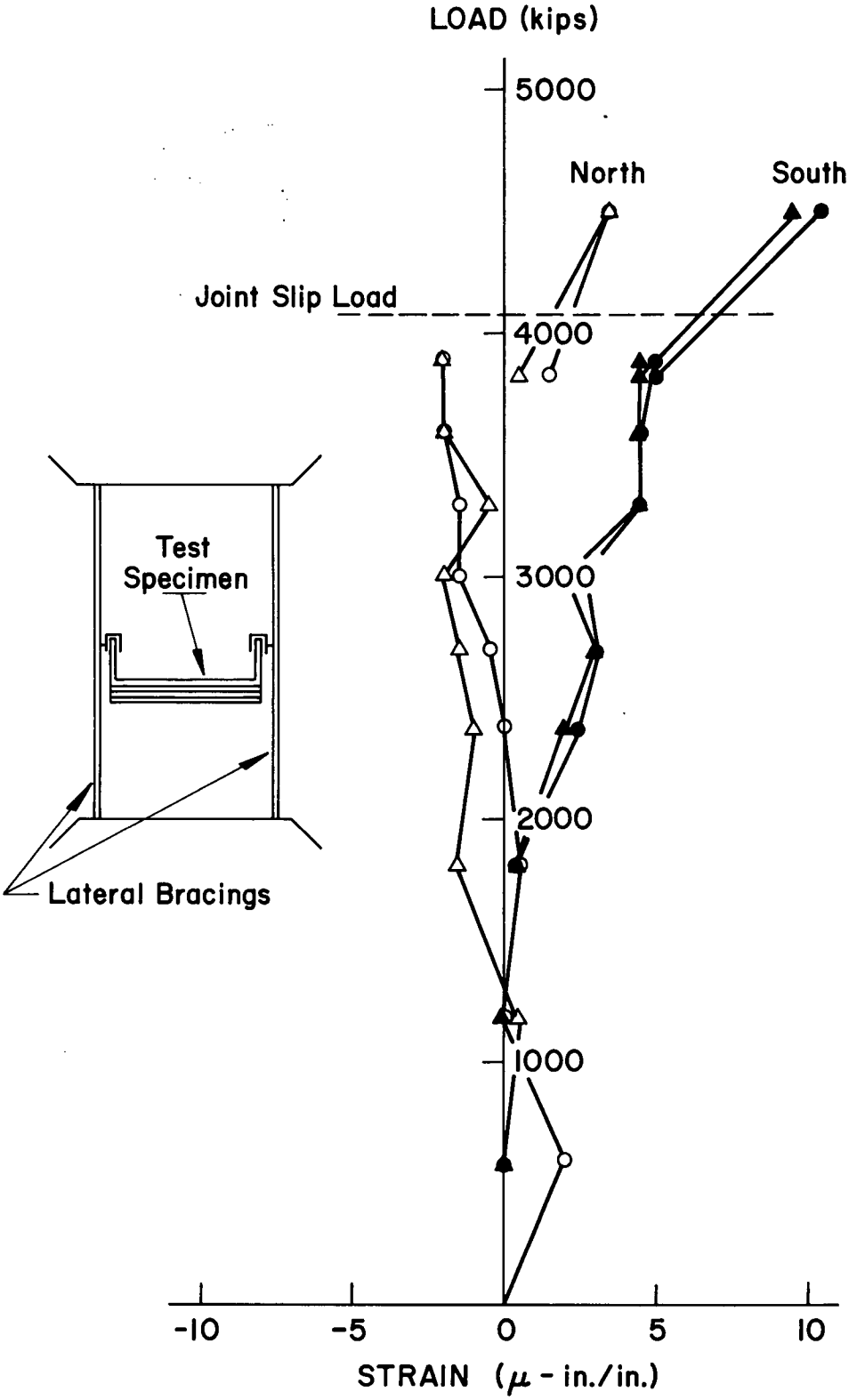

Fig. 40 Strain of Lateral Bracings

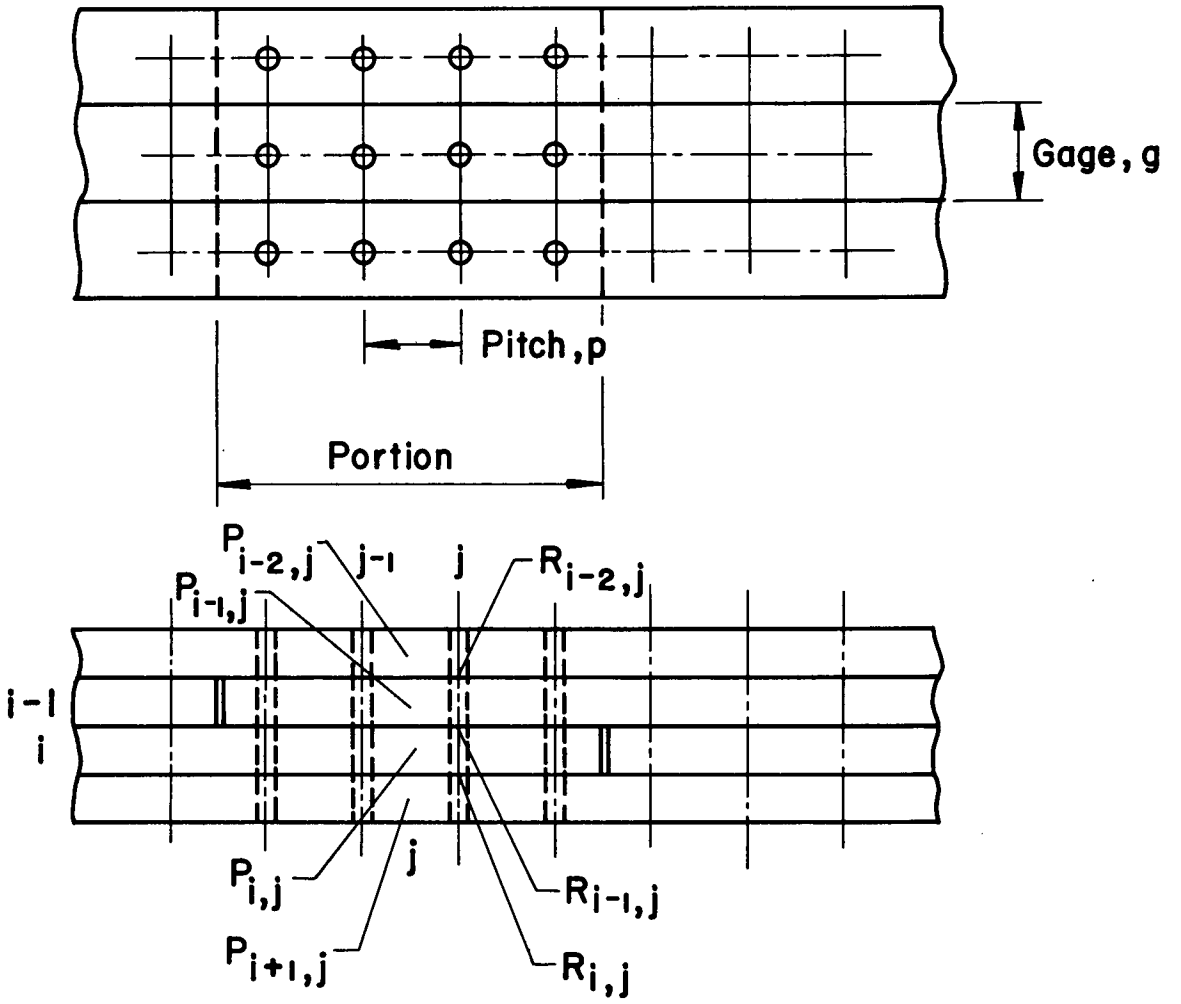

Fig. 41 Joint Geometry

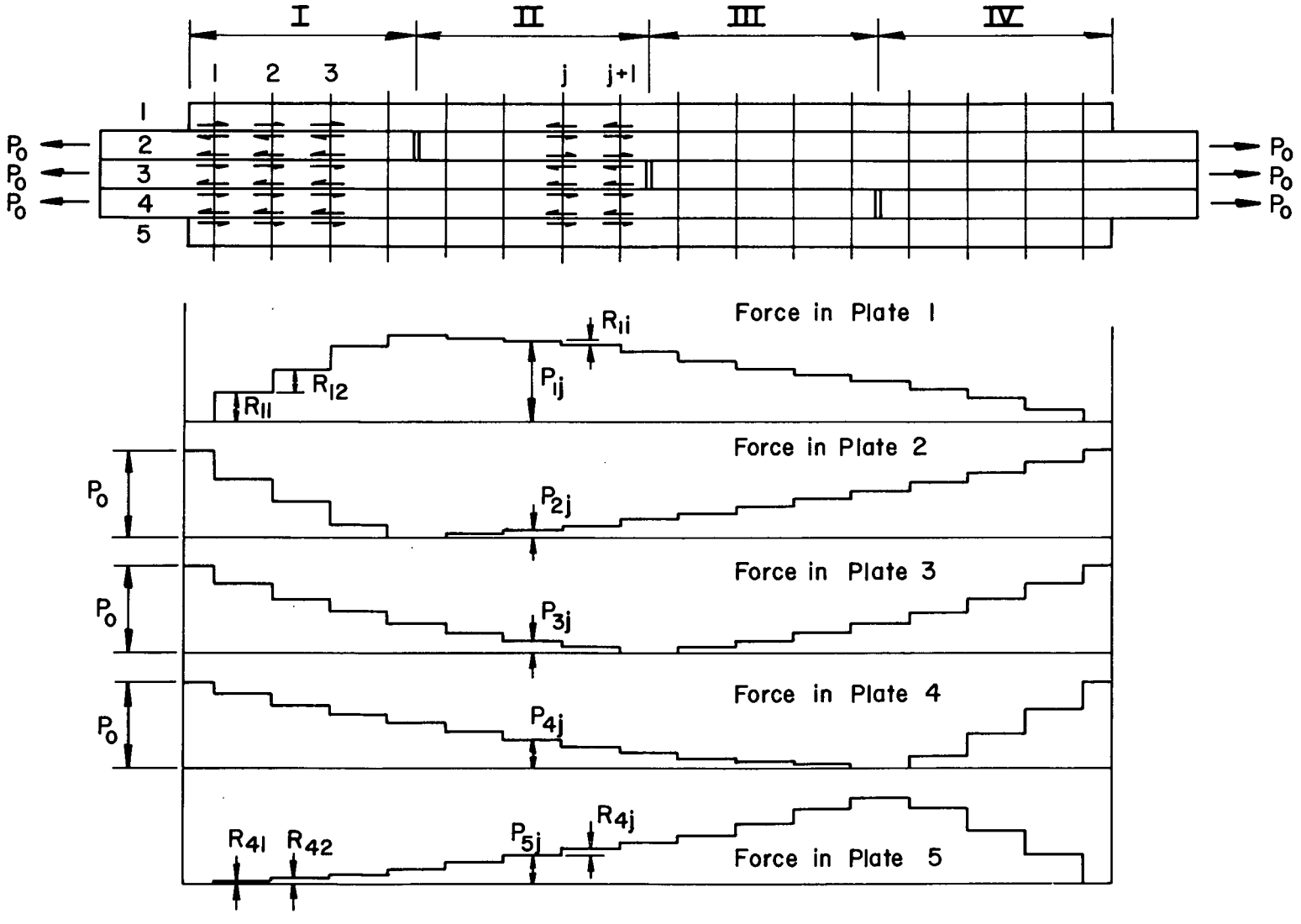

Fig. 42 Idealized Load Transfer Diagram

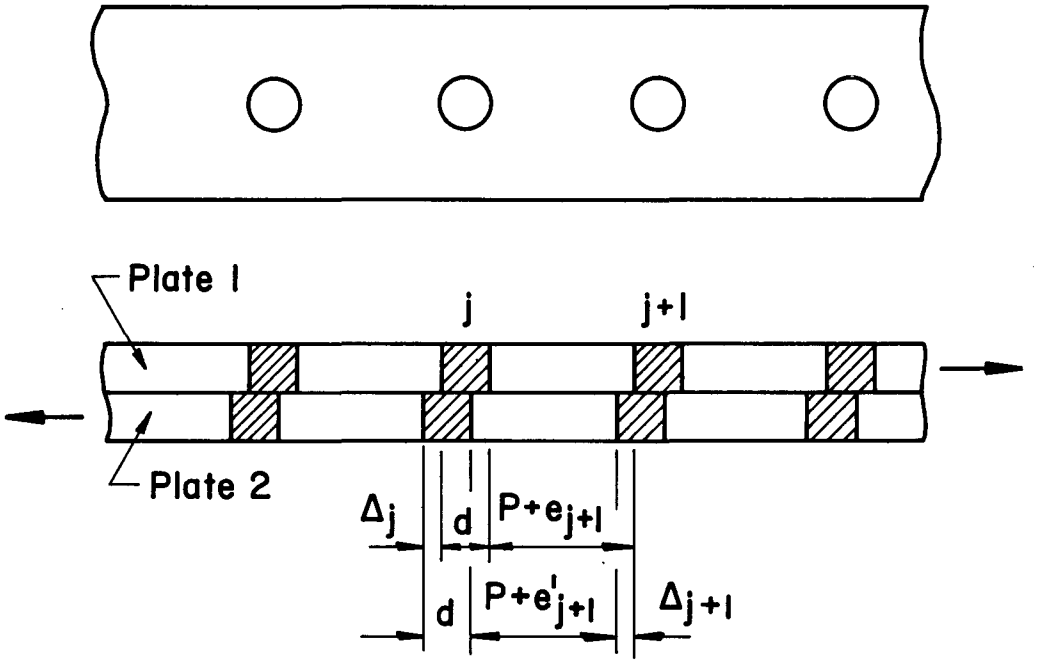

Fig. 43 Deformations in Fasteners and Plates

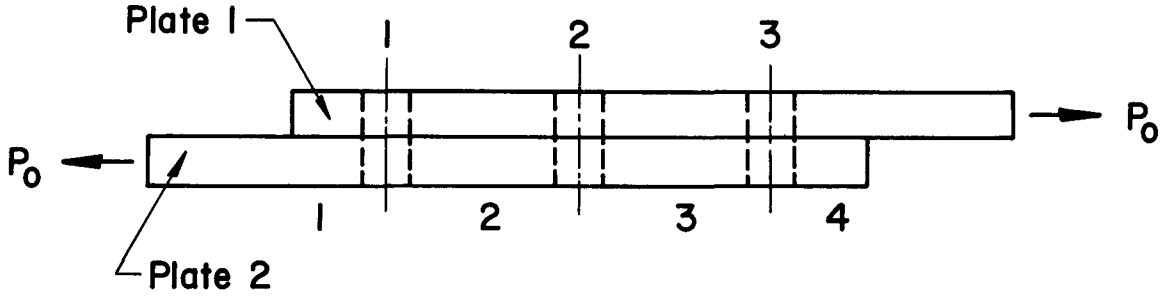

Fig. 44 A Lap Splice with Three Fasteners

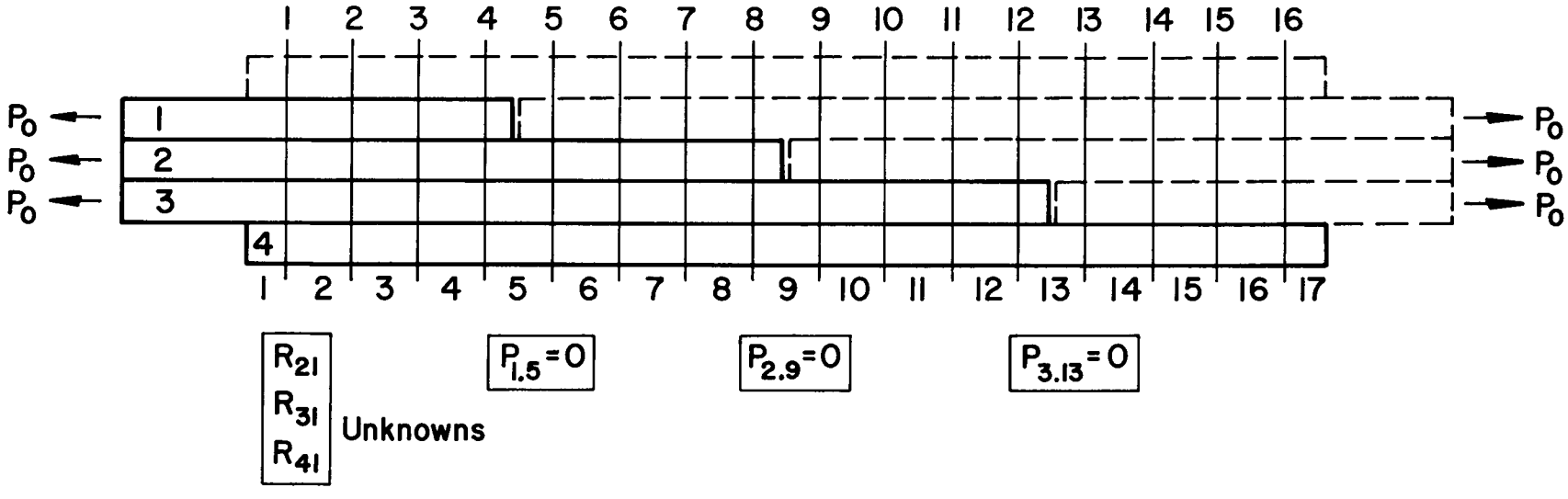

Fig. 45 Anti-Symmetric Shingle Joint

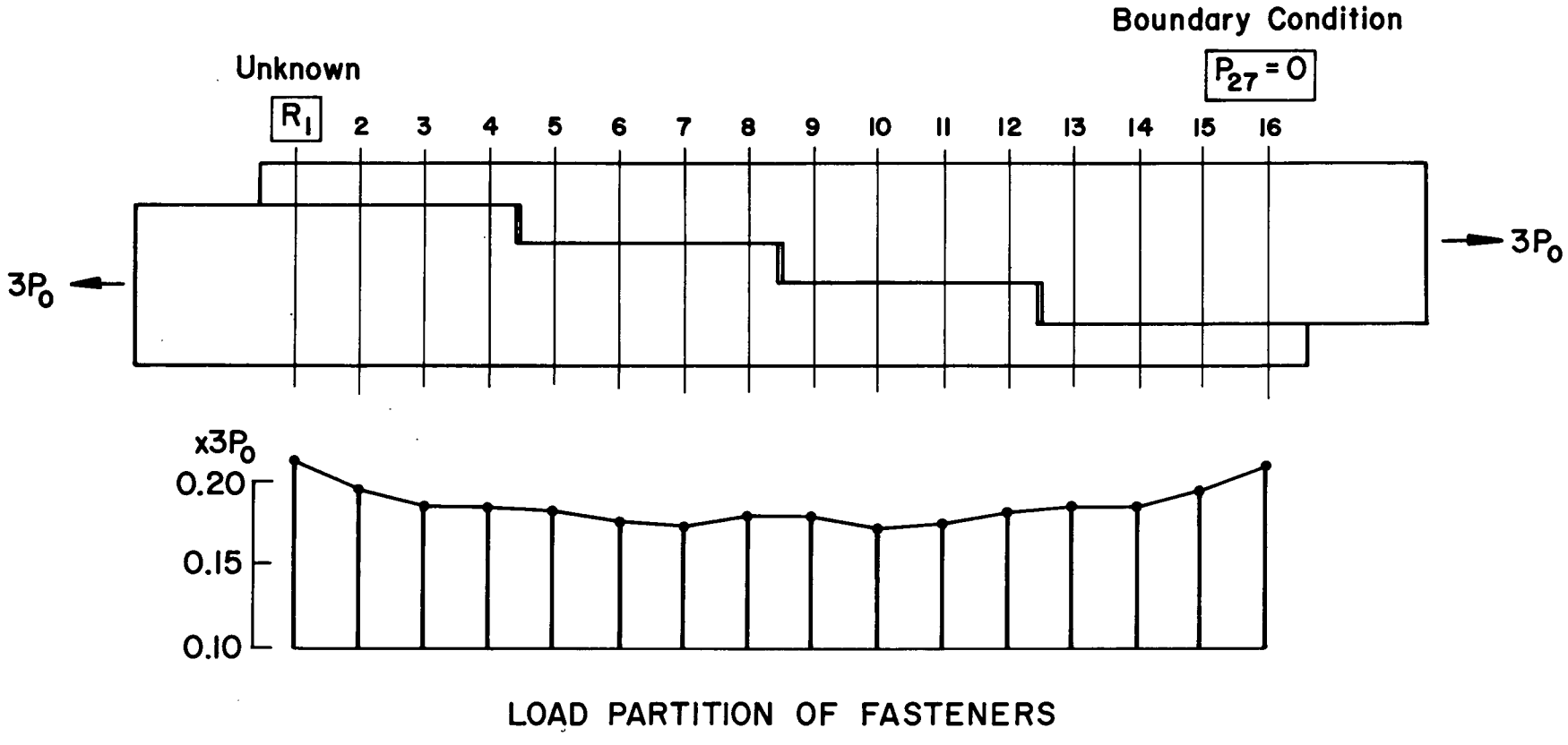

Fig. 46 Discontinuous Lap Splice

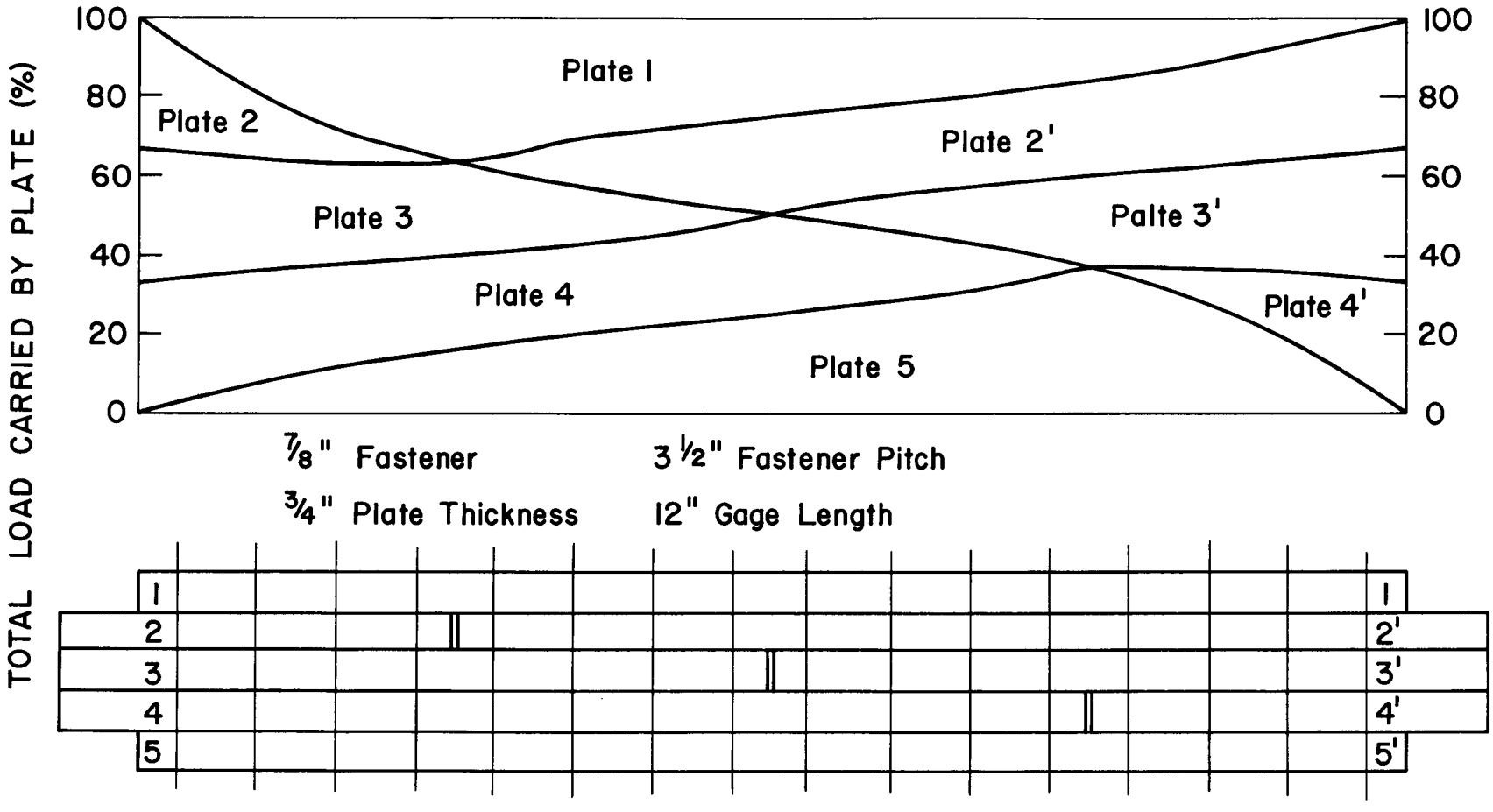

Fig. 47 Theoretical Solution of Load Partition among Plates

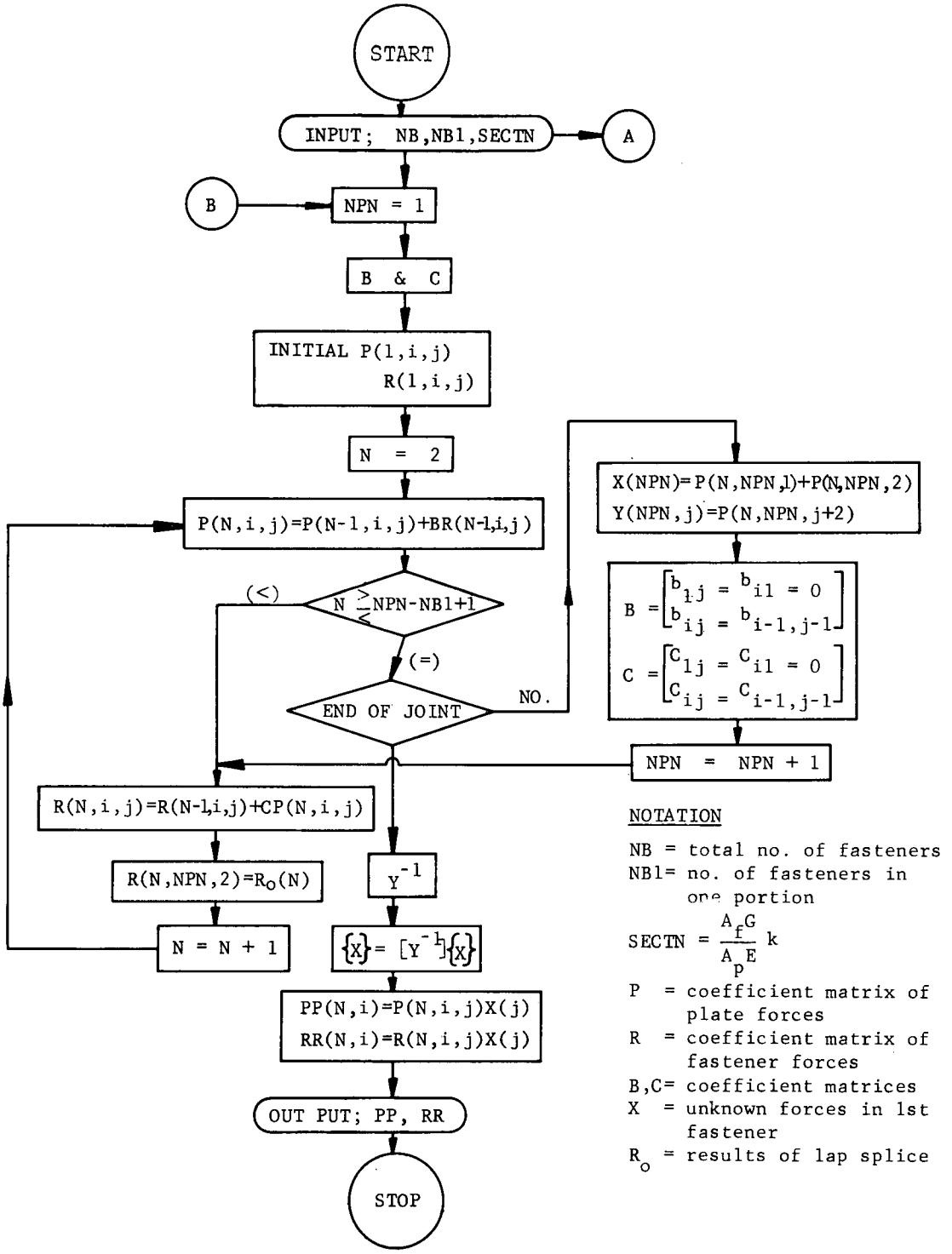

Fig. 48(1) Computation Flow Chart for Shingle Joint

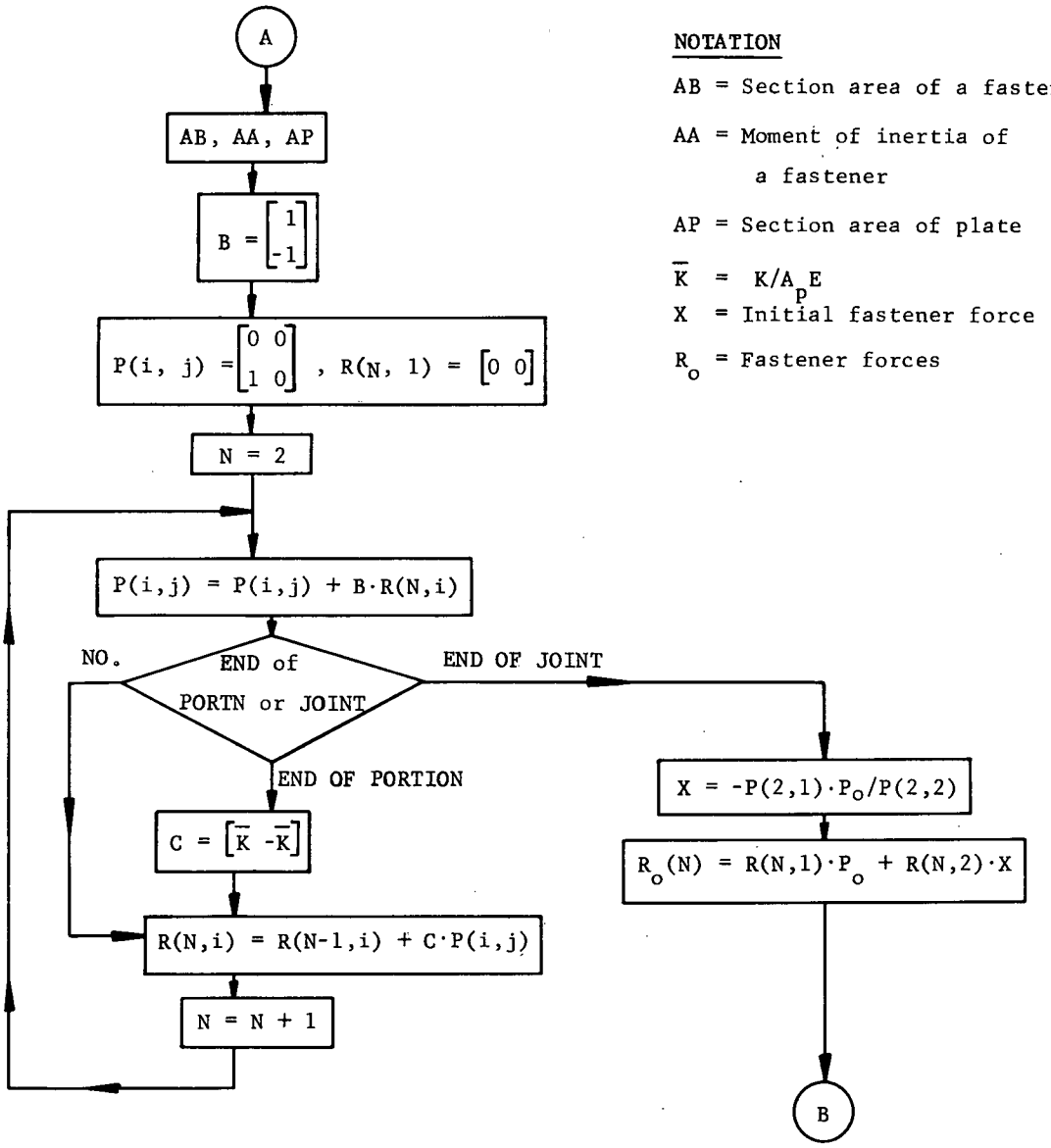

Fig. 48(2) Sub-Flow Chart for Discontinuous Lap Splice

7. REFERENCES

1. Research Council on Riveted and Bolted Structural Joints SPECIFICATIONS FOR ASSEMBLY OF STRUCTURAL JOINTS USING HIGH TENSILE STEEL BOLTS, January 1951

2. Research Council on Riveted and Bolted Structural Joints SPECIFICATIONS FOR STRUCTURAL JOINTS USING ASTM A325 or A490 BOLTS, September 1, 1966

3. Foreman, R. T. and Rumpf, J. L.
   STATIC TENSION TESTS OF COMPACT BOLTED JOINTS, Journal of the Structural Division, ASCE, No. ST6, June 1960

4. Davis, R. E., Woodruff, G. B. and Davis, H. E.
   TENSION TESTS OF LARGE RIVETED JOINTS, Transactions, ASCE, Vol. 105, 1940, p. 1193

5. Armovlevic, I.
   INANSPRUNCHNAHME DER ANSHLUSSNIETEN ELASTISCHER STÄBE, Zeitschrift fur Architekten und Ingenieure, Vol. 14, Heft, 2, 1909, p. 89

6. Batho, C.
   THE PARTITION OF LOAD IN RIVETED JOINTS, Journal of the Franklin Institute, Vol. 182, 1916, p. 553

7. Bleich, F.
   THEORIE UND BERECHNUNG DER EISERNEN BRUCKER, Julius Springer, Berlin, 1921

8. Hrennikoff, A.
   THE WORK OF RIVETS IN RIVETED JOINTS, Transactions, ASCE, Vol. 99, 1934, pp. 437 - 489

9. Vogt, F.
   LOAD DISTRIBUTION IN BOLTED OR RIVETED STRUCTURAL JOINTS IN LIGHT-ALLOY STRUCTURES, U. S. NACA Tech. Memo No. 1135, 1947

10. Francis, A. J.
    THE BEHAVIOR OF ALUMINUM ALLOY RIVETED JOINTS, The Aluminum Development Association, Research Report No. 15, London, 1953

11. Rumpf, J. L.
THE ULTIMATE STRENGTH OF BOLTED CONNECTIONS, PhD Dissertation, Lehigh University, 1960

12. Fisher, J. W.
THE ANALYSIS OF BOLTED PLATE SPLICES, PhD Dissertation, Lehigh University, 1964

13. Fisher, J. W., Ramseier, P. O. and Beedle, L. S.
STRENGTH OF A440 STEEL JOINTS FASTENED WITH A325 BOLTS, Proceedings, IABSE, Zurich 1963

14. Bendigo, R. A., Hansen, R. M. and Rumpf, J. L.
LONG BOLTED JOINTS, Journal of the Structural Division, ASCE, Vol. 89, No. ST6, 1963

15. Rumpf, J. L., and Fisher, J. W.
CALIBRATION OF A325 BOLTS, Journal of the Structural Division, ASCE, Vol. 89, No. ST6, 1963

16. Fisher, J. W. and Beedle, L. S.
CRITERIA FOR DESIGNING BEARING-TYPE BOLTED JOINTS, Transactions, ASCE, Vol. 91, No. ST5, 1965

17. Fisher, J. W. and Rumpf, J. L.
ANALYSIS OF BOLTED BUTT JOINTS, Transactions, ASCE, Vol. 91, No. ST5, 1965

18. Coker, E. G.
THE DISTRIBUTION OF STRESS DUE TO A RIVET IN A PLATE, Transactions, Institute of Naval Arch., Vol. 55, 1913, p. 207

19. Baron, F. and Larson, E. W.
THE EFFECT OF GRIP ON THE FATIGUE STRENGTH OF RIVETED AND BOLTED JOINTS, Proceedings, AREA, Vol. 54, 1953

20. Sterling, G. H. and Fisher, J. W.
A440 STEEL JOINTS CONNECTED BY A490 BOLTS, Journal of the Structural Division, ASCE, Vol. 92, No. ST3, June 1966

21. Sterling, G. H.
Discussion of COEFFICIENT OR FRICTION IN JOINTS OF VARIOUS STEELS, Journal of the Structural Division, ASCE, Vol. 94, No. ST4, April 1968, pp. 1072 - 1075

8. VITA

Noriaki Yoshida was born on December 28, 1940 in Hokkaido, Japan, the third child of Shosaku and Yoshiko Yoshida. He attended Sapporo Nishi High School for three years, graduating in 1959.

He entered Hokkaido University in 1959 and received Bachelor of Engineering Degree in Civil Engineering in 1963. During his undergraduate years he was active in the student chapter of the JSCE. He worked at Hitach Shipbuilding and Engineering Company for 3 years after graduation from Hokkaido University.

In August 1966, he came to Fritz Engineering Laboratory at Lehigh University as a Research Assistant in the Structural Division.